Mechanisms of Group B Streptococcus Colonization and Ascending Infection

Jay Vornhagen

A dissertation

submitted in partial fulfillment of the

requirements for the degree of

Doctor of Philosophy

University of Washington

2017

Reading Committee:

Lakshmi Rajagopal, Chair

Richard Darveau

David N. Fredricks

Program Authorized to Offer Degree:

Pathobiology

University of Washington

Abstract

Mechanisms of Group B Streptococcus Colonization and Ascending Infection

Jay Charles Vornhagen

Chair of the Supervisory Committee:

Lakshmi Rajagopal, Ph.D.

Pathobiology Program, Department of Global Health

Group B Streptococcus (GBS), also known as Streptococcus *agalactiae*, are bacteria that commonly reside in the vagina of healthy women. GBS is not a major cause of infection in normal adults. However, newborns can acquire GBS from colonized mothers during birth leading to neonatal infections. Alternatively, GBS can migrate from the vagina to the uterus, during pregnancy leading to *in utero* infection and significant adverse pregnancy outcomes such as preterm birth and stillbirth. To successfully establish an *in utero* infection, GBS must bypass the host immune response to traffic from the vagina into the pregnant uterus in a process known as ascending infection. Despite the significant impact on perinatal and neonatal health, the mechanisms of GBS vaginal colonization and ascending infection are not completely understood. An increased understanding of these processes will enable the development of novel therapeutic

strategies and interventions and are critical for the reduction of the burden of GBS disease. This dissertation summarizes our efforts to describe the interactions between GBS and the host during vaginal colonization, ascending *in utero* infection and preterm birth.

First, we aimed to explore the host-pathogen interactions that mediate vaginal colonization. While significant work has been done to identify GBS virulence factors involved in vaginal colonization, little attention has been given to the host response during colonization. We demonstrate that the vaginal resident immune cells known as mast cells are critical for preventing colonization of hyper-virulent GBS, which are highly associated with invasive infections. GBS virulence is largely mediated by its unique hemolytic toxin which is a pigmented rhamnolipid (hereafter-called hemolytic pigment); yet hyper-pigmented GBS strains are rarely isolated from vagina. We found that the hemolytic pigment toxin activates a subset of host immune cells known as mast cells, leading to its clearance from the vagina. Interestingly, removal of the GBS hemolytic pigment from the bacteria, which renders it avirulent, also leads to inefficient vaginal colonization. Once GBS has ascended from the vagina to infect the placenta, the hemolytic pigment is required for resistance of the host immune response, and hyper-pigmented strains are more resistant to killing by host immune defenses. These data indicate that a delicate balance of hemolytic pigment expression, and therefore regulation of the host immune response, is necessary for successful colonization and ascending infection.

Next, we sought to determine the mechanism by which GBS ascends from the vagina to the uterus. We show that GBS interactions with vaginal epithelial cells play an integral role in permitting ascending infection. GBS stimulate a process known as epithelial exfoliation that is critical for ascending infection. Epithelial exfoliation is a process wherein epithelial cells lose their junction properties and detach from the epithelial surface and basement membranes. To

induce epithelial exfoliation, GBS actives a class of proteins called integrins, which leads to β-catenin signaling and epithelial-to-mesenchymal transition (EMT), resulting in a migratory cell phenotype. EMT drives loss of junctional and adherent properties, and permits bacterial dissemination into vaginal tissues for ascending infection. Reduction of integrin activation results in less epithelial exfoliation and a reduction in ascending infection and adverse pregnancy outcomes. This work is the first to outline a mechanism of GBS ascending infection.

Finally, we endeavored to define the mechanism by which GBS establishes *in utero* infection. We observed that GBS isolated from cases of preterm birth had significantly higher levels of hyaluronidase activity than those isolated from commensal settings. The GBS hyaluronidase, HylB, is a secreted enzyme that cleaves the host extra-cellular matrix molecule hyaluronic acid into is disaccharide moiety. Hyaluronic acid disaccharides have the ability to block toll-like receptors, which are critical for the detection of pathogenic bacteria, and thus prevent immune recognition of GBS. Using a murine model of ascending infection, we show that GBS deficient for *hylB* have reduced ability to establish *in utero* infections due to increased immune recognition of the bacteria. The reduction in bacterial load in the uterus reduces bacterial invasion of placental and fetal tissues, leading to improved pregnancy outcomes.

Together, the work in this dissertation describes how GBS successfully colonizes the vagina, ascends from the vagina into the pregnant uterus, and blunts the host immune response in the uterus, leading to placental and fetal infection and adverse pregnancy outcomes.

TABLE OF CONTENTS

LIST OF FIGURES

LIST OF SUPPLEMENTARY FIGURES

LIST OF TABLES

ACKNOWLEDGEMENTS

First and foremost, I want to thank my advisor, Dr. Lakshmi Rajagopal. You have been a consistent and positive guiding force in my development as a scientist and as a person. I cannot fully express how grateful I am to you for putting up with my teasing, my pranks, and my sarcasm. You are one of the people that saw my potential, and without that support, I would not have been able to complete this process.

Secondly, I want to thank my fellow graduate students for their support in this work, especially Chris Whidbey, Blair Armistead, Justine Levan, and Taylor Stepien. You have all been integral to my success through your mentorship, advice, and most importantly, friendship. It has been an honor to work with you and to befriend you.

Finally, I want to thank my family and my partner. Mom and Dad, thank you for raising me with a strong sense of curiosity and work ethic. Without your support, constant parenting, and love, I would not have been able to complete this journey. Verónica, you have been the best partner anyone could ask for. Thank you for all of the long nights you spent with me while I worked, thank you for all of the practice talks you had to sit through and all of the drafts you had to read, and thank you for lifting my spirits when I was at out of energy. Without all of you, this dissertation would not exist.

Chapter 1. Introduction

The figures and figure legends in this chapter have been adapted from the following articles:

Jay Vornhagen, Kristina Adams Waldorf, and Lakshmi Rajagopal. (2017) Perinatal Group B Streptococcal infections: virulence factors, immunity and prevention strategies. Trends in Microbiology, accepted.

Figure numbers have been updated to conform to the dissertation. Adapted text remains as published with minor editorial changes.

1.1 INFECTION-ASSOCIATED PRETERM BIRTH

Perinates and neonates are exceedingly vulnerable to many adverse health outcomes. Every minute more than five neonates die, accounting for roughly 50% of under-five deaths (WHO World Health Statistics Report 2016). These deaths disproportionately affect people of low socioeconomic status, and are largely attributable to high rates of perinatal or neonatal infection, and preterm birth[1]. Preterm birth occurs before 37 weeks gestation[2,3], and is the primary risk factor for neonatal death[4]. Every year, approximately 6,000,000 premature births occur and more than 500,000 neonates die due to prematurity, accounting for 44% of all under-five deaths[1,5]. The long term effects of preterm birth include but is not limited to cognitive or sensory impairments[6,7], developmental disorders[6], and increased risk for cardiovascular and pulmonary disease[8]. Finally, the economic burden of preterm birth is substantial[9]. The estimated cost of preterm birth in the United States in 2007 was $26.2 billion[10], and it is certain that figure has increased over the last decade, as preterm birth only diminished slightly during that time[11]. Given its clinical impact, a better understanding of mechanisms that lead to preterm birth is critical for the improvement of global health.

The etiology of preterm birth is multi-faceted and poorly understood. Multiple factors, including microbial infection, vascular disorders, breakdown of maternal-fetal tolerance, stress, uterine distension, and cervical disease, have been associated with preterm birth[12]. A majority of early preterm births are due to infection[3], wherein bacteria have been identified by culture and/or PCR in the amniotic fluid of 15-50% of women undergoing preterm birth[3,13-16]. A wide variety of bacteria have been associated with preterm birth including: *Chlamydia trachomatis*[17], *Neisseria gonorrhea*[17], *Treponema pallidum*[18], *Escherichia coli*[19], *Gardnerella vaginalis*[19], and

Streptococcus agalactiae[20]; however, many questions regarding the mechanisms by which these bacteria cause preterm birth remain unanswered.

During infection-associated preterm birth, microbes come into contact with the placenta and may invade the amniotic cavity. This leads to inflammation of the placental membranes, referred to as chorioamnionitis, which is frequently associated with preterm birth and stillbirth[3]. During pregnancy, the placental membranes protect the fetus from infection and injury. The placental membranes are comprised of two main layers known as the chorion and amnion. The chorion faces the maternal side and the amnion is located on the fetal side and is in direct contact with the amniotic fluid and fetus. These membranes contain various types of cells. The amnion is made up of five distinct layers, the epithelial layer being most proximal to the fetus, followed by the epithelial basement membrane, the compact layer and fibroblast layers, which contain high levels of collagen that maintain the mechanical strength of the amnion, and finally, the intermediate layer, which is rich in hyaluronic acid and separates the amnion and chorion[21]. The chorion is made up of three layers: the reticulate layer followed by the basement membrane, and a trophoblast layer. Together, these layers add strength and elasticity to the placental membranes with the amnion providing more tensile strength than the chorion[22]. Upon infection of the placenta or the amniotic cavity, microbes infection can elicit inflammation, damage to the placental membranes, and fetal damage, which can lead to preterm labor. Studies have shown that bacterial penetration of the amniotic cavity is not necessary for this process, though the inflammatory cascade is critical in driving these processes. Interestingly, intra-amniotic administration of cytokines such as TNFα and IL-1β (without bacteria) also stimulated preterm labor in non-human primates[23], and multiple studies have implicated IL-1α, IL-1β, IL-6, and IL-8 in driving infection-associated preterm birth in humans[24]. In mice, IL-6 has been shown to be an

important regulator to the timing of parturition[25,26]. Thus, chorioamnionitis and inflammation induced by bacterial infection is a critical component of infection-associated preterm birth.

Currently, the only intervention for infection-associated preterm birth is the use of intra-partum broad spectrum antibiotic prophylaxis (IAP)[27-30]. While this treatment is effective, it is not without its limitations. IAP is only appropriate in at-risk situations, and is not recommended for universal administration in all cases of preterm labor[31,32]. Additionally, IAP does not prevent preterm birth, but rather minimizes the adverse perinatal and neonatal outcomes. If infection and inflammation occurs during pregnancy, preterm labor frequently occurs prior to antibiotic intervention, thus, IAP is not a preventative measure for preterm birth. Finally, antibiotic resistance is on the rise[33], and recent work suggests potential impacts of antibiotics during labor and delivery on the immediate and long-term health of the neonate[34,35]. Given these trends, more information is needed about infection-associated preterm birth and how individual bacteria stimulate preterm birth to successfully develop therapeutics and interventions to reduce this important cause of preterm birth and perinatal and neonatal mortality.

1.2 Ascending Bacterial Infection

Frequently, the bacterial agents that cause preterm birth and stillbirth originate from the mother's vagina. In order for these bacteria to infect placental tissues, they must penetrate the cervix, enter the uterus in a process called ascending infection. A variety of bacteria have been experimentally and/or clinically shown to cause ascending infection[36] (Table 1-1); however, the mechanisms by which they travel from the vagina to the uterus remains unexplored. Many studies have focused on how the host prevents ascending infection during pregnancy, but few have aimed to determine the mechanisms by which bacteria ascend, or what bacterial factors are involved. The only bacterial properties that have been suggested to play a role in ascending

infection are resistance to the anti-microbial activity of the cervical mucus plug[37], which separates the uterus and the vagina during pregnancy, modification of the host immune system through poly-microbial infection[38], and for *Streptococcus agalactiae*, expression of its hemolytic pigment toxin (described in detail below)[39]. One reason for the absence of mechanistic information regarding ascending infection is the lack of appropriate experimental models, as *in vitro* models are unsuitable, and *in vivo* models are limited in their ability to recapitulate human pregnancy[40,41]. The development of new models for the study of ascending bacterial infection is crucial for a better understanding of the mechanisms, timing, and causes of ascending infection.

1.3 GROUP B STREPTOCOCCUS

Group B Streptococcus (GBS) or *Streptococcus agalactiae*, are Gram positive, beta-hemolytic bacteria that are the leading cause of infection during pregnancy, preterm birth and neonatal infection[4,42,43]. Additionally, GBS are a cause of soft-tissue infection, pneumonia, bacteremia, and urinary tract infection in elderly or immunocompromised non-pregnant adults, and those with chronic illnesses[44,45]. GBS were first identified in 1887 as a cause of bovine mastitis[46], and later were isolated from the human vagina[47] and associated with cases of human disease[48]. Subsequently, GBS vaginal colonization was identified as a risk factor for the development of neonatal GBS disease[49,50] and preterm birth[4,43].

Neonatal GBS infection is classified into two categories: early onset neonatal disease (EOD), which manifests during the first week of life, and late onset neonatal disease (LOD), which manifests from the first week through the first three months of life. Neonatal infection by GBS results in sepsis, pneumonia, and/or meningitis, with an overall case fatality rate of 5-10%[51-54]. EOD most frequently presents as sepsis, and LOD most frequently presents as meningitis[54]. The primary risk factor for neonatal GBS infection is heavy maternal vaginal

colonization during pregnancy[43]. In the U.S. and many other countries, women are routinely screened for GBS in the late third trimester (between 35-37 weeks gestation) for GBS colonization by rectovaginal swab and subsequent culture[55]. If the rectovaginal swab is culture positive or the patient has GBS in the urine, or has a prior history of a GBS perinatal infection, intrapartum prophylactic antibiotics are administered to prevent vertical transmission of GBS to the neonate during labor and delivery.

GBS vaginal colonization during pregnancy is associated with increased rates of vertical transmission of GBS and neonatal infection[56], recurrent maternal colonization[57], and importantly, early term birth[58], preterm birth[4], and stillbirth[59]. The close proximity of the vagina and rectum is thought to enable GBS trafficking from intestinal flora into the vagina. Once GBS enters the vagina, colonization requires these bacteria to overcome a number of challenges: physical barriers created by the mucus and epithelial layers, low environmental pH, antimicrobial peptides, antibodies, microbicidal immune cells, and a vaginal microbiome dominated by lactobacilli. To overcome these barriers, GBS encodes a number of factors for vaginal colonization.

Once GBS colonizes the vagina during pregnancy, the potential exists for these bacteria to ascend into the uterus and infect the placenta and fetus. How a non-motile bacterium, such as GBS traffic from the vagina into the uterus and amniotic cavity is not fully understood. A number of animal models, including pregnant mice and nonhuman primates, have been developed to study mechanisms of ascending GBS infection[39,60-66], shedding new light on these complicated processes. While studies using these models have revealed novel insight into the role of virulence factors that contribute to ascending infection, more research is needed to fully understand the process of ascending GBS infection that leads to adverse neonatal outcomes.

The host immune response evoked in the placenta in response to GBS infection is a key determinant of perinatal outcome, microbial invasion of the amniotic cavity and fetal infection. A variety of fetal and maternal cells within the placental membranes are capable of pathogen recognition for initiating and sustaining an inflammatory response; these include chorionic cells, amniotic epithelial cells and those recruited in the context of an infection such as fetal macrophages, decidual macrophages, decidual NK cells, and neutrophils [3,62,66-69]. While a severe infection with microbial invasion of the amniotic cavity is typical for early preterm birth, an inflammatory response in the context of a limited GBS infection confined to the placenta is sufficient to induce preterm labor in some cases[61]. Thus, placental inflammation induced by bacterial infection is likely a critical component of GBS-associated preterm birth. Also, GBS suppression of placental immune responses could contribute to bacterial invasion of the amniotic cavity leading to stillbirths[70]. A better understanding of the mechanisms by which *in utero* GBS infections drive preterm births or stillbirths may lead to development of new interventions to reduce the burden of disease.

1.4 Epidemiology of Group B Streptococcus Vaginal Colonization

Significant effort has been dedicated to measuring the global rates of GBS colonization[71,72] (Figure 1-1), disease[50,73,74], and related risk factors[75,76]. These studies have revealed that global GBS colonization rates during pregnancy are approximately 20%[71], are high in many low-income countries, and parallel high rates of neonatal infection and preterm birth[1]. A variety of risk factors for GBS colonization have been identified, including obesity[75,77] and black ethnicity[78]. Vaginal colonization during pregnancy can be difficult to assess, as the dynamics of colonization during pregnancy are highly variable[79], thus more prospective cohort studies are needed to fully assess the intricacies of vaginal colonization during pregnancy. Additionally,

work has been done to determine the mode of person-to-person transmission of GBS. Some studies have identified sexual transmission of GBS leading to vaginal colonization[80-84], but vertical transmission and fecal-oral transmission may be alternative routes.

While much work has been to estimate regional GBS colonization rates[71], the colonization rate in many individual countries remains unknown. Individual country studies can be highly variable, with inter-study colonization rates differing by up to 20%[71]. This variability may be due to differences between sub-regions of large countries (e.g. India) or the means of diagnosing colonization (culture-based methods versus PCR-based methods versus serology-based methods). Additionally, few studies provide information about GBS serotype prevalence, colonization load, antibiotic resistance profiles, or valuable genetic information, such as virulence gene prevalence. It is clear that a previous GBS colonization is a risk factor for a subsequent pregnancy[76], but few risk factors for initial GBS colonization or resulting ascending infection have been identified. A better understanding of the GBS colonization and ascending infection would greatly improve our ability to reduce the global burden of GBS disease.

1.5 Mechanisms of Group B Streptococcus Vaginal Colonization and Ascending Infection

1.5.1 *Adherence and Invasion Factors*

To maintain long-term colonization, GBS encodes a number of virulence factors that allow it to persist in the harsh vaginal environment and avoid clearance (Table 1-2). Many of these factors are involved in adherence to and invasion of host epithelial cells that ultimately lead to persistent colonization[85]. Cellular adherence and invasion appears to be mediated by GBS interactions with host extracellular matrix components (ECM), and may also promote increased resistance of the pathogen to mechanical clearance, avoidance of immune surveillance, and

enable paracellular transmigration[86]. GBS interactions with host ECM molecules are mediated by a variety of mechanisms and a few are discussed below. The GBS extracellular protein BsaB (bacterial surface adhesin of GBS) has been shown to interact with host laminin and fibronectin, leading to increased adherence to cervicovaginal epithelial cells and biofilm formation[87]. GBS Srr (serine-rich repeat) family of glycoproteins have been shown to bind host fibrinogen through a unique "dock, lock, and latch" mechanism, in which fibrinogen binding leads to an ordered series of conformational changes in Srr1 and Srr2 proteins that results in enhanced adherence[88]. Deletion of the entire Srr1 glycoprotein or only the latch domain of Srr1 leads to diminished vaginal colonization[89,90]. The GBS pilus also mediates bacterial adherence during vaginal colonization via the binding of the PilA adhesin to collagen type 1[89,91]. Finally, the GBS Alpha C protein, which contains a glycosaminoglycan binding domain, is thought to mediate GBS invasion of cervical epithelial cells[92,93], however, the specific glycosaminoglycan that binds Alpha C is not known. GBS invasion has also been suggested to be driven by lipid raft association and phosphoinositide 3-kinase signaling[94]. Once ascended, GBS are able to adhere to and invade both chorionic and amnion epithelial cells[95,96], which is partially mediated by the virulence factors IagA, a glycosyltransferase that helps anchor lipoteichoic acid to the cell surface[97], the CovR/S two component system[96], and quorum sensing through the *rgf* operon[98]. Interestingly, clinical GBS isolates have been shown to be able to interact with ECM molecules[90,99] (Table 1-2), suggesting their importance to human disease. Despite these findings, the interactions between GBS and host ECM components in the setting of human vaginal colonization is yet to be explored. A better understanding of factors that regulate GBS vaginal colonization is essential for the development of preventive therapies. Given that there is no

known benefit for humans to be vaginally colonized by GBS, elimination of colonization during pregnancy may be ideal for the prevention of GBS disease.

1.5.2 *Hemolytic Pigment*

GBS are β-hemolytic and this property is conferred through the hemolytic ornithine rhamnolipid pigment (hereafter referred to as "hemolytic pigment" or "pigment")[96]. The hemolytic pigment was one of the earliest identified GBS virulence factors[100,101], and was long thought to be a proteinaceous in nature[102], until Whidbey and colleagues determined it to be a lipid[96]. Production of the pigment is necessary for full virulence in multiple infectious settings, including systemic infection[103], urinary tract infection[104], vaginal colonization[105], ascending infection[39], perinatal infection[66], and preterm birth[62]. During pregnancy, the hemolytic pigment permeabilizes the membranes of macrophages upon entry into the uterine space, leading to K^+ efflux and activation of the NLRP3 inflammasome, resulting in pyroptosis[66]. High levels of inflammatory cytokines are released in the process of pyroptosis, which induces tissue damage, fetal demise *in utero*[66], and preterm labor[62]. Interestingly, over-expression of pigment biosynthetic genes, which induces a hyper-hemolytic phenotype, leads to inefficient vaginal colonization. This is likely due to clearance due to increased inflammation and immune surveillance[106]; however, the exact mechanism by which the process occurs is unknown.

1.5.3 *Hyaluronidase*

The GBS hyaluronidase, known as HylB, also promotes GBS vaginal persistence[65]. HylB is secreted by GBS into the extracellular milieu and specifically targets and degrades host hyaluronic acid[107,108]. Hyaluronic acid is a extracellular matrix glycosaminoglycan composed of repeating disaccharide units (*N*-acetyl-D-glucosamine-D-glucuronic acid) and is important for

cell migration, cell signaling, regulation of inflammation[109] and for prevention of ascending infection[110,111]. It was recently shown that HylB degrades host hyaluronic acid into its disaccharide moieties[65], which are immunosuppressive as they bind to TLR2/4 and block immune signaling. GBS HylB diminished anti-bacterial responses by blocking TLR2/4 signaling in immune cells[65] and deletion of *hylB* led to increased clearance of GBS from the mouse vagina[65]. The suppression of key inflammatory responses is likely to pay an important role in ascending GBS infection and fetal injury.

1.5.4 *Other Virulence Factors*

Studies have described a role for extracellular membrane vesicles (MVs) in weakening placental (gestational) membranes[112]. GBS were shown to release MVs that contain multiple virulence factors, including: HylB (described above); CAMP factor (Christine, Atkins, Munch-Peterson factor[113]), which is a secreted pore-forming protein[114] that may amplify[115], but is not essential for GBS virulence[116]; IgA binding protein, which has the ability to bind human IgA[117] and has been suggested to play a role in host immune evasion[118]; and multiple enzymes that may play a role in ECM degradation[112]. Intra-amniotic administration of these MVs in pregnant mice caused significant damage to choriodecidual tissues and stimulated leukocytic infiltration and inflammation, leading to weakening of the membranes[112]. The specific role played by each virulence factors in the context of MV weakening of membranes remains unknown. The observation of MV weakening of choriodecidual membranes may represent a novel means by which GBS are able to damage placental/fetal tissues.

1.6 HOST IMMUNITY DURING GBS INFECTION OF REPRODUCTIVE TISSUES

The female reproductive tract is unique immunological environment, as it is the only mucosal site that is dually responsible for the destruction and tolerance of foreign bodies, such as invasive viruses and bacteria, commensal bacteria, sperm, and notably, the developing fetus. In order to successfully undertake this responsibility, a dynamic interplay between the various types of cells and cell products that mediate immunity and their environment is required. Conversely, pathogens such as GBS must circumvent female reproductive immunity, and thus immune cells, in order to successfully establish colonization and infection.

Evasion of the host immune response is essential for successful vaginal colonization. Vaginal immunity is mediated by many physical and cellular components, beginning with the luminal mucus layer, followed by the squamous vaginal epithelia, and finally, immune cells present in vaginal tissue. Little is known about how GBS interacts with the vaginal mucus layer or prevents epithelial immune responses, but recent work has elucidated new information regarding the immune cell response to GBS during vaginal colonization[85,105,106,119]. Cellular immunity in the vaginal tract in response to GBS is largely mediated by neutrophils[85,105,106], and macrophages[105]. The role of NK cells and dendritic cells in GBS colonization remains unexplored. Multiple soluble inflammatory cytokines and chemokines have been identified as important for reduction of colonization in animal models of GBS vaginal colonization, including IL-1β, IL-6, IL-8, IL-17, IL-23, and histamine[85,105,106]. Currently, the mucosal T cell response to GBS colonization is ill-defined. IL-17 and IL-17+ cells were indicated to play an important role in clearance of persistent colonization by a hyper-adherent and invasive strain of GBS[85], suggesting that the T_h17 differentiation pathway is important for controlling persistent GBS colonization. Similarly, another study found cytokines involved in T_{h1}, T_{h2}, and T_{h17}

differentiation pathways as important for reduction of colonization[105]; however, T cells were not directly identified as being important for the response to GBS in either study.

The progression of labor relies on inflammation derived from immune cells[120,121]. During labor, women have high levels of circulating neutrophils[122] and high levels of NK cells, macrophages, mast cells, regulatory T cells, and CD4+CD25- T cells are present in the decidua[123,124]. Inflammatory activation of these cell types leads to the progression of labor at term[120,121]. If the activation or invasion of these cells into gestational tissues occurs at an inappropriate time during parturition, labor can be induced prematurely[125]. GBS invasion of the uterus leads to a variety of adverse outcomes, including tissue damage, inflammation, lung and brain injury, pneumonia, meningitis, sepsis, and fetal death. GBS can invade multiple fetal organs, including the blood, liver, spleen, gastrovascular cavity, and lung. Fetal tissue damage has been observed in the presence and absence of bacterial invasion, likely due to inflammation in gestational tissues. GBS invasion of fetal tissues induces inflammation and fetal death[39,59,60,66], and in the case of the hemolytic pigment, this involved induction of the NLRP3 inflammasome[66], potentially accompanied by the recognition of bacterial RNA[126]. Indeed the activation of the NRLP3 inflammasome by the hemolytic pigment induced significant inflammation and tissues damage, leading to fetal injury and demise in a mouse model of ascending infection[66]. GBS has been shown to induce secretion of multiple cytokines and defensins from gestational membranes *ex vivo*, including TNF-α, IL-1α, IL-1β, IL-6, and IL-8[68,96,127-129]. Inflammation is stimulated either through pattern-recognition receptor (PRR) recognition of GBS antigens[68,127] or by pigment-mediated cell cytoxicity and activation of NF-κB[96]. GBS are also able to bind Siglecs through their sialic acid capsule or β-protein to prevent placental membrane inflammation[70], potentially leading to increased rates of GBS-associated preterm birth.

1.7 DISSERTATION SUMMARY

Understanding the complex interactions between GBS and the host during colonization and ascending infection is critical for the development therapeutic strategies to prevent perinatal infection. While much attention has been given to understanding GBS pathogenesis in *in vitro* settings and in the context of systemic infection, little research has focused on understanding GBS pathogenesis in settings that closely replicate human disease. The work presented in this dissertation attempts to address this issue by trying to understand how GBS interacts with host from initial colonization through ascending infection, and finally, during preterm birth. Chapter 2 defines the role of the GBS hemolytic pigment in vaginal colonization and placental infection. Chapter 3 explains a novel mechanism that GBS utilize to ascend from the vagina into the uterine space. Chapter 4 outlines the role of the GBS hyaluronidase in immune evasion during ascending infection and preterm birth. Finally, a summary of my findings, conclusions, and thoughts on future directions for research regarding GBS colonization, ascending infection, and perinatal infection is provided in Chapter 5.

1.8 FIGURE AND TABLES

Table 1-1 - Bacteria that cause ascending infection

Gram's Stain	Phylum	Species	Identification	Reference
Positive	Actinobacteria	*Gardnerella vaginalis*	Identified in amniotic fluid by culture or PCR, shown experimentally	130
	Firmicutes	*Mycoplasma hominis*	Identified in amniotic fluid by culture or PCR	131,132
		Peptostreptococcus spp.	Identified in amniotic fluid by culture or PCR	133
		Streptococcus agalactiae	Identified in amniotic fluid by culture or PCR, shown experimentally	36,39,60,132
		Streptococcus anginosus	Identified in amniotic fluid by culture or PCR	132
		Streptococcus dysgalactiae	Identified in amniotic fluid by culture or PCR	134
		Streptococcus anginosus	Identified in amniotic fluid by culture or PCR	132
		Ureaplasma parvum	Identified in amniotic fluid by culture or PCR	132
		Ureaplasma urealyticum	Identified in amniotic fluid by culture or PCR	38,131,135,136
Negative	Chlamydiae	*Chlamydia trachomatis*	Identified in amniotic fluid by culture or PCR, shown experimentally	137-139
	Fusobacteria	*Fusobacterium nucleatum*	Identified in amniotic fluid by culture or PCR, shown experimentally	140,141
		Leptotrichia spp.	Identified in amniotic fluid by culture or PCR	15,141
		Sneathia sanguinegens	Identified in amniotic fluid by culture or PCR	14
	Proteobacteria	*Escherichia coli*	Clinically identified in amniotic fluid, shown experimentally	36,38,111,142

Table 1-2 - GBS factors involved in vaginal colonization

Virulence Factor	Host Target	Function	Model	Reference
HylB	Hyaluronic Acid	Blocks TLR2/4 signaling for vaginal persistence	Mouse Vaginal Colonization	65
BsaB	Fibronectin and laminin	Adherence to vaginal epithelial cells	Immortalized human cell line	87
Hemolytic Pigment	PMNs	Provides resistance to PMN response	Mouse Vaginal Colonization, Primary human cells	105
Srr1/2	Fibrinogen	Adherence to vaginal epithelial cells, cervical epithelial cells	Mouse Vaginal Colonization, Immortalized human cell line	89,90
Pili	Collagen I[91]	Adherence to vaginal epithelial cells	Mouse Vaginal Colonization, Immortalized human cell line	89
Capsule	Unknown	Adherence to and invasion of cervical epithelial cells	Immortalized human cell line	86
Alpha C Protein	Host cell surface glycosaminoglycan[93]	Invasion of cervical epithelial cells	Immortalized human cell line	92
Two Component System	**External Signal**	**Function**	**Model**	**Reference**
CovRS	pH[143]	Represses inappropriate expression of the hemolytic pigment to avoid immune detection, adherence to vaginal epithelial cells and cervical epithelial cells	Mouse Vaginal Colonization, Immortalized human cell line	106,119,144
FspSR	fructose 6-phosphate	Vaginal persistence	Mouse Vaginal Colonization	145

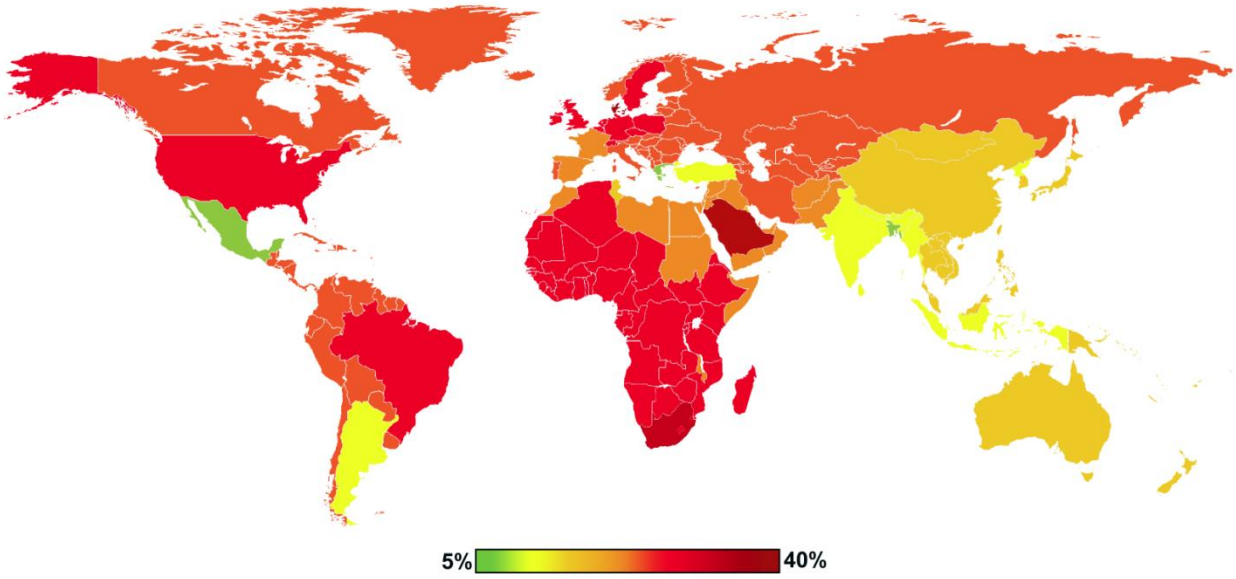

Figure 1-1 – Estimates of global GBS colonization prevalence

Heat map showing percent of the women that test positive for GBS during pregnancy. Country-level colonization prevalence data is displayed where data were available, or is displayed by WHO regional groupings. Significant portions of these data are generated in countries where universal screening for GBS does not occur, thus some country estimates may be over- or under-reported. Data are adapted from Kwata and colleagues, 2016[71].

Chapter 2. Role of hemolytic pigment toxin in GBS vaginal colonization and ascending infection

The figures, figure legends, and materials and methods in this chapter have been adapted from the following articles:

Claire Gendrin, **Jay Vornhagen**, Lisa Ngo, Christopher Whidbey, Erica Boldenow, Veronica Santana-Ufret, Morgan Clauson, Kellie Burnside, Dionne P. Galloway, Kristina Adams Waldorf, Adrian M. Piliponsky, and Lakshmi Rajagopal. (2015) Mast cell degranulation by a hemolytic lipid toxin decreases GBS colonization and infection. **Science Advances**, vol. 1, no. 6, e1400225.

Erica Boldenow, Claire Gendrin†, Lisa Ngo†, Craig Bierle†, **Jay Vornhagen†**, Michelle Coleman, Sean Merillat, Blair Armistead, Christopher Whidbey, Varchita Alishetti, Veronica Santana-Ufret, Jason Ogle, Michael Gough, Sengkeo Srinouanprachanh, James W. MacDonald, Theo K. Bammler, Aasthaa Bansal, H. Denny Liggitt, Lakshmi Rajagopal, and Kristina M. Adams Waldorf. (2016) Group B Streptococcus circumvents neutrophils and neutrophil extracellular traps during amniotic cavity invasion and preterm labor. **Science Immunology**, vol. 1, no. 4, DOI: 10.1126/sciimmunol.aah4576. †Equal contribution.

Jay Vornhagen, Kristina Adams Waldorf, and Lakshmi Rajagopal. (2017) Perinatal Group B Streptococcal infections: virulence factors, immunity and prevention strategies. Trends in Microbiology, accepted.

Figure numbers have been updated to conform to the dissertation. Adapted text remains as published with minor editorial changes.

2.1 INTRODUCTION

More than 30% of neonatal deaths are a result of preterm birth[3]. A significant cause of preterm birth is *in utero* infection by vaginal microorganisms. One microorganism frequently associated with *in utero* infection and preterm birth is Group B Streptococcus (GBS), or *Streptococcus agalactiae*. GBS are β-hemolytic, gram-positive bacteria that commonly colonize the vagina in healthy adult women; however, the factors necessary for GBS colonization of the vagina remain ill defined.

Expression of the GBS hemolysin affects vaginal colonization and infection. Hemolytic activity of GBS is due to the ornithine rhamnolipid pigment expressed by genes in the *cyl* operon[102]. Deletion of the *cylE* gene, which encodes an N-acyl transferase necessary for pigment production[96], renders GBS non-pigmented and non-hemolytic[96,102]. Absence of the hemolytic pigment reduces the ability of GBS to successfully colonize the vagina, likely due to an increased susceptibility to neutrophilic clearance[39,105]. It has been suggested that the GBS pigment is able to sequester reactive oxygen species, and GBS lacking the hemolytic pigment exhibit decreased survival in macrophages[103], and likely also in neutrophils. Expression of the hemolytic pigment is negatively regulated at the transcriptional level by the CovR/CovS two-component system[96,146], therefore, genetic ablation of *covR/S* renders GBS hyper-pigmented and hyper-hemolytic. Interestingly, deletion of *covR/S* results in ineffective vaginal colonization[106]; however, the interaction between the hemolytic pigment and the host vaginal response and how that leads to a reduction in colonization is unknown.

Additionally, the hemolytic pigment plays an important role in ascending GBS infection. Randis and colleagues observed decreased bacterial load in the placentas of pregnant mice vaginally inoculated with non-hemolytic GBS (GBS lacking *cylE*) when compared to isogenic

hemolytic GBS WT[39], suggesting a role for the GBS pigment in bacterial ascension to the uterus. This decrease in bacterial ascension results in decreased damage to fetal tissues and reduced rates of preterm birth[39]. These results support the idea that production of the hemolytic pigment must be tightly regulated for ascension to occur, but how expression of the hemolytic pigment enables GBS to bypass host defenses for ascension during pregnancy are not well understood.

In this chapter, we show that, in clinical settings, hyper-hemolytic GBS strains are rarely isolated from the vagina. Using a mouse model of vaginal colonization, we show that expression of the hemolytic pigment is important for successful colonization, but overexpression greatly diminishes colonization. Furthermore, we show that hyper-hemolytic GBS are able to activate and degranulate mast cells, leading to clearance from the vagina. Finally, we demonstrate how expression of the GBS hemolytic pigment enables GBS to surpass neutrophil extracellular traps during infection of gestational tissues. Together, these data define the role of the hemolytic pigment toxin in GBS vaginal colonization and ascending infection.

2.2 RESULTS

2.2.1 *Hyper-Hemolytic and Hyper-Pigmented Strains are Rarely Isolated from the Vagina*

It is known that non-pigmented GBS strains are also non-hemolytic[147], and it was thought that the source of the hemolytic activity was due to a protein encoded by the *cylE* gene and was independent of pigmentation[102]. Only recently was it discovered that the pigment is responsible for the hemolytic activity[96]. It has been shown described that hyper-pigmented GBS, some of which were associated with mutations in a two component repressor of the hemolytic pigment known as CovR/CovS (comprising the sensor kinase CovS and the DNA binding response regulator CovR), were present in the amniotic fluid and placental membranes of women in preterm labor[96] and can induce fetal injury[66]. To determine if hyper-hemolytic GBS exist as

colonizers in the lower genital tract of adult women, we analyzed GBS isolates obtained from rectovaginal swabs of 53 women in their third trimester of pregnancy. GBS strains were examined for their hemolytic properties and pigmentation on blood agar and tryptic soy agar, respectively. As controls, the wild type GBS strain COH1 and isogenic GBSΔ*covR* which exhibits increased hemolysis/pigmentation were used; these controls were chosen as they were used in our previous work[96] to compare hyper-hemolysis/pigmentation from GBS obtained from women in preterm labor. Quantitative titers were estimated using a modified hemolysis assay (see Materials and Methods). We observed that 2 of the 53 isolates showed increased hemolysis/pigmentation similar to GBSΔ*covR* (Table 2-1). In comparison, we previously obtained eight GBS isolates obtained from six women in preterm labor and subsequently noted that these were hyper-hemolytic[96]. Although our collection of GBS clinical isolates is not exhaustive, the frequency of hyper-hemolysis that we observed between the preterm (6 of 6 isolates[96]) and rectovaginal GBS isolates (2 of 53 isolates) is significantly different ($p = 0.001$, Fisher's exact test). These observations suggest that host immune mechanisms may diminish colonization of hyper-hemolytic/hyper-pigmented GBS strains from the vaginal microenvironment. Interestingly, the 2 hyper-hemolytic, rectovaginal isolates resembled the GBSΔ*covR* (Figure 2-1, top panel); however, DNA sequencing of the *covR/S* locus did not reveal the presence of any mutations, similar to the previously described natively hyper-pigmented strain NCTC10/84[102,148,149]. These results suggest that the presence of other regulators may influence the expression of the *covR/S* regulon in certain GBS strains. Nevertheless, these observations led us to hypothesize that an effective host immune response may diminish colonization of hyper-hemolytic/hyper-pigmented GBS strains from the human vaginal microenvironment.

2.2.2 *The Role of the Hemolytic Pigment in Murine Model of GBS Vaginal Colonization*

Mouse models have indicated an important role for the GBS hemolytic pigment during vaginal colonization. Studies have shown that hyper-pigmented GBS are less able to effectively colonize the vagina[106]. Conversely, non-hemolytic GBS strains due also exhibited diminished vaginal colonization, though this effect is more subtle than that of hyper-pigmented strains[39,105]. Given that GBS strains express different levels of hemolysin, we aimed to determine how differences in hemolytic pigment expression affect vaginal colonization. To this end, we used three different wild-type GBS strains: the weakly-hemolytic strain COH1[119], the mildly-hemolytic strain A909, and the naturally occurring hyper-hemolytic strain NCTC10/84 (Figure 2-1, bottom panel). In all cases, isogenic *cylE* mutants were used as controls for examining the role of hemolysin. To examine their vaginal colonization, we modified a version of the murine model of GBS vaginal colonization originally developed by Sheen and colleagues[89]. In this model, mice are synchronized for estrus 1 day prior to vaginal inoculation by intraperitoneal administration of 50μg of β17-estradiol. The vaginal lumen is then inoculated with 10^7 colony forming units (CFU) of GBS, and mice are inverted for 5 minutes to allow retention of the inoculum in the vaginal cavity and to prevent genital grooming. GBS colonization is tested by vaginal swab or lavage every 24-48 hours, and lavage samples can be used to measure cytokine or hormone concentrations. Unfortunately, vaginal sampling in this model is limited since lavage samples only capture bacteria and analytes in vaginal secretions or that are loosely associated with the vaginal epithelium. Bacteria that have disseminated into the deeper tissue and tissue-associated analytes are not captured. Additionally, the physical disruption caused by vaginal lavage or swab may have effects on the host immune response and the vaginal microbiome. In

order to avoid any uncontrolled effects present in the above model, we modified the murine model of GBS vaginal colonization as indicated. Instead of using vaginal lavage or vaginal swabs to test for colonization, mice are left undisturbed until the termination of the experiment. Upon termination of the experiment, mice are euthanized, a midline laparotomy is performed, and whole reproductive tissues are collected for analysis.

To test how differences in hemolytic pigment expression affects vaginal colonization., 10^8 CFU of GBS were vaginally inoculated into eight to sixteen week old female non-pregnant C57BL/6J mice. 96 hours post-inoculation, mice were euthanized and vaginal GBS burden was measured by serial dilution and plating. The results shown in (Figure 2-2a,b) indicate that deletion of *cylE* in GBS strains that were weakly- and mildly-hemolytic (COH1 and A909, respectively) diminished vaginal colonization, likely due to an increased susceptibility of these non-hemolytic GBS strains to the host immune response[103,105]. Conversely, for the naturally occurring hyper-hemolytic GBS strain NCTC10/84, deletion of *cylE* gene lead to more effective vaginal colonization (Figure 2-2c), likely due to decrease pigment-induced immune activation. Finally, a hyper-hemolytic strain of GBS derived from the weakly-hemolytic strain (COH1), through deletion of *covR*, significantly decreased vaginal colonization efficiency (Figure 2-2d). Together, these results suggest that a delicate balance of hemolytic pigment expression is required for effective vaginal colonization, as too much or too little hemolysin results in decreased vaginal colonization.

2.2.3 *Mast Cells are Important for Clearance of Hyper-Pigmented GBS from the Vagina*

We next sought to determine the host response that controls clearance of hyper-pigmented GBS from the vagina. One type of immune cell resident in the vagina and can potentially mediates the initial response to hyper-pigmented GBS are mast cells. Mast cells are

pro-inflammatory, tissue-resident immune cells that are present in the vaginal mucosa[123]. When activated by bacteria, mast cells release pre-formed pro-inflammatory granules containing a variety of cytokines, chemokines, proteases, anti-microbial peptides, and histamine[150]. Mast cell activation has been shown to be protective against many bacterial infections, including two close relatives of GBS, *Streptococcus pyogenes*[151] and *Staphylococcus aureus*[152]. To determine if the hemolytic pigment induces mast cell degranulation, we used bone marrow mast cells as model system as they represent mucosal and connective tissue mast cells found *in vivo* [153]. Scanning electron microscopy was performed on mast cells that were exposed to the GBS pigment. As controls, mast cells were either exposed to an equivalent amount of Δ*cylE* extract (GBS pigment isolation performed from the non-pigmented GBSΔ*cylE* strain), or treated with the Ca^{2+} ionophore A23187 that induces mast cell degranulaiton. Mast cells treated with GBS pigment exhibit morphological changes indicative of degranulation similar to mast cells treated with the Ca^{2+} ionophore A23187 but not with mast cells exposed only to media or the Δ*cylE* extract (Figure 2-3). These data confirm that the GBS pigment triggers mast cell degranulation.

To assess the role of mast cells during vaginal colonization with hyper-hemolytic GBS, twelve-to-sixteen week old female mast cell deficient mice (*Cpa3-Cre;Mcl-1*$^{fl/fl}$) and littermate control mast cell proficient mice (*Cpa3-Cre;Mcl-1*$^{fl/fl+}$) were vaginally inoculated with approximately 10^8 CFU of GBSΔ*covR* or the isogenic control strain GBSΔ*covR*Δ*cylE*. Remarkably, hyper-hemolytic GBSΔ*covR* was cleared from the vagina of mast-cell proficient mice, whereas it persisted in mast-cell deficient mice (Figure 2-4a). In contrast, non-hemolytic GBSΔ*covR*Δ*cylE* persisted in the vagina both mast cell proficient and deficient mice (Figure 2-4a). Moreover, vaginal persistence correlated with both vaginal and uterine bacterial burden (Figure 2-4b,c). Finally, increased histamine levels, a measure of mast cell activation and

degranulation, were observed in mast cell proficient mice inoculated with the hyper-hemolytic GBSΔ*covR* strain, whereas this was not observed in mast cell deficient mice or mast cell proficient mice inoculated with the non-hemolytic GBSΔ*covR*Δ*cylE* strain (Figure 2-4d). Together, these data indicate that mast cells are activated *in vivo* by hyper-hemolytic GBS, leading to their clearance from the vagina.

To corroborate these data, histological sections were analyzed for mast cell degranulation by toluidine blue staining. Mast cell proficient mice inoculated with the hyper-hemolytic GBSΔ*covR* strain displayed higher levels of mast cell degranulation than that of mast cell proficient mice inoculated with the non-hemolytic GBSΔ*covR*Δ*cylE* strain or control saline (Figure 2-5a, i-iii). Mast cells were not observed in mast cell deficient mice (Figure 2-5a, iv-vi). Moreover, histological findings indicated higher levels of edema an inflammation in tissues of mast cell proficient mice inoculated with GBSΔ*covR* (Figure 2-5b, ii), whereas inflammation and edema was not observed in mast cell proficient mice inoculated with the GBSΔ*covR*Δ*cylE* or control saline (Figure 2-4b, i, iii), or in mast cell deficient mice (Figure 2-5b, iv-vi). These findings were replicated in mice inoculated with the endogenously hyper-hemolytic WT NCTC10/84 strain and control NCTC10/84Δ*cylE* strain (Figure 2-6). These results show that hyper-pigmented, and thus hyper-hemolytic, strains of GBS do not persist in the vagina due to the inflammatory action of mast cells, and potentially other immune cells that migrate to sites of mast cell degranulation.

2.2.4 *The GBS Hemolytic Pigment is Critical for Survival of Neutrophil Extracellular Traps in Placental Tissues*

When hyper-pigmented strains of GBS successfully colonize the vagina, they have potential to ascend from the vagina into the uterus during pregnancy. Indeed, mouse models of

ascending infection have suggested that pigment production is integral to ascending GBS infection and resulting preterm birth[39]. In addition to causing inflammation, the hemolytic pigment permits GBS penetration of intact human chorioamnion, induces loss of barrier function in human amnion epithelial cells[96]. Studies in pregnant non-human primates confirmed the role of the GBS pigment in penetration of placental membranes and dissemination into the amniotic cavity, leading to increased inflammation, acceleration of uterine contractions or preterm labor, and neutrophilic infiltration[62]; however, the means by which GBS evades the host immune response during infection of placental tissues is unknown.

Given that neutrophilic infiltration has been observed in placental tissues in response to GBS, and neutrophils are critical for anti-bacterial responses during infection, we aimed to determine how GBS evades this response. Neutrophils are able to eradicate invading bacteria through the formation of neutrophil extracellular traps (NETs)[154]. The formation of NETs in response to GBS infection was observed in murine models of colonization[105] and ascending infection[64], but it is unknown if NET formation occurs in response to pigment. To determine if NETs are formed in response to pigment, we performed scanning electron microscopy to determine if GBS pigment or hyper-pigmented GBS induce morphological changes to neutrophils. To this end, neutrophils in NET assay buffer were treated with either GBS pigment (5 μM), equivalent amount of control (Δ*cylE* extract) or with the GBS (hyper-hemolytic Δ*covR*, or non-hemolytic Δ*covR*Δ*cylE*) at an MOI of ~ 10 for 4 hours at 37°C. Phorbol myristate acetate (PMA, 20 nM) was included as a positive control. SEM was then performed and the results shown in Figure 2-7. The top panel in Figure 2-7 shows that the hemolytic GBS pigment induced the formation of NETs similar to PMA, whereas the control Δ*cylE* extract did not induce significant NET formation. Similarly, the hyperhemolytic GBSΔ*covR* strain robustly induced

NET formation whereas the Δ*covR*Δ*cylE* strain showed slightly attenuated NET formation (Figure 2-7, lower panel). Collectively, these data indicate that the hemolytic pigment of GBS stimulates NET formation.

To determine if NETs are formed in placental tissues in response to hyper-hemolytic GBS, chronically catheterized pregnant non-human primates (NHPs) where inoculated in the choriodecidiual space with hyper-hemolytic GBSΔ*covR*, non-hemolytic GBSΔ*covR*Δ*cylE*, or control saline (see Materials and Methods for details)[61]. Following cesarean section, gestational tissues were excised, and NET formation was assessed by immunostaining. Interestingly, NHPs inoculated with GBSΔ*covR* displayed substantially more extracellular DNA and neutrophil elastase, both indicators of NET formation[155,156], than NHPs inoculated with GBSΔ*covR*Δ*cylE* or control saline (Figure 2-8). Quantification of these images using ImageJ revealed significantly more NETs in GBSΔ*covR* inoculated tissues than GBSΔ*covR*Δ*cylE* or control saline inoculated tissues (Figure 2-9). These data indicate that indeed, NETs are formed in gestational tissues in a pigment-dependent manner.

We then examined the ability of the GBS strains to resist killing by NETs. To this end, neutrophils were induced to produce NETs and the ability of the GBS strains (WT GBS, hyper-hemolytic GBSΔ*covR*, and non-hemolytic GBSΔ*covR*Δ*cylE*,) to resist killing by NETs was evaluated. As sialic acid deficiency on the GBS polysaccharide capsule was previously described to increase sensitivity to NET killing[157], we included the sialic acid deficient GBSΔ*cpsK* strain[158] as a control in the NET killing assay. The hyper-hemolytic GBSΔ*covR* strain was resistant to killing by NETs unlike the non-hemolytic GBSΔ*covR*Δ*cylE* strain or the control capsule deficient GBSΔ*cpsK* strain (Figure 2-10). Our observations suggest that the increased virulence of the hyper-hemolytic GBSΔ*covR* strain is primarily due to its ability to induce neutrophil cell

death and may be augmented by resistance to NETs. Together, these data indicate a critical role for the pigment in GBS dissemination upon entry into placental tissues following ascending infection.

2.3 DISCUSSION

Understanding the mechanisms by which GBS are able to colonize the vagina is vital for the reduction of neonatal and perinatal GBS disease. The work presented in this chapter refines our knowledge of the role the hemolytic pigment during colonization, ascending infection, and infection of placental tissues, leading to preterm birth. Furthermore, this work provides insight into the biology of the organism by examining the delicate balance of expression of a single virulence factor and the drastic consequences of genetic dysregulation.

The fine-tuned regulation of pigment expression by the CovR/S two-component system (TCS) is crucial for successful vaginal colonization and invasion of the amniotic cavity, wherein low levels of pigment expression permit vaginal colonization (Figure 2-2, Table 2-1), whereas high levels of pigment expression are necessary for penetration of gestational tissues (Figures 2-8 through 2-10), and stimulation of preterm birth. In addition to colonization and ascending infection, studies have demonstrated a role for the hemolytic pigment in fetal damage[39,66], sepsis[103], prosthetic joint infection[159], septic arthritis[159], conjunctivitis[159], tonsillopharnyngitis[66,159], necrotizing fasciitis[159], and urinary tract infection[159,160]. While the function of the pigment has not been identified in the pathogenesis of all of these diseases, it is clear that it vital for the survival of GBS in the human host. The tight control of pigment expression is critical for successful vaginal colonization, and as such, makes the GBS pigment an intriguing target for vaccine development.

While these studies have advanced our knowledge of GBS virulence in the context of vaginal colonization, significant work is still needed to fully understand the role of the CovR/S TCS during vaginal colonization. The CovR regulon includes over 150 genes[106], and the role of most of these genes in vaginal colonization has yet to be explored. Interestingly, the CovR/S TCS is responsive to pH[143,144], and studies have determined pH to be an important factor for GBS colonization[144]. Some studies have shown GBS to have enhanced adhesive properties[161] and biofilm formation[162,163] in highly acidic conditions, whereas other studies have found the opposite to be true[144,164]. Despite these inconsistencies, the interplay between pH and CovR/S likely plays a role in colonization given the acidic environment of the vagina. This may explain why women of African descent, who generally have a high vaginal pH and non-lactobacilli dominated vaginal microbiome[165] have higher GBS colonization rates[71,166,167] and are more predisposed to preterm birth and neonatal GBS disease[19,52,168]. The relationships between vaginal microflora, increased GBS colonization, and increased adverse pregnancy outcomes have been described in obese women[75,169,170]. Further studies are needed to delineate the complex interplay between human physiology, the microbiome, and GBS virulence.

The role of mast cells in the response to pathogenic bacteria in vagina is a novel aspect of the work presented in this chapter. The response of neutrophils and macrophages to GBS has been well studied[66,103,126,171-173], but little is known about how other types of immune cells respond to GBS, and even less is known about the role of the hemolytic pigment. The vaginal mucosa contains higher numbers of natural killer cells and T cells than macrophages and granulocytes[123], yet the effects of pigment on these cells remains unexplored. Moreover, the interaction between more minor, yet vital, subsets of vaginal immune cells, such as dendritic cells, regulatory T cells, or mucosal-associated invariant T cells, is unknown. Given the

importance of the hemolytic pigment to almost every aspect of GBS pathogenesis studied to this point, studies focused on the various interactions between immune cells and the hemolytic pigment will reveal crucial information about the mechanisms of GBS colonization, and potentially inform strategies of preventing or treating vaginal colonization.

Additionally, the work presented in this chapter refine our understanding of the response of neutrophils to GBS, namely, NET formation. Typically NET formation is associated with the ability of neutrophils to ensnare bacteria for further antimicrobial action. However, we observed that GBS strains that overexpress the hemolytic pigment were resistant to killing by NETs when compared to the non-hemolytic strain. This may in part be due to the ability of the unsaturated polyene chain in the hemolytic pigment toxin to quench reactive oxygen species (ROS). Previous work by Liu *et. al.*[103] demonstrated the antioxidant nature of the GBS pigment. They observed that hyper-pigmented GBS strains are more resistant to ROS such as hydrogen peroxide, superoxide and singlet oxygen *in vitro* and in macrophages[103]. Although expression of an extracellular nuclease (nuclease A) in GBS was shown to degrade NETs[174], previous work by others and us showed that expression of nuclease A is not under CovR/S regulation in GBS[146,175]. This suggests that differences in resistance to NET killing between GBSΔ*covR* and GBSΔ*covR*Δ*cylE* is likely not due to altered endogenous DNAse activity. Our observations suggests that increased expression of the hemolytic toxin enables GBS to induce neutrophil cell death and likely resist killing by NETs, which may promote microbial invasion of the amniotic cavity during ascending infection. It is also noteworthy that a few reports have indicated that NETs may only entrap bacteria to prevent dissemination and wall off infection, without actually inducing bacterial cell death[176,177]. Addition of DNase at the end of the NET killing assay is thought to relieve the clumping effect and provide accurate results for discrimination between

ensnaring of bacteria by NETs versus bacterial killing by NETs[176], While we repeated these experiments with addition of DNase at the end of the experiment to confirm increased sensitivity of the GBSΔ*covR*Δ*cylE* to NETS, it remains plausible that GBS entrapment by NETs rather than NET associated killing regulates microbial invasion of the amniotic cavity *in vivo*.

In this chapter, data are presented that further define the role of the hemolytic pigment in GBS colonization and ascending infection. While these studies are not exhaustive, they provide novel insight into the host-pathogen interaction during GBS vaginal colonization. These data show that the hemolytic pigment is necessary for effective colonization, but hyper-pigmented GBS are also not able to colonize the vagina, likely as a result of induction of inflammation through mast cell degranulation. Furthermore, pigment aids in survival of the host immune response during infection of placental tissues through resistance to NET killing. Future work should aim to develop better diagnostic tools to determine if a woman is colonized with a hyper-pigmented strain of GBS during pregnancy, and to identify therapies and interventions to prevent colonization with hyper-pigmented GBS.

2.4 MATERIALS AND METHODS

2.4.1 *Ethics Statement*

All mouse experiments were approved by the Seattle Children's Research Institutional Animal Care and Use Committee (protocol #13907) and performed in strict accordance with the recommendations in the Guide for the Care and Use of Laboratory Animals (8th Edition).

All non-human primate experiments were carried out in strict accordance with the recommendations in the Guide for the Care and Use of Laboratory Animals of the National Research Council and the Weatherall report, "The use of non-human primates in research". The

protocol was approved by the University of Washington Institutional Animal Care Use Committee (Permit Number: 4165-01). All surgery was performed under general anesthesia and all efforts were made to minimize pain and distress.

2.4.2 *Bacterial Strains*

The wild type (WT) GBS strains A909 and COH1 used in this study are clinical isolates obtained from infected human newborns[178,179]. The Δ*cylE*, Δ*covR*, and Δ*covR*Δ*cylE* mutants were previously derived from A909, COH1[96,180,181]. The previously described natively occurring hyper-pigmented GBS strain NCTC10/84[149] and its non-pigmented NCTC10/84Δ*cylE* control[102] were also used in this study. The clinical isolate RM003 was isolated at the University of Washington[182]. GBS were grown in Tryptic Soy Broth (Difco Laboratories) at 30° or 37°C in 5% CO_2. Cell growth was monitored at 600 nm.

2.4.3 *Human Subjects*

GBS clinical isolates from rectovaginal swabs were obtained from women in their third trimester of pregnancy at the University of Washington Medical Center and Harborview Medical Center in 2007 under University of Washington IRB# 30308; samples were collected without any identifiers or clinical information and a waiver for written informed consent was obtained for testing anonymous samples. Written informed patient consent for donation of human blood was obtained with approval from the Seattle Children's Research Institute Institutional Review Board (protocol #11117).

2.4.4 *Hemolytic Titer Estimation of GBS Strains*

To measure hemolytic activity from the various GBS isolates, hemolytic titer assays were performed as described previously[183] with a few modifications. Briefly, TSB containing 1% glucose and 3% tween-20 was inoculated with the GBS isolates and grown overnight at 30°C in a 96 well plate. Bacteria were pelleted and the supernatants were transferred to a new plate. Two-fold serial dilutions were performed in PBS, and a 1% suspension of human red blood cells (RBC) was added at a ratio of 1:1. Cells were incubated for one hour at 37°C. Unlysed RBCs were pelleted by centrifugation, and hemoglobin release in the supernatant was measured as absorbance at 420nm using a plate reader (BioTek). Absorbance's were normalized to control wells containing either PBS (0% lysis) or 0.1% SDS (100% lysis), and the reciprocal of the highest dilution giving at least 50% lysis was considered to be the hemolytic titer.

2.4.5 *Mouse Model of Vaginal Colonization*

Eight-to-sixteen week old female, non-pregnant C57BL/6J (The Jackson Laboratories), mast cell deficient (*Cpa3-Cre;Mcl-1*$^{fl/fl184}$), and mast cell proficient (*Cpa3-Cre;Mcl-1*$^{fl/+}$) littermate control mice were used to define the role of mast cells in GBS vaginal colonization. Briefly, female mice were synchronized for estrous by cohabiting in the same cage for >10 days if not from birth, or by intraperitoneal administration of 50 µg 17β-estradiol suspended in sterile corn oil. 17β-estradiol was not administered in mast cell studies, as this agent has been described to activate mast cells[185]. Mice were anesthetized using 3-4% isoflurane and GBS (approximately 10^8 CFU in 10µl sterile PBS) was inoculated into the lower genital. Mice were left inverted for an additional 5 min under anesthesia. Subsequently, the mice were returned to their cages and monitored until ambulatory. At 4 days post infection, mice were euthanized and the lower genital

tract and uterine horns were excised and analyzed for CFU and mast cell activation. Briefly, tissues were homogenized and GBS CFU were enumerated by serial dilution and plating on both nonselective and selective media (TSA, TSA containing 50 μg/ml spectinomycin). Of note, Δ*covR* and Δ*covR*Δ*cylE* strains of GBS are spectinomycin resistant as *covR* was replaced with a gene conferring spectinomycin resistance in these strains[181,186]. All plates were incubated for 24 hrs at 37°C and the nonselective TSA plates were then left on the bench for an additional 24-48 hrs to distinguish GBS from other commensal bacteria. As further confirmation, ~100 GBS colonies from each experiment were patched on selective media *i.e.* TSA containing spectinomycin and the level of CAMP factor activity was tested on sheep blood agar plates with the inoculum strain included in parallel. CHROMagar^{TM}StrepB (DRG International, Inc.) was also used to distinguish GBS from commensal organisms. Supernatants of tissue homogenates were analyzed for histamine using the ALPCO histamine ELISA assay as described above. For histology, the lower genital tract and uterine horns were excised from mast cell proficient and deficient mice at 4 days post infection. Tissues were fixed in 10% phosphate buffered formalin at 4°C overnight and stored in 70% ethanol. The tissues were subsequently embedded in paraffin, sectioned, and stained with hematoxylin and eosin (H & E) or toluidine blue. All tissues were mounted and stained by the Histology and Imaging Core located at the University of Washington (Seattle, WA) and were scored by a pathologist blinded to group assignment. Images were captured in bright field using a DM4000B Fluorescent upright microscope (Leica) under 20X and 40X magnifications. The microscope was attached to a DFC310FX camera (Leica) and the acquisition software used was the Leica application suite (version 4.0.0). The experiment was repeated using natively hyper-pigmented WT GBS NCTC10/84 and isogenic non-pigmented NCTC10/84Δ*cylE* using WT C57BL6/J mice (*n=8/group*).

2.4.6 *Purification of the GBS Hemolytic Pigment*

The GBS hemolytic pigment was purified as previously described[96]. Briefly, pigment was extracted from WT GBS A909 using DMSO:0.1% TFA, precipitated using NH_4OH and column purified using a Sephadex LH-20 (GE Healthcare) column as described[96]. Fractions containing purified pigment were pooled, precipitated with NH_4OH, washed three times with HPLC grade water, twice with DMSO and lyophilized as described[96]. The pigment extraction procedure was also performed in parallel on the non-pigmented strain GBSΔ*cylE* and this extract was used as a control for pigment in all experiments, along with buffer DTS (DMSO+0.1% TFA+20% starch), which was used to resuspend pigment and control Δ*cylE* extract. Three independent pigment preparations were used in this study and all preparations were confirmed to be hemolytic as described previously[96]. Mass Spectrometry and NMR were used to confirm the presence of pigment exclusively in the pigment samples and not in the control Δ*cylE* extract as shown previously[96].

2.4.7 *Generation of Bone Marrow-Derived Mast Cells (BMCMCs)*

BMCMCs were isolated and cultured as described previously[184]. Briefly, femoral bone marrow cells from WT C57BL6/J mice were cultured for 6 weeks in cell culture media (DMEM+10% FBS+50 μM BME) supplemented with 10 ng/ml IL-3 to generate BM-derived cultured mast cells (BMCMCs).

2.4.8 *Scanning Election Microscopy of Pigment Activation of Mast Cells*

Approximately 10^6 BMCMCs were centrifuged, washed twice and resuspended in 0.5 mL of DMEM. BMCMCs were then treated with either 0.5 μM pigment or an equivalent amount

of control Δ*cylE* extract or A23187 (0.83 ng/μL, 1.66 μM) for 10 min. at 37^{o}C. One volume of Karnovsky fixative was added to the samples and incubated for an additional 10 min at room temperature. Subsequently, the cells were centrifuged and resuspended in 1.4 mL of Karnovsky's Fixative and incubated overnight at 4^{o}C. Samples were then prepared for scanning electron microscopy as described[96,187]. Images were captured using a JEOL 5800 Scanning Electron Microscope equipped with a JEOL Orion Digital Acquisition System.

2.4.9 *Isolation of Neutrophils from Adult Human Blood*

Neutrophils were isolated from fresh human adult blood. Briefly, approximately 20 - 30 mL of blood was collected from independent healthy human donors in EDTA tubes (BD Bioscience). Neutrophils were then isolated using a MACSxpress neutrophil isolation kit following manufacturer's instructions (Miltenyi Biotec). Following neutrophil isolation, the cells were pelleted and any residual red blood cells (RBC) were removed using the RBC lysis solution (0.15nM NH_4Cl, 1mM $NaHCO_3$) as per manufacturer's instructions. Cells were then washed with RPMI 1640 containing L-glutamine (Corning Cellgro; hereafter referred to as RPMI-G). To assess neutrophil purity, neutrophils (purified as described above) and control whole blood (after 2 erythrocyte lysis steps as indicated above) were stained for the neutrophil markers CD15 and CD16 (BD Biosciences). Approximately 5 x 10^5 cells were washed and placed in Fc receptor block (1:200, BD Biosciences) for 15 min at room temperature (RT). Following blocking, immunofluorescent antibodies were added to the cells at manufacturer recommended concentrations (1:10, CD15; 1:200, CD16) and incubated at RT for 30 min. Stained cells were washed twice in FACS (fluorescence-activated cell sorting) buffer (1mM EDTA, 25mM HEPES, 1% BSA (w/v) in PBS) and analyzed immediately or re-suspended in 1.0% paraformaldehyde

until analysis by flow cytometry. Flow cytometry experiments were conducted using an LSR II (BD Biosciences. and analyzed using FlowJo v. 10.1 (FlowJo, LLC).

2.4.10 *Scanning Electron Microscopy of NET Formation*

Approximately 1×10^6 neutrophils were washed with RPMI and resuspended in 0.5 ml of RPMI. The cells were then treated with either pigment (0.5 μM) or an equivalent amount of control (Δ*cylE* extract) or media (RPMI) or with bacteria (hyper-hemolytic GBSΔ*covR*, or non-hemolytic GBSΔ*covR*Δ*cylE*) at MOI 100 for 10 min at 37°C. One volume of ½ Karnovsky's fixative was added to the samples, and the cells were incubated for an additional 10 min at RT. Subsequently, the cells were centrifuged and resuspended in 1.4 ml of ½ Karnovsky's fixative and incubated overnight at 4°C. Samples were then prepared for scanning electron microscopy as described[188,189]. Images were captured using a Sigma 500 variable pressure Field Emission Scanning Electron Microscope (FESEM) using Smart SEM version 5.09.

2.4.11 *Chronically Catheterized NHP Model*

In this study, ten chronically catheterized pregnant NHP (*Macaca nemestrina*) containing catheters surgically implanted via laparotomy into the maternal femoral vein, amniotic cavity, and choriodecidual interface in the lower uterine segment (between uterine muscle and fetal membranes, external to amniotic fluid) received one of two experimental treatments: *i.e.* choriodecidual inoculation of either GBS COH1Δ*covR* (n=5; hyper-pigmented strain) or GBS COH1Δ*covR*Δ*cylE* (n=5; isogenic, non-pigmented strain). Results obtained from these animals were compared to saline controls (n=5; choriodecidual and amniotic fluid saline inoculations) that were performed previously[61,190]. Experiments involving chronically catheterized pregnant

NHP model of choriodecidual GBS infection was performed as previously reported[61,191] with one exception; for all the NHP animals enrolled in this study, we omitted catheterization of the fetal internal jugular vein. This was due to fetal catheter entanglement observed in two previous animals where fetal death occurred prior to experimental start.

Briefly, in this model, pregnant pigtail macaques were time-mated and fetal age determined using early ultrasound. Temperature in the animal quarters was maintained between 72-82° F. Animals were fed a commercial monkey chow, supplemented daily with fruits and vegetables and drinking water was available at all times. Each animal was first conditioned to a nylon jacket/tether system for several weeks before surgery, which allowed free movement within the cage, but protected the catheters. Between days 116-125 of pregnancy (term=172 days), catheters were surgically implanted via laparotomy into the maternal femoral artery and vein, amniotic cavity, and choriodecidual interface in the lower uterine segment (between uterine muscle and fetal membranes, external to the amniotic cavity). Choriodecidual and amniotic fluid catheters were comprised of polyvinyl tubing and maternal artery and vein catheters were made from silicone tubing. Fetal ECG electrodes and a maternal temperature probe (AD Instruments) were also implanted. Post-operative analgesia was provided via a fentanyl patch applied the day prior to surgery, in addition to postoperative indomethacin or ketoprofen as described[61].

After surgery, the animal was placed in the jacket and tether with the catheters/electrodes tracked through the tether system. Cefazolin and either terbutaline sulfate or atosiban 0.12mg/kg/hour were administered intravenously to reduce postoperative infection risk and uterine activity. Cefazolin, terbutaline or atosiban were stopped at least 72 hours before experimental start (~ 240 half-lives for atosiban, ~18 half-lives for terbutaline, ~40 half-lives for cefazolin, >97% of drugs eliminated), which represented approximately a 7-10 day period of

postoperative terbutaline administration. Experiments began approximately two weeks after catheterization surgery to allow recovery (~30-31 weeks human gestation). AF and maternal blood were collected for culture, cytokine and prostaglandin analysis during the course of the experiment. Intra-amniotic pressure was continuously recorded, digitized, and analyzed as described previously[61]. The integrated area under the intrauterine pressure curve was used as a measure of uterine activity and reported as the hourly contraction area (HCA; mmHg * sec/hour) over 24 hours.

Preterm labor was defined as progressive cervical dilation associated with increased uterine activity (>10,000 mmHg*sec/hour). Cesarean section was performed at the following endpoints to allow for tissue collection: 1) preterm labor, 2) three days after GBS inoculation if no preterm labor was observed, or 3) seven days after saline inoculation[61]. After Cesarean section, fetuses were euthanized by barbiturate overdose (1-2 ml, 390mg/ml, Beuthanasia-D Special, Schering-Plough Health Corp) followed by exsanguination and fetal necropsy[61]. Complete gross and histopathologic examination was performed.

A three-day endpoint to assess the effects of GBS infection on placental tissues and fetal injury was chosen in order to study the earliest events in the pathway of infection/inflammation associated preterm birth. The seven-day endpoint for saline controls was chosen at the inception of our research program and provides a close gestational age match for the current study. Using this model, we previously showed that saline inoculation in five pregnant NHP induced minimal to no inflammation without signs of preterm labor[61]. Data from saline control animals was used in this study for comparison as needed.

GBS strains used in the NHP model were derived from the clinical isolate obtained from an infected newborn known as COH-1 which is a ST-17 clone belonging to capsular serotype

III[192,193]. The hyper-hemolytic/hyper-pigmented Δ*covR* isogenic non-pigmented Δ*covR*Δ*cylE* were derived from wild type (WT) GBS COH-1 and were previously described[96]. Routine cultures of GBS were grown in tryptic soy broth (TSB) or tryptic soy agar (TSA, Difco Laboratories) at 37°C in 5% CO_2. For inoculations in the NHP model, GBS strains were grown to mid-log phase ($O.D_{600}$ = 0.5) and ~ 1-3 X 10^8 CFU in 1mL PBS was inoculated into the choriodecidual space, as described previously[61].

The hyper-pigmented GBSΔ*covR* strain exhibits an orange color on TSA and non-pigmented GBS strains are white in color[96,148]. Also, Δ*covR* and Δ*covR*Δ*cylE* strains of GBS are spectinomycin-resistant because the gene *covR* was replaced with a gene conferring spectinomycin resistance in these strains[96,181]. To confirm that the GBS strains recovered from infected NHP were the correct strains, a few colonies obtained from each sampled tissue and fluid per experiment were patched on selective medium (*i.e.* TSA containing spectinomycin), and the level of CAMP factor activity was tested on sheep blood agar plates with the inoculum strain included in parallel.

2.4.12 *Placental Immunostaining*

After cesarean section, placenta samples underwent tissue fixation in 10% neutral buffered formalin. Complete gross and histopathologic examination was performed on the chorioamnion and placenta. For immunostaining, full thickness paraffin sections of fetal roll were deparaffinized and epitopes were revived overnight at 60°C in citrate buffer (10 mM sodium citrate, 0.05% Tween 20, pH 6.0). After epitope revival, slides were washed, blocked for 1 hour at 23°C in 5% (v/v) goat serum and 1% (w/v) BSA, then incubated overnight at 4°C with rabbit anti-neutrophil elastase antibody (1:2000, Abcam). Anti-neutrophil elastase antibody was detected using anti-rabbit IgG antibody conjugated to Cy3 (1:2500, Abcam). Extracellular and

nuclear DNA was detected using DAPI (4',6-diamidino-2-phenylindole) in Vectashield (Vector Laboratories). Images were captured using a DM4000B Fluorescent upright microscope (Leica) under 20× magnifications. The microscope was attached to a DFC310FX camera (Leica) and the acquisition software used was the Leica application suite (version 4.0.0). Images were quantified using ImageJ v. 1.6.0_24.

2.4.13 *NET Killing Assay*

To observe neutrophil extracellular trap (NET) -mediated killing, neutrophils in NET assay buffer (RPMI-G + 1mM CaCl2 + 1% BSA) were incubated with cytochalasin D and B (10 μM in 0.25% DMSO, Cayman Chemical) for 30 min at 37°C to block phagocytosis as described[194]. To induce NETs, neutrophils from above were seeded in a 24 well plate at ~ 9 X 105 cells /ml per well and were stimulated with PMA (20nM in 0.02% DMSO, Cayman Chemical) for 2 hours at 37°C. Subsequently, the PMA-containing media was removed and replaced with 500μL fresh NET assay buffer. Wells containing NETs were inoculated with the GBS strains described above at an MOI of 0.1. To inhibit NET-mediated bacterial killing, selected wells were treated with 20kU DNase I (Qiagen) for 15 min at 37°C as described[194], prior to infection with GBS. After 1 hour of incubation at 37°C, Triton X-100 was added to a final concentration of 0.025% and media was pipetted up down thoroughly to dislodge any NET-associated bacteria. The supernatant was serially diluted and plated on TSA for GBS enumeration. The survival index was calculated as the ratio of CFU recovered in the presence of neutrophils to CFU recovered in the absence of neutrophils for each condition (i.e. with and without DNAse), respectively.

2.4.14 *Statistical Analysis*

Students *t*-test, Mann-Whitney test, Bonferroni's, Tukey's or Dunnett's multiple comparison tests following ANOVA, Fisher's exact test or Barnard's test was used to estimate differences as appropriate and p value <0.05 was considered significant. These tests were performed using GraphPad Prism version 6.0, GraphPad Software, USA, www.graphpad.com or SciStatCalc.

2.5 Acknowledgements, Author Contributions, and Conflict of Interest

2.5.1 *Acknowledgements*

We are grateful to Dr. Denny Liggitt for his expert advice, Dr. Maia Chan for assistance with animal experiments and Phuong Truong, Leticia Campos, Phoenicia Quach and Varchita Allishetti for technical assistance, Joyce Karlinsey for experimental advice, Dr. Brad Cookson for his support, and Connie Hughes for administrative assistance. We acknowledge Drs. Craig Rubens and Michael Gravett, who helped us obtain grant funding for the saline controls and contributed to study design related to performance of the original nonhuman primate experiments.

2.5.2 *Author Contributions*

For[62]: E. B., C.G., L.N., C. B., J. V., M.C., S.M., B.A., C.W., V.A., V. S-U., J.O., M.G., S.S., L.R and K.A.W collected samples and performed the experiments, E. B., C.G., J.V., L.R and K.A.W designed the research, E. B., C.G., L.N., C. B., J. V., M.C., S.M., B.A., C.W., V.A.,

S.S., J. W.M., T.K.B., A.B., H.D.L., L.R., and K.A.W analyzed the results and E.B., C.G., J. V., T.K.B., H.D.L., L.R., and K.A.W wrote the paper. For[119]: C.G., J. V., L.N., C.W., E.B., V. S-U., M.C., K.B., A.M.P performed the experiments, D.P.G collected and provided GBS strains, C.G., J.V., L.N., C.W., A.M.P and L. R designed the research, C.G., J. V., L. N., C.W., K.B., D.P.G., K.A.W., A.M.P and L.R analyzed the results and wrote the paper.

2.5.3 *Conflict of Interest*

The authors declare no competing financial interests.

2.6 FIGURES AND TABLES

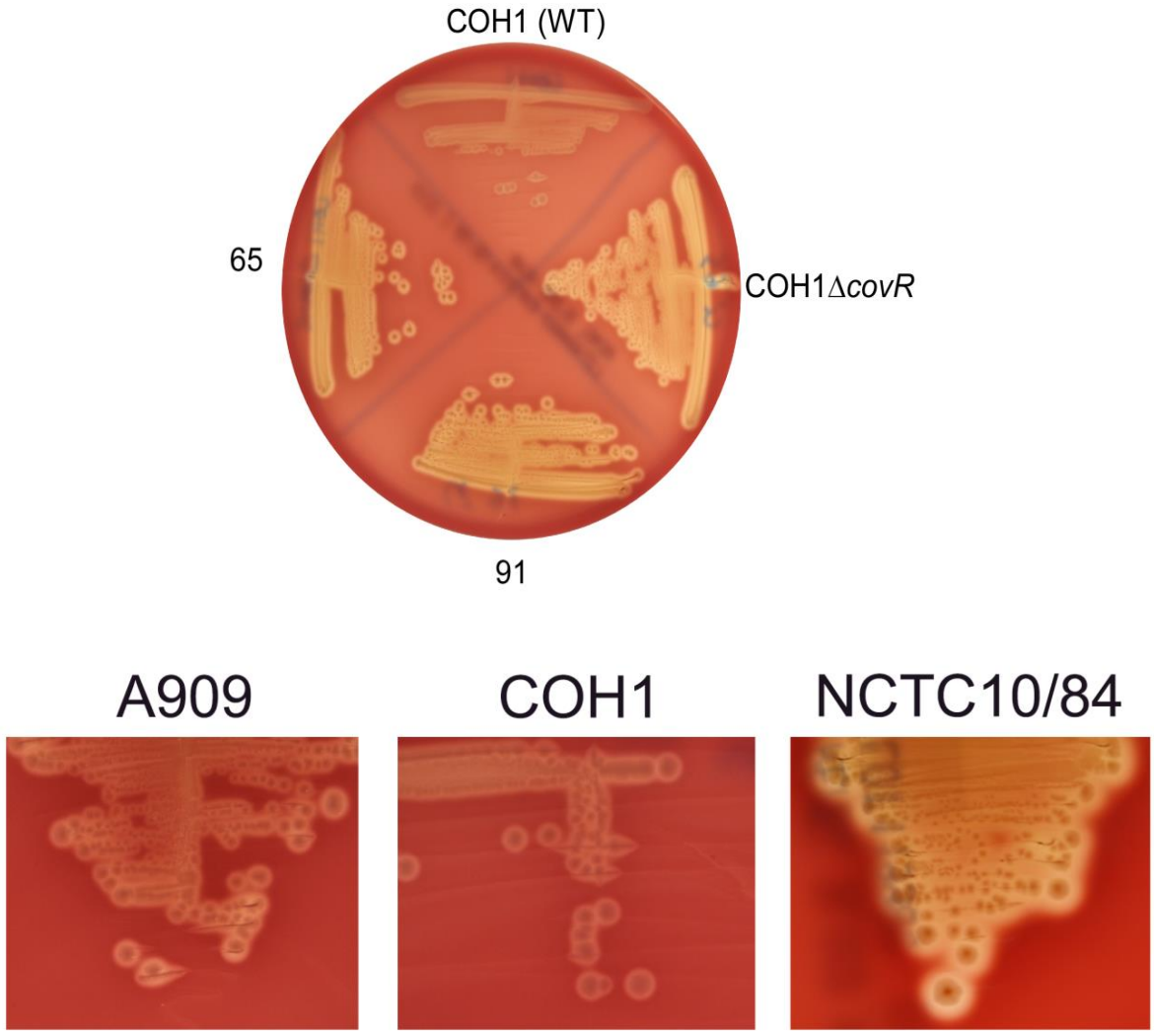

Figure 2-1 – Hemolytic factor activity of GBS isolates

The top panel shows hemolytic factor activity of rectovaginal GBS isolates. COH1 is a wild type (WT) GBS clinical isolate from an infected newborn and belongs to the hyper-virulent ST-17 clone. COH1Δ*covR* is a mutant derived from COH1 and exhibits increased hemolytic activity. Strains 65 and 91 are rectovaginal GBS isolates that exhibit increased hemolysis and decreased CAMP factor expression similar to COH11Δ*covR*. The bottom panel shows the wildtype strains

A909, COH1, and NCTC10/84. A909 is mildly hemolytic, COH1 is weakly hemolytic, and NCTC10/84 is naturally hyper-hemolytic. The top panel is adapted from Gendrin *et al.* 2015[119].

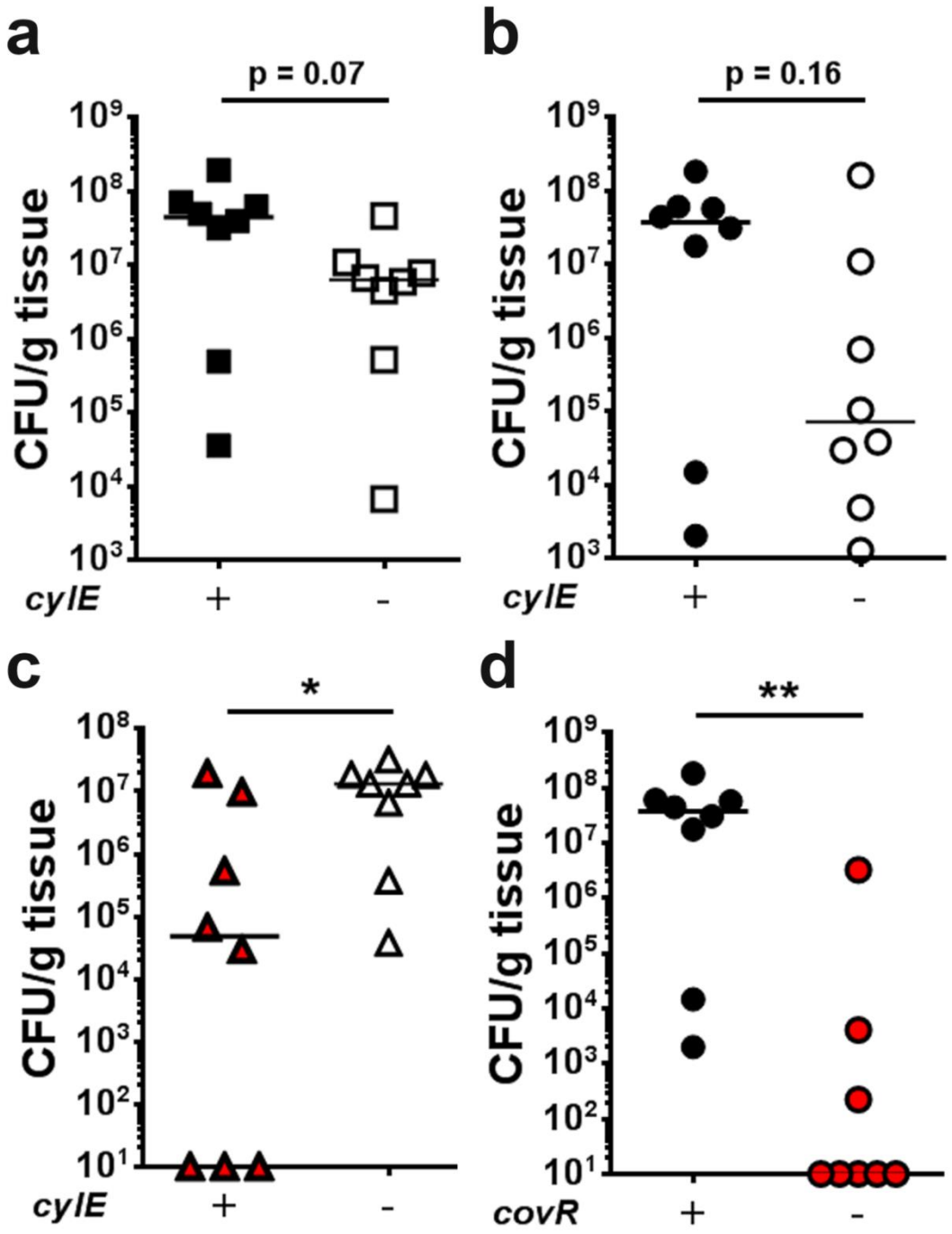

Figure 2-2 – Role of hemolytic pigment in GBS vaginal colonization.

a-d, Female, non-pregnant C57BL6/J mice were intra-vaginally inoculated with ~10^8 CFU of GBS. At 4 days post inoculation, bacterial persistence was evaluated in the lower genital tract. **a**, Vaginal bacterial burden of mice inoculated with the mildly-hemolytic WT GBS strain A909 and

isogenic non-pigmented A909Δ*cylE* mutant. **b**, Vaginal bacterial burden of mice inoculated with the mildly-hemolytic WT GBS strain COH1 and isogenic non-pigmented COH1Δ*cylE* mutant. **c**, Vaginal bacterial burden of mice inoculated with the natively hyper-pigmented NCTC10/84 and isogenic non-pigmented NCTC10/84Δ*cylE* (*n*=8/group, *$p < 0.05$). **d**, Vaginal bacterial burden of mice inoculated with WT COH1 and isogenic hyper-pigmented COH1Δ*covR* (*n*=8/group, **$p < 0.005$). Statistical significance assessed by Mann-Whitney test. Panel **c** adapted from Gendrin *et al.*, 2015[119].

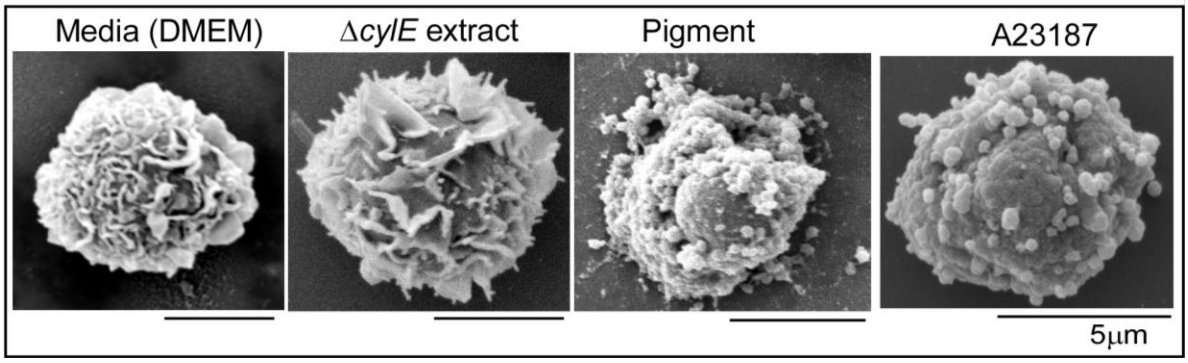

Figure 2-3 – Role of hemolytic pigment in GBS vaginal colonization.

Scanning electron micrographs showing membrane morphology of BMCMCs that were briefly exposed to 0.5 μM pigment or controls (cell culture media, Δ*cylE* extract or 1.66 μM Ca^{2+} ionophore A23187) for 10 min. A representative image from two independent experiments is shown, a minimum of 30 cells were examined in a blinded fashion. Adapted from Gendrin *et al.*, 2015[119].

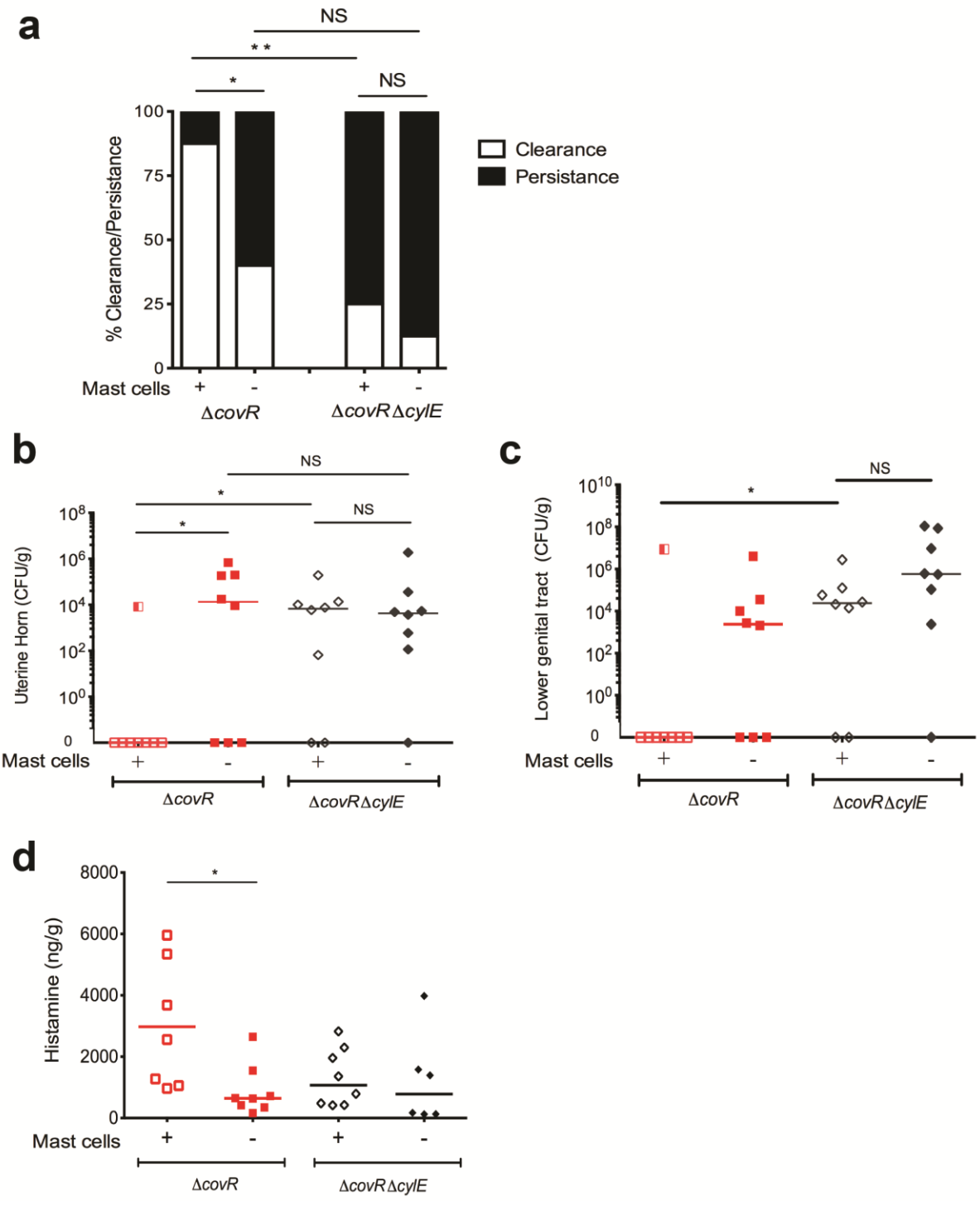
a
NS
**
*
NS
100
75
50
25
0
% Clearance/Persistance
Clearance
Persistance
Mast cells
+
-
+
-
ΔcovR
ΔcovRΔcylE
b
NS
*
*
NS
10^8
10^6
10^4
10^2
10^0
0
Uterine Horn (CFU/g)
Mast cells
+
-
+
-
ΔcovR
ΔcovRΔcylE
c
NS
*
10^10
10^8
10^6
10^4
10^2
10^0
0
Lower genital tract (CFU/g)
Mast cells
+
-
+
-
ΔcovR
ΔcovRΔcylE
d
*
8000
6000
4000
2000
0
Histamine (ng/g)
Mast cells
+
-
+
-
ΔcovR
ΔcovRΔcylE

Figure 2-4 – Mast cells activation promotes clearance of hyper-hemolytic GBS from the lower genital tract

a-c, Mast cell deficient mice or heterozygous littermate controls were intra-vaginally inoculated with ~10^8 CFU of GBS Δ*covR* or Δ*covR*Δ*cylE*. At 4 days post inoculation, bacterial persistence and dissemination was evaluated in the lower genital tract and both uterine horns. (**a**) Negative or positive bacterial cultures obtained from the lower genital tract and both uterine horns of mast cell proficient mice and mast cell deficient mice that were inoculated with either GBSΔ*covR* or Δ*covR*Δ*cylE*. Data are represented as % Clearance compared to Persistence (**a**, *n*=8/group, **p = 0.028*, ***p = 0.007*, Barnard's Test), as bacterial burden in the uterine horns (**b**) or in the lower genital tract (**c**, *n*=8/group, **p < 0.05*). In the mast cell proficient group inoculated with GBSΔ*covR*, the same mouse had bacterial CFU in both the lower genital tract and uterine horn (denoted as a partially filled symbol). **d,** Histamine levels in the lower genital tract of mast cell proficient and deficient mice infected with GBSΔ*covR* or Δ*covR*Δ*cylE*. (*n*=8/group, **p < 0.05*). Adapted from Gendrin *et al.*, 2015[119].

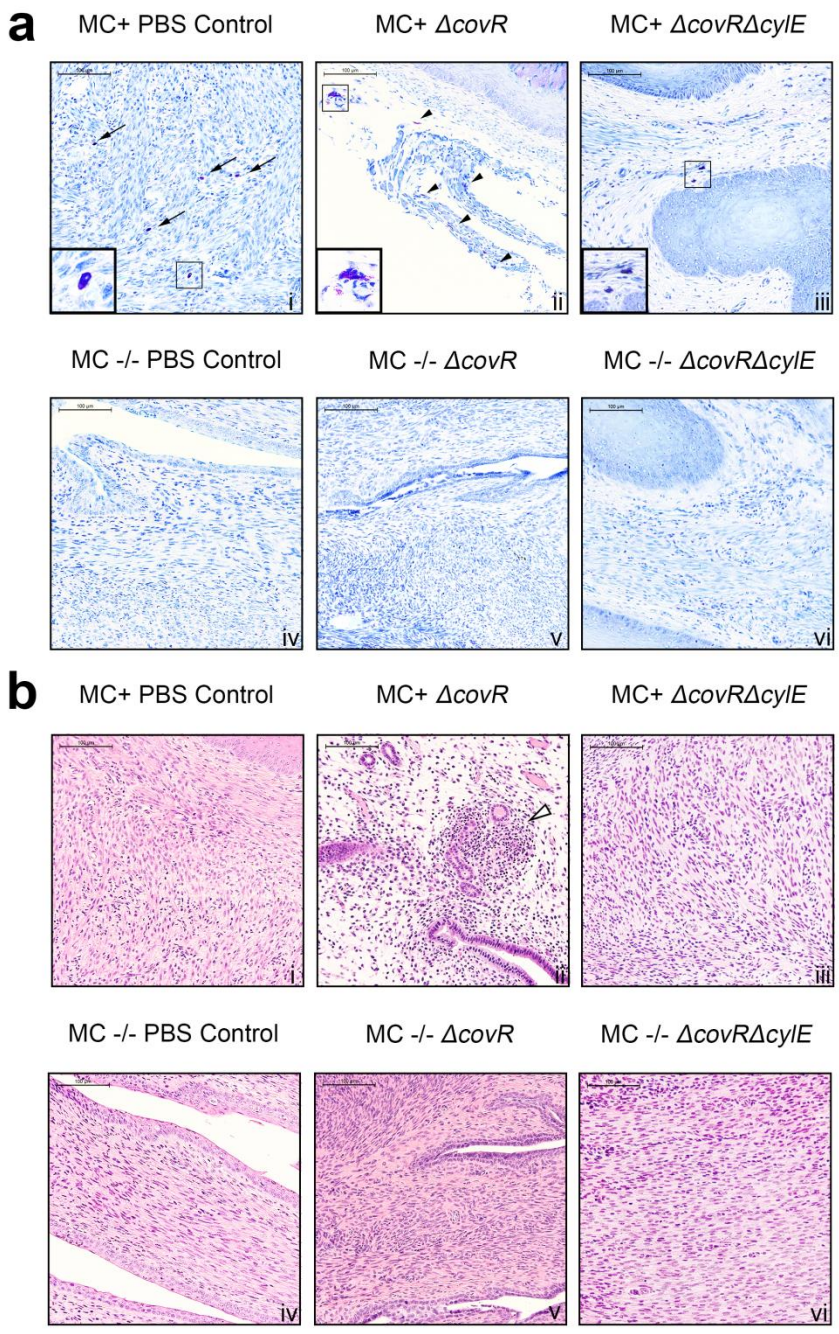

Figure 2-5– Histological sections of the genital tracts of female mast cell proficient and mast cell deficient mice infected with hyper-pigmented and non-pigmented GBS strains. **a-b**, Histology of mouse genital tracts at 4 days post inoculation with GBS (Δ*covR* or Δ*covR*Δ*cylE*) or PBS controls. Sections were stained with toluidine blue (**a**) and hematoxylin

and eosin (**b**). Arrows and boxed area indicate non-degranulated mast cells in mast cell proficient mice treated with control PBS or GBSΔ*covR*Δ*cylE* (see **a**, panels i & iii and magnified insets). In mast cell proficient mice treated with GBSΔ*covR*, arrowheads indicate degranulated mast cells (see **a**, panel ii and magnified inset). Hematoxylin and eosin stained sections of mouse genital tracts reveals the presence of inflammatory foci in mast cell proficient mice infected with GBSΔ*covR* (see **b**, arrow in panel ii) and not in mast cell proficient mice treated with PBS or GBS Δ*covR*Δ*cylE* (see **b**, panels i & iii). Inflammatory foci are also not seen in mast cell deficient mice treated with PBS, GBSΔ*covR* or GBSΔ*covR*Δ*cylE* (see **b**,panels iv-vi). Scale bar =100μm. Adapted from Gendrin *et al.*, 2015[119].

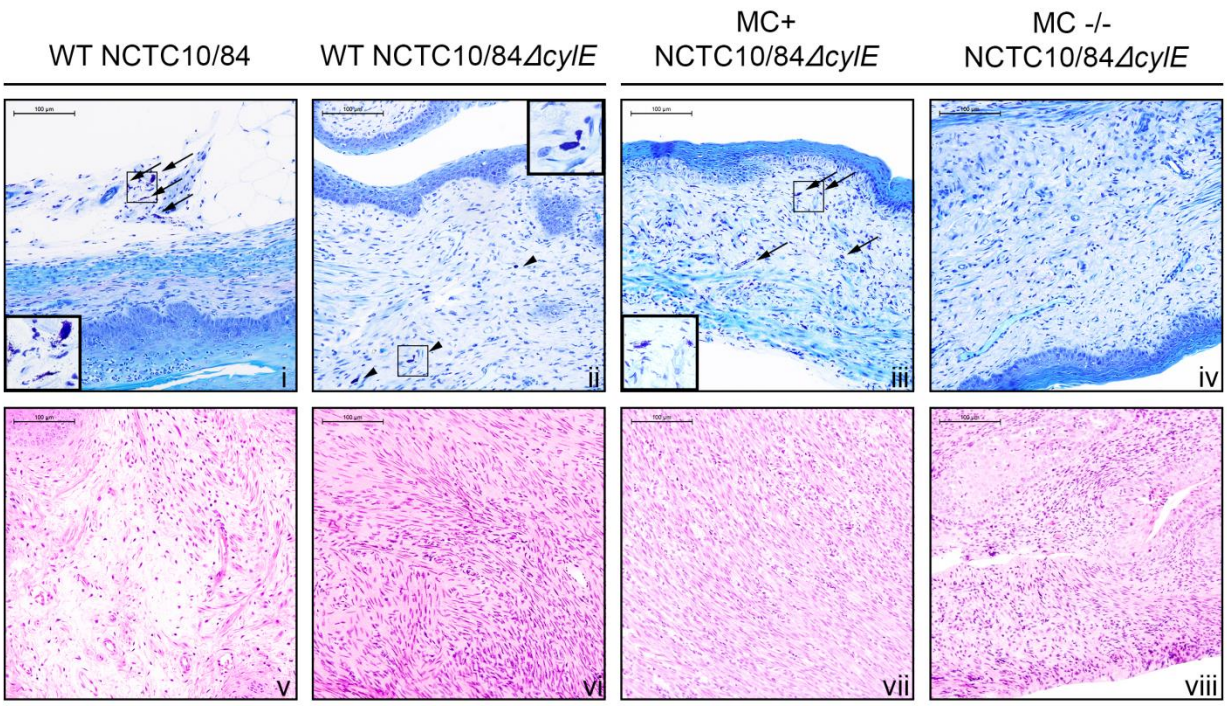

Figure 2-6 – Histological sections of the genital tracts of female mast cell proficient and mast cell deficient mice infected with endogenously hyper-pigmented GBS strain.

Toluidine blue and hematoxylin and eosin stained sections of mouse genital tracts. Arrows and boxed area indicate degranulated mast cells in mice infected with hyper-pigmented NCTC10/84 and non-degranulated mast cells in NCTC10/84Δ*cylE* (see panels i-iv and magnified insets). Hematoxylin and eosin stained sections reveal the presence of edema in mice infected with NCTC10/84 (see panel v) and not in mice infected with NCTC10/84Δ*cylE* (panel vi-viii). WT indicates C57BL/6J mice, and MC+ indicates *Cpa3-Cre;Mcl-1*$^{fl/+}$ heterogeneous mice. Scale bar =100μm. Adapted from Gendrin *et al.*, 2015[119].

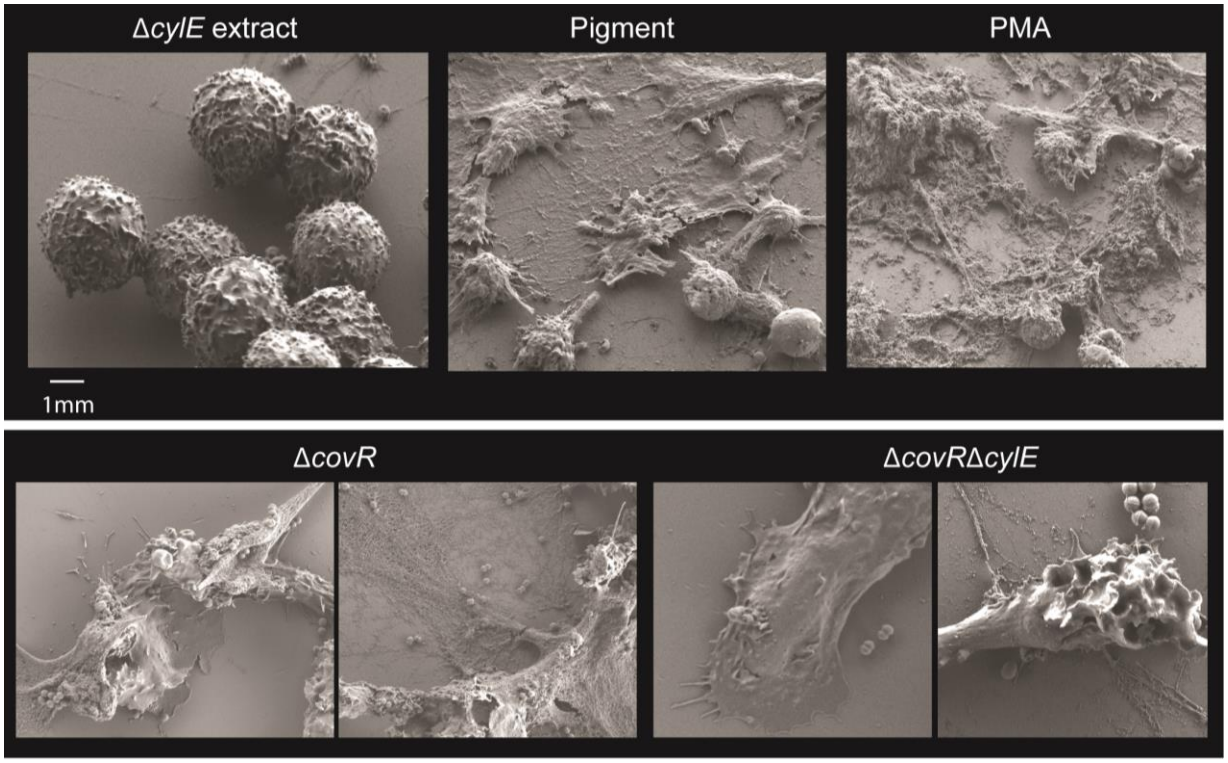

Figure 2-7 – Hemolytic pigment stimulates NET formation

Top Panel: SEM of neutrophil extracellular traps (NETs) in neutrophils treated with GBS pigment (5 μM), negative control (*ΔcylE* extract) or positive control PMA (20 μM). Bottom panel: SEM of NETS due to hyper-pigmented GBSΔ*covR* or non-pigmented GBSΔ*covR*Δ*cylE*. Adapted from Boldenow *et al.*, 2016[62].

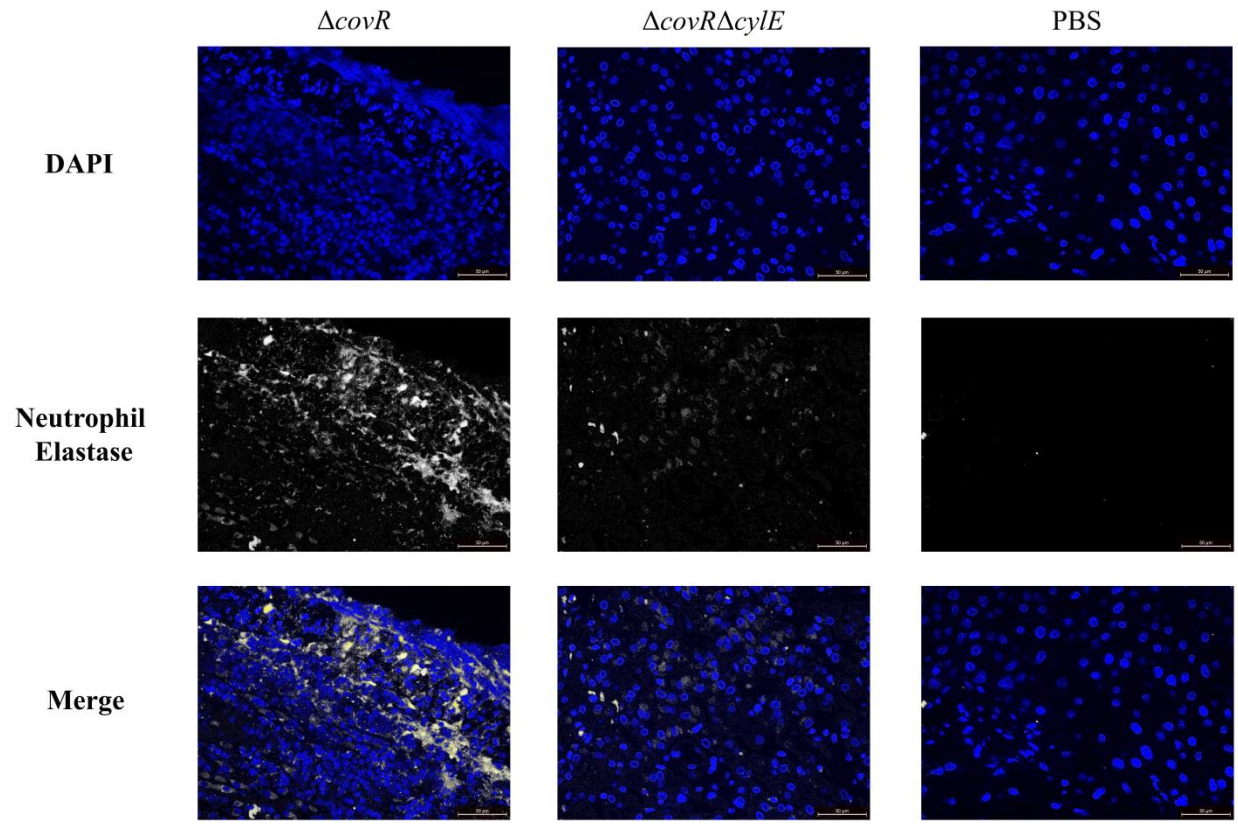

Figure 2-8 – NETs are formed in the chorioamnion during *in vivo* GBS infection.
Immunofluorescence staining for neutrophil elastase and extracellular DNA was performed on chorioamniotic membranes from NHPs inoculated with either hyper-pigmented GBSΔ*covR*, non-pigmented GBSΔ*covR*Δ*cylE*, or control saline. Data are representative of five animals from each group that were examined for NETs. Neutrophil elastase staining is shown in grayscale mode for ease of visualization. PBS, phosphate-buffered saline; DAPI, 4′,6-diamidino-2-phenylindole. Adapted from Boldenow *et al.*, 2016[62].

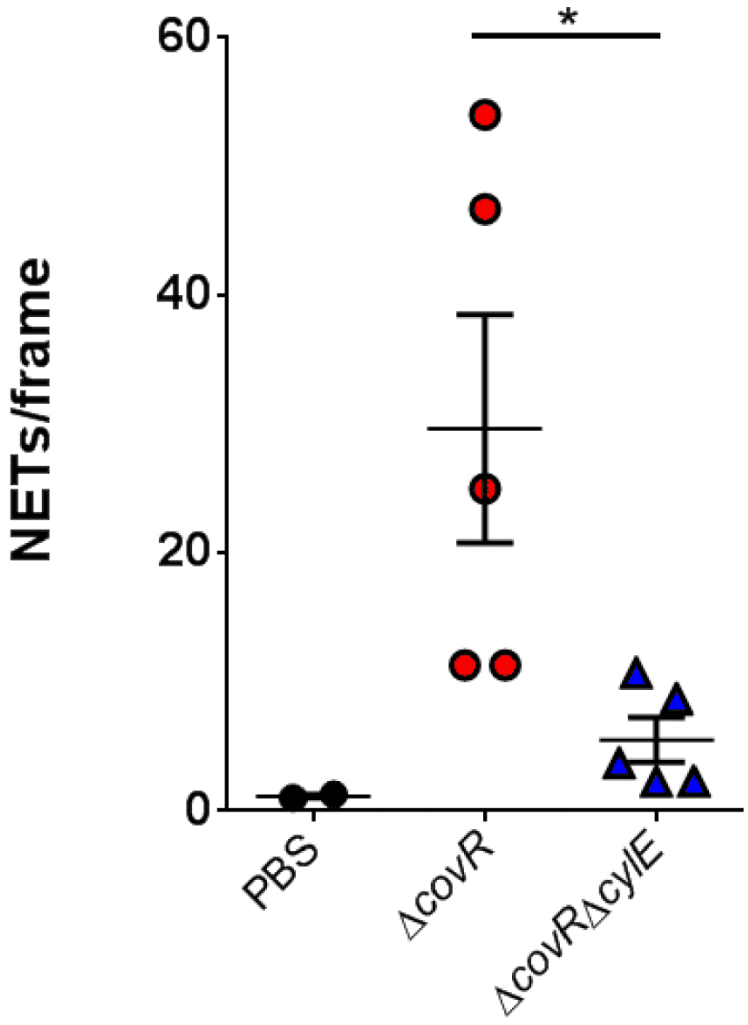

Figure 2-9 – Increased NETs in the chorioamnion of NHPs infected with hyper-pigmented GBSΔ*covR*.

NET formation was quantified on immunofluorescent images obtained from chorioamniotic membranes inoculated with GBSΔ*covR* (n = 5), GBSΔ*covR*Δ*cylE* (n = 5), or saline controls (PBS, n = 2). Three random frames of equal area were collected from each sample and NETs were counted using ImageJ by thresholding images and analyzing particles >10 pixels in size. Particle counts from each frame were then averaged for each sample (mean ± SEM, Tukey's multiple comparison test following ANOVA, *$p < 0.05$). Adapted from Boldenow *et al.*, 2016[62].

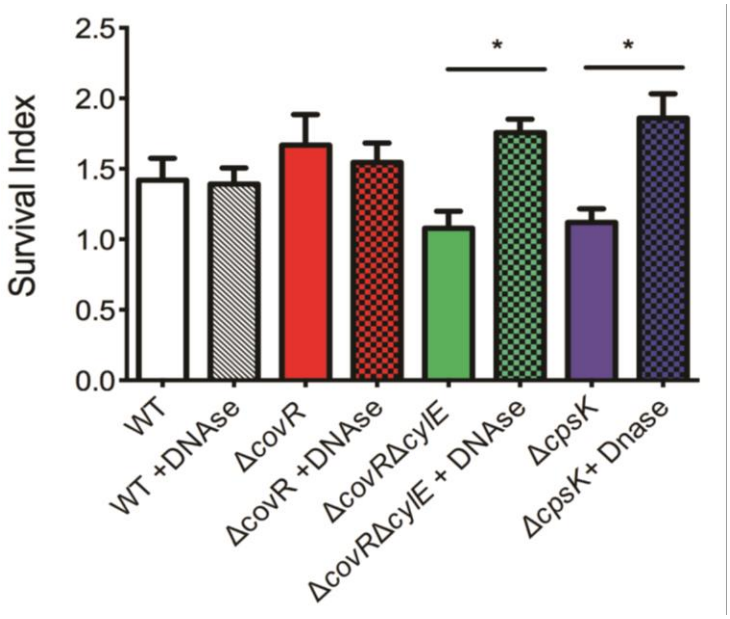

Figure 2-10 – Increased expression of the hemolytic pigment enables GBS to resist killing by neutrophil extracellular traps

Neutrophils were incubated with cytochalasin D and B (10 μM) to block phagocytosis and NETs were induced by stimulation with PMA. Subsequent NET killing of the GBS strains (WT GBS, isogenic hyper-hemolytic GBSΔ*covR*, non-hemolytic GBSΔ*covR*Δ*cylE* and GBSΔ*cylE* and capsule deficient GBSΔ*cpsK*) was compared. To inhibit NET-mediated bacterial killing, control wells were treated with DNase I. Data shown are the average of three independent experiments performed in duplicate, error bars ± SEM. Significance was determined using Bonferroni's multiple comparison test following ANOVA, * $p < 0.05$. Adapted from Boldenow *et al.*, 2016[62].

Strain	Hemolytic Titer
Clinical Isolates	
WT GBS (COH1)	**2**
COH1Δ*covR*	**>32**
Rectovaginal Isolates	
Strain 65	**> 32**
Strain 91	**> 32**
Remaining 51 isolates	**≤ 2**

Table 2-1 – Hemolytic titers of GBS strains isolated from rectovaginal swabs of women in their third trimester of pregnancy.

COH1 is a wild type (WT) GBS clinical isolate from an infected newborn and belongs to the hypervirulent ST-17 clone. COH1Δ*covR* is a mutant derived from COH1 and exhibits increased hemolytic activity. Strain 65 and 91 are rectovaginal GBS isolates that exhibit increased hemolysis expression similar to COH1Δ*covR* (see Fig. 2-1). Adapted from Gendrin *et al.*, 2015[119].

2.7 SUPPLEMENTAL FIGURES

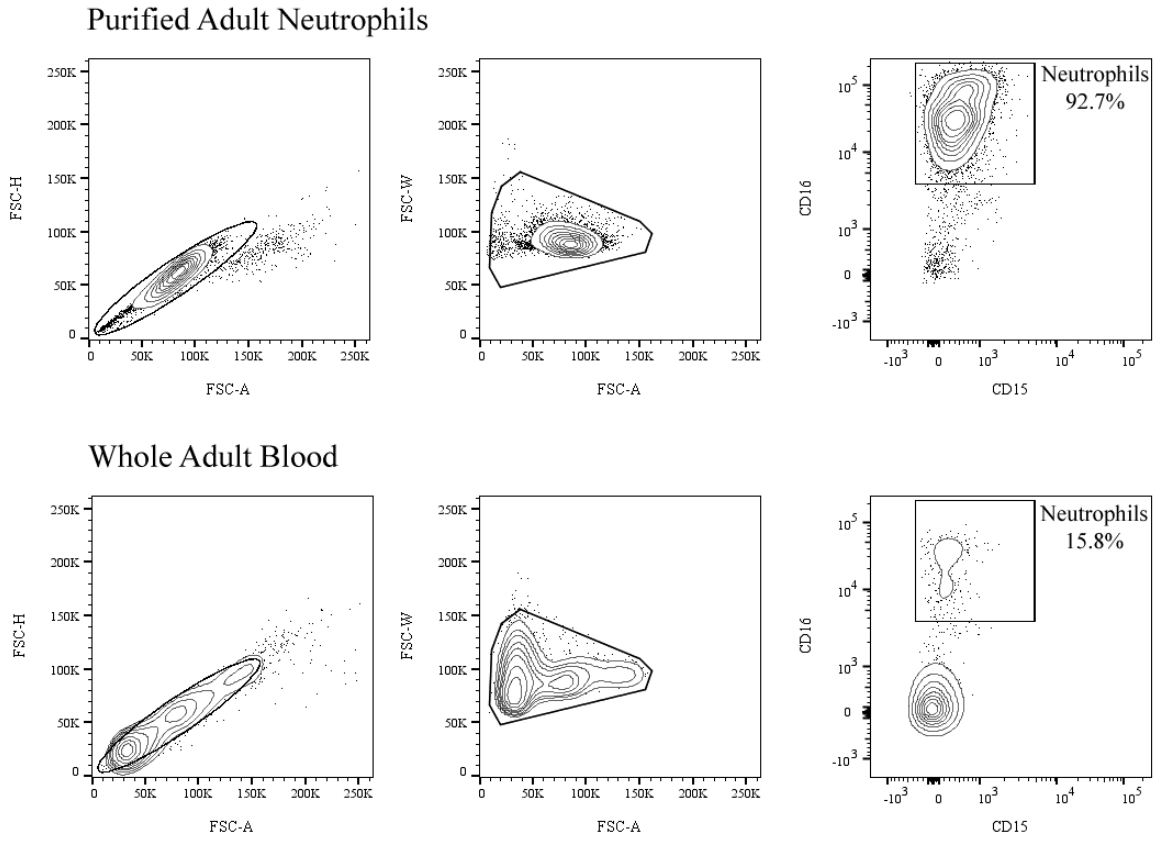

Figure 2-S1 – FACS (fluorescence-activated cell sorting) of neutrophils purified from human blood.

Flow cytometry was used to assess neutrophil purity from purified neutrophils and whole blood was included for comparison. Samples were first gated for single cells using FSA (forward scatter area) and FSH (forward scatter height, see LHS panels), and then by FSA and FSW (forward scatter width, see center panels). Finally, single cells were assessed for the neutrophil markers CD16 and CD15 (RHS panels). Note that ~ 15.8% of cells in whole blood were CD15+CD16+ prior to purification, whereas ~ 92.7 % of cells that were isolated after neutrophil purification were CD15+CD16+. Adapted from Boldenow *et al.*, 2016[62].

Chapter 3. Role of epithelial exfoliation in ascending GBS infection

The following text is from the article:

Jay Vornhagen, Blair Armistead†, Verónica Santana-Ufret†, Claire Gendrin†, Sean Merillat†, Michelle Coleman†, Phoenicia Quach, Erica Boldenow, Varchita Alishetti, Christina Leonhard-Melief4, Lisa Y. Ngo, Christopher Whidbey, Kelly S. Doran, Chad Curtis, Kristina M Adams Waldorf1, Elizabeth Nance, Lakshmi Rajagopal. (2017) Group B Streptococcus exploit vaginal epithelial exfoliation for ascending infection and fetal injury. In review, **Nature Medicine**. †Equal contribution.

Figure numbers have been updated to conform to the dissertation. The text remains as published with minor editorial changes.

3.1 ABSTRACT

Eleven percent of all pregnancies worldwide are preterm, accounting for roughly fifteen million preterm births and one million deaths per year. Premature birth increases the risk of adverse birth outcomes and is the leading cause of neonatal mortality. A significant cause of preterm birth is *in utero* infection by vaginal microorganisms. To establish an *in utero* infection, vaginal microbes must ascend from the vagina into the pregnant uterus by a process called ascending infection. The mechanisms by which vaginal organisms gain access into the uterus are not known. Previous studies have implicated vaginal epithelial exfoliation as a mechanism to diminish bacterial colonization. Here, we demonstrate how a vaginal commensal known as Group B Streptococcus (GBS), which is frequently associated with preterm birth, uses exfoliation for ascending infection. Using a murine model of vaginal colonization and ascending infection, we show that GBS induces vaginal epithelial exfoliation. This process is driven by extracellular activation of β_1 integrin signaling, which stimulates β-catenin signaling, and epithelial-to-mesenchymal transition (EMT). EMT induces loss of barrier function and cellular detachment, leading to epithelial exfoliation. Interestingly, epithelial exfoliation does not diminish vaginal colonization, but rather permits bacterial dissemination and ascending infection. Abrogation of epithelial exfoliation by interruption of β_1 integrin signaling and EMT leads to reduced rates of ascending infection and preterm birth. These data indicate that for some vaginal bacteria, epithelial exfoliation permits ascending infection rather than preventing colonization. This study provides novel mechanistic insight into ascending infection, potentially leading to novel interventions to prevent preterm birth.

3.2 INTRODUCTORY PARAGRAPH

Fifteen million babies are born prematurely each year[9], making preterm birth the leading cause of neonatal morbidity and mortality[4]. Intrauterine infection is the most frequent cause of preterm birth, which occurs when bacteria ascend from the vagina into the cervix and, ultimately, the uterus[12,195]. Once in the uterus, bacteria cross the placenta and invade the amniotic cavity, leading to inflammation, tissue damage, and preterm labor[3]. The mechanisms by which bacteria ascend from the vagina to the uterus remain unknown[3]. Here, we show how pathogenic bacteria such as Group B Streptococcus (GBS), which are associated with ascending infection and preterm birth[42,60,62,66,96], hijack host cellular processes to enable bacterial trafficking into the uterus. Although vaginal epithelial exfoliation is thought to prevent pathogen colonization of the genitourinary tract[196,197], we found that GBS exploits epithelial exfoliation for ascending infection, fetal injury and preterm birth. GBS activates β_1 integrin and β-catenin signaling leading to loss of barrier function, epithelial-to-mesenchymal transition (EMT) and exfoliation of vaginal epithelium. Preventing GBS induced vaginal epithelial exfoliation decreased ascending infection and improved pregnancy outcomes. Herein, we describe a novel mechanism by which GBS utilize epithelial exfoliation to establish an invasive perinatal infection. This work represents a shift in the current paradigm that vaginal epithelial exfoliation prevents pathogen colonization and infection.

3.3 MAIN TEXT

Heavy vaginal colonization is a primary risk factor for GBS-associated preterm birth[43]. Prior studies have demonstrated a role for epithelial exfoliation in decreasing bacterial colonization of the urinary tract[197] and vagina[198,199]. Upon challenge with pathogenic bacteria such as

Escherichia coli and *Neisseria gonorrhoeae*, vaginal epithelial cells lose their junctional and adhesive properties and exfoliate from their basement membrane along with the colonizing bacteria, thus preventing long term colonization and dissemination[197-199]. This phenomenon has yet to be explored in the context of GBS vaginal colonization and preterm birth. To determine how vaginal epithelial cells respond to GBS, female mice were vaginally inoculated with the GBS wild-type (WT) serotype III strain COH1, or saline, as previously described[119]. Interestingly, increased exfoliation of vaginal epithelial cells was observed in response to GBS over time (Figure 1a-b; Figure 3-S1a-c). Although a slight increase in epithelial exfoliation was observed in saline controls at 48-72 hours post-inoculation (Figure 3-S1c), which is consistent with the natural estrus cycle[200], levels of vaginal exfoliation were significantly higher in GBS treated animals compared to saline controls at 72 and 96 hours post-inoculation (Figure 1a-b, Figure 3-S1a-c). Similar levels of vaginal epithelial exfoliation was also observed with a GBS WT serotype V strain CJB111 (Figure 3-S2), previously described to exhibit increased vaginal persistence[85]. These data indicate that GBS stimulate epithelial exfoliation during vaginal colonization.

We next hypothesized that epithelial exfoliation would reduce GBS burden in the vagina, as observed with *N. gonorrhoeae* lacking the Opa protein[199]. Despite GBS being present on exfoliating vaginal epithelial cells (Figure 1c), epithelial exfoliation did not correlate with significantly decreased bacterial burden in the vagina (Figure 1d). Rather, a significant increase in GBS colony-forming units (CFU) was observed in the uterus (Figure 1e), suggesting a potential association between increased epithelial exfoliation and GBS ascending infection.

To determine if bacteria in the uterus primarily represented those ascending from the vagina or those arising by replication of initially ascended bacteria, we vaginally inoculated mice

with a WT GBS strain expressing a plasmid-encoded GFP[201]. Retention of this plasmid requires the presence of erythromycin. In the absence of antibiotic pressure, daughter cells do not inherit the plasmid (Figure 3-S3a), and GFP+ (mother) and GFP- (daughter) populations are generated (Figure 3-S3b). We confirmed that GFP fluorescence was observed under microaerobic and anaerobic conditions that represent genitourinary oxygen levels[202] (Figure 3-S3c). These data indicate that any potential differences in GFP expression observed *in vivo* is not solely due to differences in environmental conditions. Flow cytometry analysis of GFP+ GBS in vaginal and uterine tissues (Figure 3-S3d-e) demonstrated a modest decrease in GFP+ GBS in the vagina (Figure 1f) over 96 hours; in contrast, a significant increase in GFP+ GBS was observed in the uterus (Figure 1g). These data suggest that GBS recovered from the uterus likely ascended from the vagina. Although growth dynamics that occur *in vivo* are difficult to recapitulate *in vitro*, our results indicate that there is an association between epithelial exfoliation and GBS trafficking into the uterus.

We next sought to understand how GBS induces vaginal epithelial exfoliation. We first explored signaling via toll-like receptor 2 (TLR2) as a potential means of stimulating epithelial exfoliation, as it has been shown to be an important regulator of the host response to GBS[203]. Vaginal epithelial exfoliation and ascending GBS infection were independent of TLR2, as no differences in either exfoliation (Figure 3-S4a-b) or vaginal or uterine GBS burden (Figure 3-S4c-d) were observed between WT mice and TLR2 knockout mice. Similarly, mice deficient for the critical TLR2 adaptor molecule MyD88 displayed high levels of vaginal epithelial exfoliation in response to GBS colonization (Figure 3-S4a). We next explored cell death as a mechanism of GBS stimulation of epithelial exfoliation, as caspase 1-controlled lytic cell death has been shown to be a critical component of the host response to genitourinary GBS[66]. Vaginal epithelial

exfoliation due to GBS was not associated with induction of cytotoxicity or cell death. GBS infection of immortalized human vaginal epithelial cells (hVECs) did not correlate with a significant increase in cytotoxicity (Figure 3-S5a). Exfoliated CD326+ murine vaginal epithelial cells collected from GBS and saline inoculated animals did not display any differences in propidium iodide uptake, indicating that GBS does not induce cell permeabilization (Figure 3-S5b). Moreover, exfoliated CD326+ murine vaginal epithelial cells did not display external phosphatidylserine, a marker of apoptosis, as determined by Annexin V staining (Figure 3-S5c). Finally, no differences in vaginal exfoliation (Figure 3-S5d-e) or uterine GBS CFU (Figure 3-S5f) were observed between WT mice and Caspase 1 knockout mice, indicating that caspase 1 does not control epithelial exfoliation. Together, these data indicate that epithelial exfoliation and ascending GBS infection is independent of TLR2 signaling and cell death.

We then hypothesized that GBS triggers loss of barrier function in vaginal epithelial cells, leading to exfoliation. Epithelial exfoliation is a complex process influenced by multiple factors including failure of barrier function, as observed in intestinal cells[204]. Indeed, GBS infection resulted in loss of barrier function in hVECs, as measured by electric cell–substrate impedance sensing[205] (Figure 2a) and by trans-epithelial permeability assays (Figure 2b). Notably, loss of barrier function in hVECs correlated with increased cellular detachment (Figure 2c-d) and differences in cell shape and structure (Figure 2d) of detached hVECs similar to epithelial exfoliation observed *in vivo* (Figure 1c). To determine if exfoliation also disrupted underlying epithelia, we used fluorescent nanoparticles (hydrodynamic size: 118.7 ± 1.5 nm, surface charge -9.8 ± 0.7 mV) to probe vaginal epithelial barrier function *in vivo*. Interestingly, more nanoparticles penetrated the epithelial barrier over time in GBS-inoculated mice (Figure 2e,iii-iv), when compared to control animals (Figure 2e,i-ii). This increase in epithelial

permeability suggests that GBS may be able penetrate the epithelial due to exfoliation. Finally, intra-epithelial GBS were observed in conjunction with epithelial disruption (Figure 2f), indicating that indeed GBS are able to disseminate into epithelial tissues. Collectively, these data indicate that GBS disruption of epithelial barrier function is associated with increased cell detachment and exfoliation.

We next examined if GBS induced loss of barrier function in vaginal cells correlated with induction of epithelial-to-mesenchymal transition (EMT). EMT is a process wherein non-motile epithelial cells lose their cell-cell adhesions and gain migratory and invasive properties, which disrupts epithelial barrier function[206]. EMT is characterized by the loss of the epithelial marker E Cadherin and gain of the mesenchymal marker N Cadherin[206]. Interestingly, GBS-infected hVECs exhibited decreased surface expression (hVEC gating strategy shown in Figure 3-S6) of E Cadherin (Figure 2g) and increased surface expression of N cadherin (Figure 2h). Loss of E Cadherin observed in GBS-infected hVECs could not be attributed to either direct cleavage by GBS (Figure 3-S7) or its serine protease HtrA (Figure 3-S8), in contrast to the effect of HtrA in *Helicobacter pylori*[207]. GBS infection of hVECs induced changes in gene transcription that are well-characterized markers of EMT[206]. We observed decreased expression of *miR200c* and increased *snail1*, *zeb1*, and *zeb2* expression in GBS-infected hVECs compared to controls (Figure 2i). Further, infection of hVECs with the common vaginal commensal *Lactobacillus crispatus* failed to induce EMT or loss of barrier function (Figure 3-S9), indicating that induction of EMT is GBS specific. To corroborate these findings *in vivo*, E Cadherin levels in murine vaginal tracts were analyzed by immunohistochemistry. Interestingly, decreased levels of E Cadherin were observed in vaginal tissues of GBS-inoculated mice compared to control animals (Figure 2j). Additionally, flow cytometry of primary murine vaginal epithelial cells isolated from

GBS infected mice (see Figure 3-S10 for murine vaginal epithelial cell isolation and gating strategy) displayed significantly less E Cadherin compared to control animals (Figure 2k). Finally, EMT does not appear to be dependent on bacterial invasion. Inhibition of GBS invasion of hVECs (Figure 3-S11a) did not impact E Cadherin and N Cadherin surface expression in response to GBS infection (Figure 3-S11b-c). These data demonstrate that GBS induce EMT in vaginal epithelial cells *in vitro* and *in vivo*.

We next examined if GBS can trigger the β-catenin signaling pathway, which can regulate EMT[206]. β-catenin is sequestered at the membrane by E Cadherin, and when released, is either degraded or translocated to the nucleus. There, β-catenin binds the transcription factors T-cell factor 1 (TCF1) and lymphoid enhancer factor 1 (LEF1), resulting in transcription of genes associated with cell cycle progression, EMT, and oncogenesis[208]. Intriguingly, β-catenin regulated genes were significantly up-regulated during GBS infection of vaginal cells (Figure 3a). Visualization of β-catenin in GBS-infected hVECs demonstrated that β-catenin did indeed re-localize to the cytoplasm and nucleus (Figure 3b). A subset of these findings was recapitulated *in vivo*. Many β-catenin regulated genes were significantly upregulated in vaginal tissues of GBS-inoculated mice compared to controls (Figure 3c). Additionally, increased levels of the β-catenin target c-Myc were observed in GBS-inoculated mice compared to control animals (Figure 3d). Finally, inhibition of β-catenin signaling by a chemical inhibitor FH535[209] blocked cell detachment and loss of E Cadherin in response to WT GBS infection of vaginal cells *in vitro* (Figure 3-S12). These data show that β-catenin signaling controls EMT in vaginal epithelial cells and that GBS exploits this signaling mechanism to induce epithelial exfoliation.

Integrins are a widely expressed family of proteins, controlling various cellular processes ranging from proliferation to migration to organogensis[210]. Activation of β_1 integrins through

clustering at the cell surface stimulates a signaling cascade beginning with focal adhesion kinase (FAK), which is auto-phosphorylated at Tyr397[211]. FAK activates protein kinase B (AKT) by phosphorylation at Ser473[212], which proceeds to phosphorylate glycogen synthase kinase-3 beta (GSK3β) at Ser9, leading to its deactivation. Deactivation of GSK3β permits nuclear translocated of β-catenin, thus resulting in integrin control of β-catenin signaling. To test if β_1 integrin signaling is induced by GBS in vaginal epithelial cells, we used the 9EG7 β_1 integrin antibody, which specifically recognizes the active conformation of β_1 integrin[213]. Interestingly, GBS-infected vaginal epithelial cells displayed significantly more active β_1 integrin than mock-infected cells (Figure 3e). Additionally, vaginal epithelial cells infected with WT GBS showed increased phosphorylation of FAK, AKT and GSK3β (see FAKpTyr397, AKTpSer473, and GSK3βpSer9 in Figure 3f, Figure 3-S13) compared to mock infected cells. Furthermore, vaginal tissues from GBS-inoculated animals had substantially higher levels of active β_1 integrin at the epithelial layer near vaginal lumen in contrast to control tissues, where active β_1 integrin staining is localized to the basement membrane (Figure 3g). These findings are similar to those observed in carcinoma biology, wherein active integrins are normally expressed at the basement membrane of healthy stratified squamous epithelia; in contract, expression above the basement membrane is typical in cancerous tissues or tissues undergoing EMT[214]. Finally, intravaginal administration of recombinant murine $\alpha_1\beta_1$ integrin significantly diminished epithelial exfoliation and ascending infection without affecting vaginal colonization (Figure 3h-j). Although it is difficult to discern the independent effects of the integrin α_1 chain compared to the β_1 chain in the *in vivo* experiments, increased active β_1 integrin was observed in vaginal cells and tissues during GBS infection and competitively inhibited epithelial exfoliation and ascending infection.

Together, these data indicate that GBS are able to stimulate β_1 integrin signaling, which results in nuclear translocation of β-catenin, EMT, barrier disruption, and vaginal epithelial exfoliation.

We posit that GBS induced epithelial exfoliation compromises epithelial barrier function thereby permitting ascending infection. Thus, we sought to determine the effects of attenuated GBS-mediated β1 integrin signaling on ascending infection and preterm birth. Previous work has shown that GBS deficient for the invasion associated gene A (GBSΔ*iagA*) are less able to invade human brain microvascular endothelial cells and are less virulent than WT GBS[97]. We hypothesized that GBSΔ*iagA* may exhibit decreased interaction with vaginal epithelial cells leading to diminished β_1 integrin signaling. Interestingly, in contrast to brain microvascular endothelial cells, both WT GBS and GBSΔ*iagA* invaded vaginal epithelial cells similarly *in vitro* (Figure 3-S14a) and *in vivo* (Figure 3-S14b-c). Despite this, hVECs infected with GBSΔ*iagA* displayed less active β_1 integrin (Figure 4a) and reduced levels of FAKpTyr397 and GSK3βpSer9 (Figure 4b), consistent with reduced activation of the β-catenin signaling pathway. Additionally, GBSΔ*iagA* did not induce loss of barrier function in vaginal epithelial cells (Figure 4c), exhibited reduced β-catenin signaling (Figure 4d), and did not stimulate EMT (Figure 4e-f). Although the exact mechanism of how the absence of IagA reduces GBS β_1 integrin signaling is still to be elucidated, we used the strain as a model to test the effects of reduced GBS-mediated β_1 integrin signaling *in vivo*. We observed that mice inoculated with GBSΔ*iagA* had significantly decreased vaginal epithelial exfoliation (Figure 4g-h) and less ascending infection (Figure 4i), compared to mice inoculated with WT GBS. Additionally, the amount of GFP+ GBS observed in the uterus of mice inoculated with GBSΔ*iagA* was significantly less than that of WT GBS (Figure 4j). Together, these data demonstrate that a reduction in epithelial exfoliation leads to a decrease in ascending GBS infection. Given the importance of ascending GBS infection for

preterm birth[3], we vaginally inoculated pregnant mice with WT GBS or GBSΔ*iagA*. Pregnant mice inoculated with GBSΔ*iagA* exhibited substantially fewer CFUs in the uterus, placenta, and fetal tissues (Figure 4k, see Figure 3-S15 for a diagram of the murine female reproductive tissues). Moreover, the number of pups affected by an adverse birth outcome (either born premature or died *in utero*) was significantly reduced in mice inoculated with GBSΔ*iagA* (Figure 4l). These data are the first to indicate that GBS attenuated for their ability to stimulate β_1 integrin signaling *in vivo* exhibit reduced epithelial exfoliation, ascending infection and preterm birth. These results highlight the importance of these processes to GBS-associated preterm birth.

This work suggests a shift in the current paradigm of vaginal epithelial exfoliation in response to pathogen colonization. Previous studies on pathogenic *Neisseria* and uropathogenic *E. coli* (UPEC) have extensively demonstrated a role for vaginal epithelial exfoliation in the prevention of bacterial colonization[197-199], whereas we have found the opposite to be true for GBS (see model in Figure 3-S16). It appears that GBS lost with exfoliating cells do not significantly diminish the bacterial load in the vagina or uterus. This may be due to replicating GBS in the vagina, as evident by the decrease in number of GFP+ GBS in vaginal tissues (Figure 1f). One potential explanation for the difference between GBS and other bacteria that prevent vaginal epithelial exfoliation lies at the host-pathogen interface. Both *N. gonorrhoeae* and UPEC express proteins that target a family of host epithelial cell glycoproteins known as CEACAMs, and for these bacteria, CEACAM engagement prevents vaginal epithelial exfoliation[197,198]. We have not found CEACAM-binding proteins in GBS, indicating differences in the interactions between vaginal-resident microbes and host epithelial cells. These differences in host-microbe interactions explain the functional consequences on epithelial exfoliation, and are an interesting example of divergent evolution between the bacteria. It is intriguing that GBS and bacteria such

as *N. gonorrhoeae* and *E. coli* that prevent epithelial exfoliation both target integrin signaling[197,199]. It is logical that pathogens would target these proteins as a means of controlling cellular behaviors and circumventing host defenses, and that different pathogens would subvert integrin signaling in different ways for their benefit. CEACAM binding leads to integrin activation and increased epithelial adhesion[197,199], whereas integrin activation without CEACAM binding leads to decreased epithelial adhesion. This suggests that activation of integrin signaling is a conserved strategy for pathogen interaction with vaginal epithelial cells, but the host target is an important determinant of cell behavior. Although *N. gonorrhoeae* and *E. coli* target integrin signaling to prevent exfoliation[197,199], the downstream signaling components of this process are currently unknown, and may explain the divergent strategies used by these bacteria and GBS. Additionally, identifying other host determinants of cell adhesion in response to bacteria that stimulate integrin signaling is an interesting area for further research. Modification of integrin signaling may be a common mechanism for pathogenic manipulation of host cells, as it has been in shown to play a role in viral infection[215], fungal infection[216], Gram negative bacterial infection[197,199,217], and now, Gram positive bacterial infection. Interestingly, *N. gonorrhoeae* also targets $\alpha_1\beta_1$ integrins during urethral mucosa infection[218]. The ubiquitous occurrence of integrin signaling during host-pathogen interactions, as well as the increasingly limited availability of antibiotics, makes integrin signaling an attractive target for therapeutic intervention, and thus warrants further research.

GBS induction of epithelial exfoliation and loss of barrier function is a result of β_1 integrin activation and induction of β-catenin signaling and EMT (Figure 3-S16). The role of EMT, β-catenin signaling, and β_1 integrin activation in response to GBS are novel findings, but the role of EMT during bacterial infection remains poorly understood. Bacterial induction of

EMT is largely thought to be a TLR-mediated process[219] rather than an integrin-mediated process; however, we have found this process to be TLR2 independent for GBS. Recent studies have focused on induction of EMT by bacterial pathogens that are either associated with or are causal agents of cancer[220-222]; however, the induction of EMT by bacterial pathogens that are not associated with cancer receives little attention. β-catenin is a master regulator of many different processes, including organogenesis, cell adhesion, and cancer development[223]. Similar to EMT, its role in bacterial infection is not known. Interestingly, direct and indirect inhibition of the Wnt/β-catenin signaling pathway is an active area of research in cancer progression and metastasis[224-226]. Insights from this field may reveal novel mechanisms applicable to bacterial disruption of the epithelial barrier and for the development of therapeutic compounds that prevent bacterial epithelial colonization. Given the importance of EMT and β-catenin signaling in maintaining the vaginal epithelial barrier, which is the primary defense against many pathogens, more insight is necessary to fully understand how bacterial pathogens colonize and disrupt epithelial surfaces.

While there are many novel findings in this study, we acknowledge limitations. First, our findings stem from experiments performed with immortalized cells and animal models. As performing these studies in humans is not possible, these models are extensively used to provide insight into mechanisms of disease processes[197-199]. However, there are significant biological differences between humans and animal and cell culture models. To fully confirm the importance of EMT and epithelial exfoliation during ascending bacterial infection, these processes should be explored in humans. Secondly, we were unable to attribute vaginal epithelial exfoliation to one microbial factor. In this study, GBS lacking *iagA* acts was used as a model to define the outcome of reduced epithelial exfoliation; however, IagA is a glycosyltransferase[97] that likely does not

directly interact with β_1 integrin. It is possible that multiple GBS factors are directly or indirectly involved in these processes, and this warrants further exploration. Identification of key virulence factors that control GBS induction of integrin signaling and EMT may reveal novel vaccine targets for the prevention of GBS-associated preterm birth. Finally, this study shows an association between a cellular process occurring in the vagina (epithelial exfoliation), and a phenotypic result of this process (ascending bacterial infection), but does not comprehensively identify the mechanism of bacterial trafficking. We speculate that 1) the loss of epithelial barrier function may permit pathogen entry into microvasculature and dissemination into uterine tissues, 2) increases in cellular mobility may inadvertently enable bacterial trafficking to new locations, and/or 3) changes in the cellular architecture may prevent clearance of disseminated bacteria thereby permit bacterial trafficking and persistence.

The importance of preterm birth as a leading cause of neonatal morbidity and mortality cannot be overstated. Premature neonates are at higher risk for respiratory distress syndrome, intracranial hemorrhage, necrotizing enterocolitis, severe neurological disorders, and death[227]. Unfortunately, our knowledge of the causes of preterm birth is incomplete, thus available interventions are limited[3]. A significant portion of this disease burden is attributable to ascending bacterial infection[3]. For successful infection, pathogen-specific factors must be involved in circumventing host defenses. Previously, we have identified multiple bacterial virulence factors that promote ascending infection and preterm birth[60,66], and in this study, we have identified a novel host mechanism that inadvertently promotes entry of GBS into the uterus. GBS strains that are more proficient in inducing integrin signaling, EMT, and vaginal epithelial exfoliation are better able to establish ascending infection. Furthermore, these studies give insight into mechanisms that predispose some individuals to ascending infection and preterm birth, which is

critical for the development of effective interventions. To fully confirm the importance of EMT and vaginal epithelial exfoliation during infections occurring in pregnancy, clinical studies should be designed to explore these processes in humans, and we hope these will ultimately lead to interventions that reduce the global burden of preterm birth.

3.4 MATERIALS AND METHODS

3.4.1 *Ethics Statement*

All animal experiments were approved by the Seattle Children's Research Institutional Animal Care and Use Committee (protocol #13907) and performed in strict accordance with the recommendations in the Guide for the Care and Use of Laboratory Animals of the National Institutes of Health (8th Edition).

3.4.2 *Materials, Bacterial Strains, and Cell Lines*

Chemicals in this study were purchased from Sigma Aldrich, unless stated otherwise. The WT GBS strains COH-1 and CJB111, used in this study, are clinical isolates obtained from infected newborns. COH-1 is a capsular serotype III, hypervirulent ST-17 clone[172] and CJB111 is a capsular serotype V strain[228] (Carol Baker Collection, Division of Infectious Diseases, Baylor College of Medicine, Houston). The Δ*iagA* mutant was previously derived from COH1[97,102]. The *htrA* allelic replacement mutant was generated using methods previously described[229]. GBS were grown in Tryptic Soy Broth (TSB) or on Tryptic Soy Agar (TSA, Difco Laboratories) at 30° or 37° C in 5% CO_2. Erythromycin (5 μg/mL) was added to GBS growth media to retain the plasmid expressing green fluorescent protein (GFP). The *Lactobacillus crispatus* strain used in this study was obtained as a gift from Dr. Michael Fischbach (University

of California, San Francisco). *L. crispatus* was cultured in MRS broth at 37° C under anaerobic conditions. Human vaginal epithelial cells (hVECs) were originally obtained from the American Type Culture Collection (ATCC CRL-2616) and cultured as previously described[106]. Cells were maintained in keratinocyte serum-free medium (KSFM, Invitrogen), supplemented with 65 μg/mL bovine pituitary extract (Invitrogen), 67.419 pg/mL human recombinant epidermal growth factor (Invitrogen), and 50 to 100 I.U./mL penicillin and 50 to 100 μg/mL streptomycin (Corning). Cells were split every 3-4 days and passaged at a 1:10 dilution. All assays were performed at passages 14-30, and prior to infection, antibiotic-containing media was aspirated, cells were washed 2 times with sterile PBS, and media was replaced with antibiotic-free supplemented KSFM. Cells were determined to be mycoplasma free using the Universal Mycoplasma Detection Kit (ATCC).

3.4.3 *Murine Model of GBS Vaginal Colonization and Ascending Infection*

To determine sample size, power calculations (alpha level 0.05) were performed to detect a pre-determined effect size for adverse birth outcomes or changes in bacterial load in genital tissue to obtain 80% power.

3.4.3.1 Vaginal Colonization

Six-to-eight week old female C57BL/6J, B6.129-Tlr2^{tm1Kir}/J (TLR2 knockout), and B6N.129S2-Casp1^{tm1Flv}/J (Caspase 1 knockout) mice were obtained from The Jackson Laboratory and used for colonization studies at 8- to 16-weeks as previously described[119] with some modifications. One day prior to colonization, mice were intraperitoneally injected with 500 μg of 17β-estradiol suspended in 100 μL sterile canola oil as previously described[89], and randomly assigned to an experimental group. No blinding was performed during group

assignment. Overnight GBS cultures were sub-cultured 1:20, grown to OD_{600} = 0.3, pelleted at 2300 x g for 8 min, washed once with sterile PBS, and re-suspended in sterile PBS to a final concentration of 10^{10} CFU/mL. Mice were anesthetized using 4% isoflurane and 10 µL (~10^8 CFU) of GBS was administered into the vaginal tract using a micropipette. Mice were left inverted for an additional 5 minutes under anesthesia, then returned to their cages and monitored until ambulatory, as previously described[119]. After inoculation, mice were monitored daily for signs of distress, euthanized at specified times, and vaginal and uterine tissues were excised for further analysis. For inhibitor studies, 300 ng of recombinant murine $\alpha_1\beta_1$ integrin (R and D Systems) dissolved in 10 µL PBS was administered 1 day prior to GBS inoculation, 2 hours prior GBS inoculation, and every 24 hours up to 96 hours post GBS inoculation. To obtain vaginal lavage fluids, mice were euthanized, and the vaginal lumen of each mouse was lavaged twice with 20 µL sterile PBS using a standard 200 µL pipette tip. Collected fluid was dispensed into a 1mL microcentrifuge tube.

3.4.3.2 Ascending Infection

Six-to-eight week old female C57BL/6J mice were obtained from The Jackson Laboratory, mated for pregnancy, randomly assigned to an experimental group, and inoculated with GBS as previously described[60]. No blinding was performed during group assignment. GBS inoculum was prepared and administered as described above. After inoculation, pregnant mice were monitored twice per day for up to 3 days post-inoculation for signs of preterm labor (vaginal bleeding and/or pups in cage). At 72 hours post-infection, or earlier if preterm labor was observed, mice were euthanized and a midline laparotomy was performed to identify fetal injury or loss of pregnancy. For CFU enumeration, maternal and fetal tissues were excised, homogenized in 1 mL of PBS, serially diluted, and plated on TSA and confirmed as GBS by Granada media or

ChromAgar StrepB as described[119]. In order to minimize use of pregnant mice, data shown in this study for ascending infection of WT GBS (Figure 4h-i) were recently reported in a previous publication[60]. All other mouse work was conducted as part of this study and is not previously reported.

3.4.4 *Scanning Election Microscopy*

Vaginal GBS colonization was performed as above. Excised vaginal tissues were split vertically at one side of the tissue to expose the entire vaginal lumen. Tissues were then pinned onto 3.5% agarose pads using 30-gauge needles and immediately fixed with ~3 mL of ½ Karnovsky's fixative. After 5-10min of fixation, tissues were transferred to ~10 mL of fixative and stored at 4°C until imaging. For hVEC imaging, hVEC monolayers were grown in 6-well tissue culture treated plates on glass coverslips and infected with WT GBS at an MOI = ~1.0. At 24 hours, media was aspirated and 1 mL of ½ strength Karnovsky's fixative was added and stored at 4°C until imaging. Samples were prepared for SEM by the Electron Microscopy Core of Fred Hutch Cancer Research Center. Fixed tissues were washed in 0.1 M Cacodylate Buffer, and then dehydrated using a series of ethanol washes (50%, 70%, 95%, 2 x 100%, 30 min each). After dehydration, samples were dried using a critical point dryer (Tousimis), mounted, and sputter coated with Au/Pd. Images were captured using a JEOL 5800 Scanning Electron Microscope equipped with a JEOL Orion Digital Acquisition System. For quantification, at least 3 images of equal surface area from at least 2 tissues were de-identified, and individual exfoliated cells were counted in a blinded manner.

3.4.5 *GBS GFP Expression Validation*

3.4.5.1 pDEST-erythromycin-GFP Plasmid Loss

WT GBS containing the *pDEST-erythromycin-GFP* plasmid[230] were grown at 30° C in 5% CO_2 overnight in 5 ml TSB with 5 ug/mL erythromycin. The following day, the bacteria were pelleted at 10,000 x g for 10 minutes and washed twice with 5 ml TSB and re-suspended in 5 ml TSB. The bacteria were then sub-cultured 1:20 in 10 ml TSB, grown at 37° C in 5% CO_2 for 8 hour, then sub-cultured 1:20 in 10 ml TSB. This process was repeated for the following four days and CFU were enumerated by serial dilution onto TSA or TSA containing erythromycin. CFU on TSA were compared with CFU on TSA containing erythromycin to detect loss of erythromycin resistance and therefore plasmid loss.

3.4.5.2 GFP expression in response to oxygen availability

WT GBS containing the *pDEST-erythromycin-GFP* plasmid[230] were grown at 30° C in 5% CO_2 overnight in 5 ml TSB with 5 ug/mL erythromycin. The bacteria were then sub-cultured and grown at 37° C in 5% CO_2 or at 37° C in an anaerobic chamber (Coy Laboratory Products). Sub-cultures were then incubated for 24 hours and then pelleted at 10,000 x g for 10 minutes. Bacterial pellets were re-suspended in 500 µl 10% formalin and then FACS buffer was added to a total volume of 1 ml. All data was collected using an LSR II instrument (BD Biosciences) using the following voltages: SSC – 220, FSC – 300, GFP/FITC – 300.

3.4.6 *Cytotoxicity Assay*

Cell cytotoxicity was measured by lactate dehydrogenase (LDH) release assay (Clontech) as per manufacturer's instructions. Briefly, hVEC monolayers grown in 6-well tissue culture

treated plates were infected with WT GBS at an MOI = ~1.0 for 16 or 24 hours. One hour before analysis, an untreated well was treated with 1.0% (v/v) Triton X-100, which served as a positive control. At 16 or 24 hours, 10 µL of media was removed and mixed with the assay reagent supplied in the kit and incubated for 20 min at RT. Following incubation, absorbance was measured with a Spectramax i3x plate reader (Molecular Devices) at 492 nm and referenced at 600 nm. Data are represented as percent cytotoxicity, which is calculated as: $\frac{infected - mock\ infected}{Triton\ X{-}100\ treated - mock\ infected} * 100.$

3.4.7 *Cell Detachment Assay*

For cell detachment experiments, hVEC monolayers grown in 6-well tissue culture treated plates were infected with WT GBS at an MOI = ~1.0. At 0, 16, or 24 hours, 100% crystal violet was added to each well to a final concentration of 10% and incubated at 37° C for 30 min. After 30 min, an empty 6-well plate was inverted over the top of the hVEC-containing 6-well plate and secured with tape. The plates were then inverted and placed in a swinging bucket centrifuge and spun at 1000 x g for 10 min to detach loosely adherent cells. Following centrifugation, the amount of crystal violet associated with remaining adherent cells was measured with a Spectramax i3x plate reader (Molecular Devices) at 585 nm. For FH535 experiments, 1.5 µL of 50 mM FH535 in DMSO was added to 5 mL culture media. One hour before infection, culture media was aspirated from hVEC monolayers and replaced with FH535-containing media. Following pre-incubation with FH535, GBS infection and cell detachment assay was performed as described above. Data are represented as percent cell detachment, which is calculated as: $\frac{remaining\ adherence\ mock\ infected\ cells - remaining\ adherence\ GBS\ infected\ cells}{remaining\ adherence\ mock\ infected\ cells} * 100.$

3.4.8 *Barrier Function Analysis*

Electric cell-substrate sensing (ECIS) was used to measure changes in hVEC barrier function in real time using methods previously described[96,180]. hVEC monolayers were grown to confluence on polyethylene 8W10E+ arrays (Applied BioPhysics). Cells were infected with ~10^5 CFU of WT GBS, *Lactobacillus crispatus*, or GBSΔ*iagA* and monitored for changes in resistance at 1000 Hz over 24 hours using an ECIS ZTheta Instrument (Applied BioPhysics). Data were then normalized to resistance values at the point of infection and subtracted from the mock infected resistance values. For permeability assays, hVECs were grown to confluence on tissue culture treated polycarbonate 0.4 µm transwells (Corning). Cells were infected with 5x10^5 CFU of WT GBS, GBSΔ*iagA*, or mock infected for 24 hours. One hour before analysis, an untreated well was treated with 0.1% (v/v) Triton X-100, which served as a positive control. After 24 hours, the media from both the apical and basal compartments was aspirated, and replaced with either Hank's Balanced Salt Solution (HBSS, Corning) alone (basal), or HBSS containing 50 µg/mL FITC (apical). After 1 hour, 300 µL of media from each basal compartment was removed, and fluorescent intensity was measured in triplicate with a Spectramax i3x plate reader (Molecular Devices) with excitation at 485 nm and emission at 535 nm.

3.4.9 *Nanoparticle Preparation and Characterization*

Red fluorescent COOH-modified polystyrene (PS)[231] particles, 110 nm in hydrodynamic diameter (Molecular Probes) were covalently modified with methoxy (MeO)–PEG–amine (NH_2) (molecular size, 5 kDa; Creative PEGWorks) by COOH-amine reaction, following a modified protocol described previously[232]. PEG, MW 5 kDa, is expected to increase the size of nanoparticles by 10-20 nm[232,233]. 50 µL of PS particle suspension was washed and re-suspended to 4-fold dilution in ultrapure water. An excess of MeO-PEG-NH_2 was added to the particle

suspension and mixed to dissolve the PEG. N-Hydroxysulfosuccinimide was added to a final concentration of 7 mM, and 200 mM borate buffer (pH 8.2) was added to a 4-fold dilution of the starting volume. 1-Ethyl-3-(3-dimethylaminopropyl) carbodiimide (EDC, Invitrogen) was added to a concentration of 10 mM. Particle suspensions were placed on a rotary incubator for 4 hours at 25 °C, centrifuged, and re-suspended in ultrapure water to the initial particle volume (50 µL) and stored at 4 °C. PEG-coated fluorescent nanoparticles were measured by laser Doppler anemometry for net surface charge (ξ-potential), and PDI and hydrodynamic diameter using a Zetasizer NanoZS (Malvern Instruments). Size measurements and PDI were performed at 25°C at a scattering angle of 90°. Samples were diluted 1000-fold in 10 mM NaCl for measurements.

3.4.10 *Nanoparticle Administration in vivo*

Vaginal GBS colonization was performed as above. Following euthanasia, fluorescent nanoparticles (10 µL total volume in PBS) were administered intravaginally by micropipette, as described above. Vaginal tracts were then excised, embedded and frozen in OCT (Tissue-Tek), and stored at -80° C until sectioning. Following sectioning, slides were stored at -80° C until staining. Sectioned tissues were stained with 2 µg/mL 4',6-diamidino-2-phenylindole (DAPI, Life Technologies) for 10 min, then washed twice for 2 min in PBS and stored in SlowFade Gold anti-fade reagent (Life Technologies) until imaging. Images were captured using a Keyence BZ-X710 fluorescent microscope and were quantified using ImageJ v. 1.6.0_24.

3.4.11 *Flow Cytometry Analysis*

3.4.11.1 Surface Expression of EMT Markers in vitro

hVEC monolayers grown in 6-well tissue culture treated plates were infected with WT GBS or GBSΔ*iagA* at an MOI = ~1.0. After 24 hours, tissue culture media was aspirated and

replaced with 1mL of buffer containing 1mM EDTA, 25mM HEPES, and 0.1% BSA (w/v) in PBS (FACS buffer). Cells were then collected using a cell scraper, pelleted at 300 x g for 5 min, washed once in 1mL FACS buffer, re-suspended in FACS buffer containing human Fc block (cat. no. 564219, BD Biosciences), and incubated at RT for 15 min. Approximately 10^6 cells were then pelleted, washed once in FACS buffer, and stained with either PE-conjugated anti-E Cadherin (clone 36, BD Biosciences) or Alexa Fluor 488-conjugated anti-N Cadherin (affinity-purified polyclonal, cat. no. FAB6426G, R&D Systems) for 30 min at RT. Cells were washed twice to remove the antibody, re-suspended in FACS buffer. All data was collected using an LSR II instrument (BD Biosciences). Gates for cell size and nonspecific fluorescence were based on unstained cells, which underwent the same processing in parallel. Surface marker expression was analyzed using FlowJo software version 10 (Tree Star).

3.4.11.2 Surface Expression of Active β_1 Integrin in vitro

For β_1 integrin staining, cells were prepared as above and stained with a 1:200 dilution of anti-β_1 integrin primary antibody (clone 9EG7, BD Biosciences) for 1 hour at 4° C. Following primary antibody staining, cells were pelleted, washed once in FACS buffer, and stained with a 1:200 dilution of Cy3 conjugated secondary antibody (affinity-purified polyclonal, cat. no. ab6953, Abcam). Data collection and analysis was performed as described above.

3.4.11.3 Surface Expression of EMT Markers in vivo

For flow cytometry analysis of isolated murine epithelial cells, cells were stained with either PE-conjugated anti-E Cadherin (clone DECMA-1, BioLegend) and APC-conjugated anti-CD326 (clone G8.8, BioLegend) as described above. PE and APC stained beads (BD

Biosciences) were used for flow cytometry compensation. Data collection and analysis was performed as described above.

3.4.11.4 Detection of GFP Expression in vivo

For flow cytometry analysis of GFP expression GBS in murine tissues, whole vaginal and uterine tissues were homogenized in 1 mL of PBS, pelleted at 300 x g for 5 min, washed once in 1mL FACS buffer, re-suspended in FACs buffer containing human Fc block (cat. no. 564219, BD Biosciences), and incubated at RT for 15 min. Cells were then incubated with a 1:1000 dilution of anti-GBS antibody[234] for 1 hour at 4° C. Following primary antibody staining, cells were pelleted, washed once in FACS buffer, and stained with a 1:200 dilution of Cy3 conjugated secondary antibody (affinity-purified polyclonal, cat. no. ab6939, Abcam). FITC and Cy3 stained beads (BD Biosciences) were used for flow cytometry compensation. Data collection and analysis was performed as described above.

3.4.11.5 Cell Death Phenotyping of Lavaged Vaginal Epithelial Cells

Collected cells from the vaginal lavage were washed once with PBS and then re-suspended at a concentration of ~10^6 cells/mL in FACS buffer anti-mouse CD16/CD32 (1:200, eBioscience) at RT for 15 minutes. Then, cells were stained with anti-mouse CD326-APC (1:100, BioLegend) for 35 minutes at RT, protected from light. Cells were washed twice with FACS buffer and then re-suspended in annexin V binding buffer (10mM HEPES, 140mM NaCl, and 2.5mM CaCl2, pH 7.4) containing Alexafluor 488 conjugated annexin V (1:20, Invitrogen) at RT for 15 minutes, protected from light. Annexin V staining among epithelial cells (CD326+) was analyzed using an LSR II flow cytometer (BD Biociences). Positive events were identified by comparing to unstained control cells.

3.4.12 *Immunohistochemistry*

Vaginal GBS colonization was performed as above. At 24 or 96 hours, mice were euthanized, whole vaginal tracts were excised, mounted on cardboard, and immediately fixed in formalin overnight at 4 °C. Following overnight fixation, formalin was replaced with 70% ethanol and stored at 4 °C until sectioning. Tissues were sectioned, then baked and deparaffinized for 30 min at 60 °C. Antigens were revived in EDTA buffer (pH 9.0 Lieca Bond Epitope Retrieval Solution 2) at 100 °C for 20 min, blocked for in 10% normal goat serum at RT, and stained with a 1:400 dilution of E Cadherin primary antibody (clone 24E10, Cell Signal Technology), a 1:2500 dilution of c-Myc primary antibody (clone D84C12, Cell Signal Technology), a 1:250 dilution of anti-β_1 integrin primary antibody (clone 9EG7, BD Biosciences), or a 1:1000 dilution of rabbit IgG for 30 min at RT. Following primary antibody incubation, slides were treated with Bond Polymer Refine DAB reagent (Leica) for 8 min at RT, blocked with peroxide block (Leica) for 5 min at RT, treated twice with Bond Mixed Refine DAB detection reagent for 10 min at RT, and finally, counterstained with Hematoxylin (Leica) for 4 min. Images were collected with a Leica DMI6000B inverted microscope equipped with a Leica DFC310FX camera. Leica application suite, version 4.0.0 was used as acquisition software.

3.4.13 *Inhibition of Bacterial Invasion by Cytochalasin D*

For Cytochalasin D experiments, 5 or 10 μg/mL Cytochalasin D in culture media was used. One hour before infection, culture media was aspirated from hVEC monolayers and replaced with Cytochalasin D-containing media. Following pre-incubation with Cytochalasin D, WT GBS infection and flow cytometry analysis or cellular invasion assays were performed as described above.

3.4.14 *Primary Murine Vaginal Epithelial Cell Isolation*

Vaginal GBS colonization was performed as above. At 96 hours, mice were euthanized, entire vaginal tracts were excised, placed in RPMI media, and minced for 2 min into pieces < 2 mm in diameter. After mincing, tissues were enzymatically digested (Multi Tissue Dissociation Kit 1, Miltenyi Biotec) at 37 °C in a gentleMACS Octo Dissociator (Miltenyi Biotec) using the Human Tumor Dissociation Kit 1 protocol, per manufacturer's instructions. Following dissociation, dead cells and debris were removed by purifying the samples through the MS MACS Column (Miltenyi Biotec) and the flow through was collected. The flow through samples were then magnetically labeled with CD326 Microbeads (Miltenyi Biotec) and positively selected using a Large Cell MACS Column (Miltenyi Biotec), per manufacturer's instructions. Following isolation, cells were stained and analyzed by flow cytometry as described above.

3.4.15 *Direct E Cadherin Cleavage Analysis*

For recombinant E Cadherin experiments, 20 μg of recombinant human E Cadherin (Advanced BioMatrix) was added to 50 μL overnight GBS culture or and equal volume of PBS. At specified time points, bacterial cells were pelleted and supernatants were transferred to 1.5 mL collection tubes. Directly after transfer, Laemmli buffer (6x) was added to the supernatants and the samples were boiled at 95 °C for 5 min. Following denaturation, samples stored at 4 °C until analysis by western blot.

3.4.16 *Western Blot Analysis*

All primary antibodies used for western blotting were obtained from Cell Signal Technology (anti-E Cadherin, clone 24E10; anti-Phosho-AKT, cat. no. 9271; anti-Phosho-FAK, clone D20B1; anti-Phospho-GSK3β, clone D3A4; anti-AKT, cat. no. 9272; anti-FAK, cat. no.

3285; anti-GSK3β, clone D5C5Z), except anti-GAPDH (affinity-purified polyclonal, cat. no. sc20357, Santa Cruz Biotechnology). For western blot experiments, hVEC monolayers grown in 6-well tissue culture treated plates were infected with WT GBS at an MOI = ~1.0 for 4 or 24 hours or ~100 for 1 hour. Tissue culture media was aspirated and replaced with 500 µL of lysis buffer (recipe above) with protease inhibitor plus phosphatase inhibitor (1 tablet per 5 mL, PhosphoSTOP, Roche), and cell lysates were harvested as described above. Protein concentration was measured by Bradford assay with an 8-point standard curve. Equal amounts of total protein (20 or 40 µg) was added to Laemmli buffer (6x), boiled at 95 °C for 5 min, loaded into precast 10% or 4-20% acrylamide Mini-PROTEAN TGX protein gels (BioRad), and run at 200 V for 40 min. Proteins were then transferred onto PVDF membranes at 100 V for 75 min or at 30 V overnight. Membranes were blocked for at least 1 hour in 1:1 Odyssey blocking buffer (Li-Cor Biosciences) in PBS or TBS and then incubated with primary antibody at 4°C overnight. Membranes were washed 3 times for 5 minutes in PBS or TBS with 1.0% Tween20 (Fisher Scientific) and incubated with Alexa Fluor 680-conjugated anti-rabbit IgG antibody (1:5000 dilution, cat. no. A-21076, Invitrogen) or Alexa Fluor 680-conjugated anti-goat IgG antibody (1:5000 dilution, cat. no. A-21084, Invitrogen) for 30 minutes. Finally, membranes were washed 3 times for 5 minutes in PBS or TBS with 1.0% Tween20, rinsed several times in PBS or TBS, and visualized with the Odyssey Li-Cor infrared imager (Li-Cor Biosciences). Western blot images were quantified using ImageJ v. 1.6.0_24.

3.4.17 *qRT-PCR Analysis*

For qRT-PCR experiments, hVEC monolayers grown in 6-well tissue culture treated plates were infected with WT GBS at an MOI = ~1.0. After 24 hours, tissue culture media was aspirated and total RNA was isolated using the RNeasy miniprep kit (Qiagen) according to

manufacturer protocol. cDNA was generated from whole RNA using the iScript cDNA synthesis kit (BioRad). Equal amounts of cDNA were used to determine gene expression as previously described[180]. A list of primers used in this study can be found in Supplementary Table 1.

3.4.18 *Immunofluorescence*

For immunofluorescence experiments, hVEC monolayers on glass coverslips were infected with WT GBS at an MOI = ~1.0. After 24 hours, tissue culture media was aspirated, replaced with 1 mL 10% formalin, and fixed at 4° overnight. Following fixation, formalin was removed, cells were washed once in PBS, and permeabilized for 20 minutes in 1.0% Triton X-100. Coverslips were washed twice with PBS, then blocked for at least 1 hour in 1 mL SuperBlock PBS blocking buffer (Life Technologies). Next, coverslips were incubated overnight with anti-β catenin antibody (affinity-purified polyclonal, cat. no. ab16051, Abcam), washed twice for 5 minutes in PBS, then incubated with Alexa Fluor 594-conjugated anti-rabbit IgG antibody (1:1000 dilution, cat. no. A-11037, Invitrogen) for 2 hours. For actin staining, cells were solely incubated with ActinGreen 488 ReadyProbes reagent (Life Technologies) for 30 minutes. Finally, coverslips were washed twice for 5 minutes in PBS and mounted in DAPI-containing VectaSheild anti-fade mounting media (Vector Laboratories) and imaged using a Leica DMI6000B inverted microscope equipped with a Leica DFC310FX camera. Leica application suite, version 4.0.0 was used as acquisition software. For immunohistofluorescent imaging, paraffin sections were deparaffinized and epitope revival was performed overnight at 60 °C in citrate buffer (10 mM sodium citrate, 0.05% Tween 20, pH 6.0). Slides were then blocked in 5.0% bovine serum albumin (Sigma) for 2 hours, then incubated for 2 hours at room temperature a 1:1000 dilution of anti-GBS antibody[234]. GBS antibody was detected using anti-rabbit IgG antibody conjugated to Cy3 (1:1000, Abcam) and nuclei were stained with 2 μg/mL

4',6-diamidino-2-phenylindole (DAPI, Life Technologies) and stored in SlowFade Gold anti-fade reagent (Life Technologies) until imaging. Images were captured using a Keyence BZ-X710 fluorescent microscope.

3.4.19 *Inhibition of EMT by FH535*

For FH535 experiments, 1.5 μL of 50 mM FH535 (Tocris Biosciences) in DMSO was added to 5 mL culture media. One hour before GBS infection, culture media was aspirated from hVEC monolayers and replaced with FH535-containing media. Following pre-incubation with FH535, WT GBS infection and flow cytometry or cellular detachment assays were performed as described above.

3.4.20 *Cellular Invasion Assay*

3.4.20.1 In vitro Invasion Assays

For invasion assays, hVEC monolayers grown in 6-well tissue culture treated plates were infected with WT GBS or GBSΔ*iagA* at an MOI = ~1.0 for 30 min or one hour. Then the culture media was aspirated, cells were washed six times with sterile PBS, and antibiotic-containing media (50 μg/mL gentamicin and 5 μg/mL penicillin G) was added to cells for two hours to kill extracellular bacteria. Following killing of extracellular bacteria, culture media was aspirated, cells were washed two more times with sterile PBS, trypsinized, and lysed with 0.1% (v/v) Triton X-100. Intracellular bacteria were enumerated by serial dilution and plating of the cell lysates. Invasive index was calculated as the number of invaded bacterial CFU divided by number adherent bacterial CFU.

3.4.20.2 In vivo Invasion Assays

Collected cells from the vaginal lavage were washed twice in sterile PBS, counted, and then divided into two groups with equal cell numbers. To measure total bacteria recovered from the cells (extracellular and intracellular) one group of cells was lysed with 0.1% (v/v) Triton X-100 and bacterial counts were enumerated by serial dilution and plating onto trypsin soy agar (TSA). To measure intracellular bacteria, the other group of cells was treated with antibiotic-containing media (50 μg/mL gentamicin and 5 μg/mL penicillin G) for 2 hours to kill extracellular bacteria. Following killing of extracellular bacteria, cells were washed twice with sterile PBS and lysed with 0.1% (v/v) Triton X-100. Intracellular bacteria were enumerated by serial dilution and plating of the cell lysates onto TSA. All CFU counts were normalized to the number of cells in each group, and extracellular CFU/100 cells was calculated by subtracting the number of intracellular CFU/100 cells from the total CFU/100 cells.

3.4.21 *Integrin Activity Assay*

For integrin activity assays, hVECs monolayers were infected with WT GBS or GBSΔ*iagA* strains at an MOI = ~100, or treated with an equal volume of sterile PBS. After 1 hour, cells were scraped, counted, washed once with PBS, centrifuged at 300 x g for 5 mins and fixed with 4% paraformaldehyde. 2.5 x 10^5 cells from each group were plated onto a 96-well plate, washed once with PBS, and blocked in 2% BSA in PBS for 30 mins, prior to staining with primary antibody (clone 9EG7, BD Biosciences) diluted 1:1000 in 2% BSA in PBS. After 1 hour, cells were washed once with PBS, and incubated for 20 mins with secondary antibody (recombinant Protein A/G, peroxidase conjugated; ThermoFisher), diluted 1:20,000 in PBS. Cells were washed twice with PBS and developed with TMB Microwell Peroxidase Substrate System (KPL, Gaithersburg, MD, USA). Samples were read at 620 nm before reaction was stopped with 2 M H_2SO_4 and read at 450 nm.

3.4.22 *Statistical Analysis*

All experimental replicates represent biological replicates. Two-sided Students t-test, two-sided Mann-Whitney test, two-sided Fisher's Exact test, or Sidak's multiple comparison test following ANOVA was used to estimate differences as appropriate and p value <0.05 was considered significant. These tests were performed using GraphPad Prism version 5.0 for Windows, GraphPad Software, USA, www.graphpad.com.

3.5 Acknowledgements, Author Contributions, and Conflict of Interest

3.5.1 *Acknowledgements*

We thank Bobbie Schneider, Sharmon Knecht, and Steve MacFarlane for their invaluable assistance with the scanning electron microscopy. We also thank Drs. Adam Lacy-Hulbert, Caroline Stefani, Barry Gumbiner and Bill Carter for insightful discussions. We thank Jan Hamanishi for assistance with the model figure and Seattle Children's Research Institute Vivarium Staff for their assistance and Connie Hughes for administrative assistance.

3.5.2 *Author Contributions*

J.V., B.A., C.G., S.M., M.C., C.L.M., E.N., and L.R. designed the experiments. J.V., B.A., V.S-U., C.G., S.M., M.C., P.Q., E.B., V.A., L.Y.N., and C.W. performed the experiments. C.C. prepared the nanoparticles. K.S.D provided reagents and K.M.A.W. provided the model figures. J.V., E.N., K.M.A.W., and L.R. analyzed the results and wrote the manuscript. All authors reviewed the final version of the manuscript.

3.5.3 *Conflict of Interest*

The authors declare that they have no conflict of interests.

3.6 FIGURES

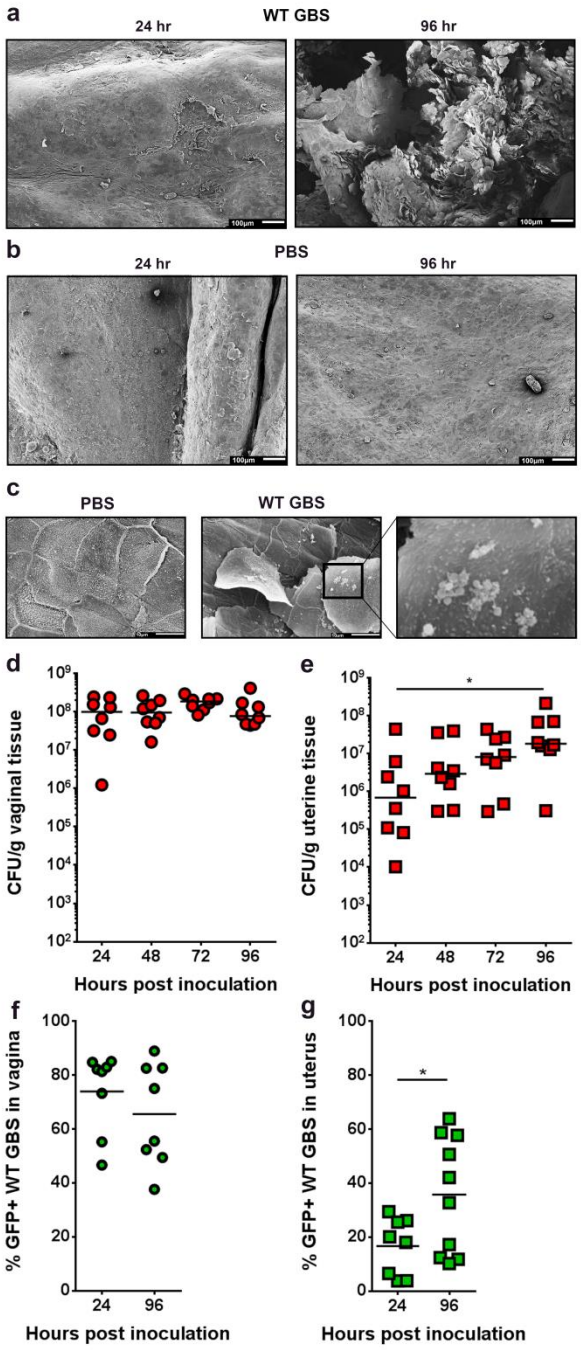
a
WT GBS
24 hr
96 hr
b
PBS
24 hr
96 hr
c
PBS
WT GBS
d
CFU/g vaginal tissue
Hours post inoculation
e
CFU/g uterine tissue
Hours post inoculation
f
% GFP+ WT GBS in vagina
Hours post inoculation
g
% GFP+ WT GBS in uterus
Hours post inoculation

Figure 3-1 – GBS induce vaginal epithelial exfoliation *in vivo*, which correlates with ascending infection

a-d Female WT C57BL6/J mice were vaginally inoculated with approximately 10^8 CFU of either WT GBS or an equal volume of control PBS (n=3/group). Vaginal tissues were analyzed by scanning electron microscopy (SEM) and bacterial burden was assessed in vaginal and uterine tissues. The SEM images show vaginal epithelial exfoliation at 24 and 96 hours post-inoculation with WT GBS (**a**) and not in control PBS (**b**). Scale bar = 100 μm. **c**, High magnification images of the vaginal epithelium show WT GBS associated with exfoliated epithelial cells. Scale bar = 10 μm. Representative images are from one of at least three independent experiments. **d**, Bacterial burden in the vagina (*$p<0.05$, Sidak's multiple comparison test following ANOVA, median displayed). **e**, Bacterial burden in the uterus (*$p<0.05$, Sidak's multiple comparison test following ANOVA, median displayed). **f**, Flow cytometry analysis of GFP positive (GFP+) GBS in the vagina at 24 and 96 hours post-infection (*$p<0.05$, two-sided, unpaired t test with Welch's correction, mean displayed). **g**, Flow cytometry analysis of GFP positive (GFP+) GBS in uterine tissue at 24 and 96 hours post-infection (*$p<0.05$, two-sided, unpaired t test with Welch's correction, mean displayed).

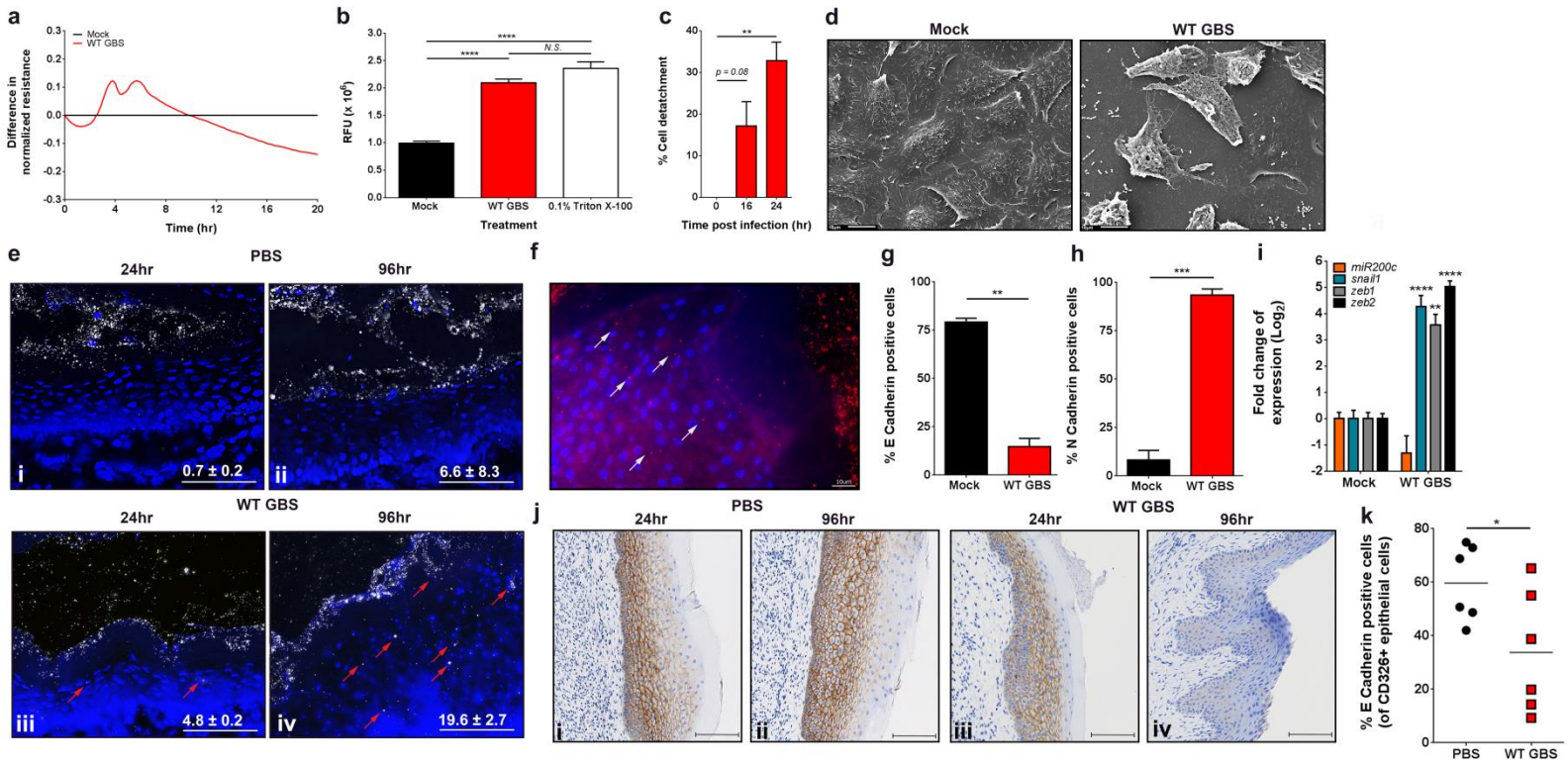

Figure 3-2 – GBS induce loss of barrier function and epithelial-to-mesenchymal transition in vaginal epithelial cells

a, Barrier function of human vaginal epithelial cell (hVEC) monolayers was monitored in real time using electric cell-substrate impedance sensing (ECIS). Infection with WT GBS leads to a disruption in barrier function as determined by the decrease in resistance of the infected monolayers compared to mock (uninfected control, n=3, mean displayed). **b**, hVECs grown on transwells were infected with WT GBS for 24 hours or treated for 1 hour with Triton X-100 (0.1%, positive control). After treatment, fluorescein dye was added to the apical compartment of the transwell, and migration of the dye to the basal compartment was measured after 1

hour (n=3, ****p<0.00005, Sidak's multiple comparison test following ANOVA, data shown represents the average of three independent experiments, error bars ± SEM). **c**, hVECs were infected with WT GBS for 0, 16, or 24 hours and stained with 10% crystal violet for 30 min. Loosely adherent cells were removed by centrifugation, and crystal violet stain intensity for remaining strongly adherent cells was measured. Data are normalized to mock infected controls (n=3, **p<0.005, Sidak's multiple comparison test following ANOVA, mean displayed, error bars ± SEM). **d**, hVECs were infected with WT GBS for 24 hours and analyzed by SEM. Representative images show hVEC detachment 24 hours post-treatment with (i) control PBS or (ii) WT GBS. Scale bar = 10 μm. **e**, Nanoparticle penetration in mouse vaginal epithelia in control saline or WT GBS animals at 24 (i, iii) or 96 (ii, iv) hours post vaginal inoculation, respectively. Nuclei are stained with DAPI and are shown in blue, PEGylated nanoparticles (120 nm diameter) are shown in white, and red arrows indicate intraepithelial nanoparticles. Scale bar = 100 μm. Representative images are from one of at least two independent experiments. Quantitative measurements were calculated using the formula ((mean area intra-epithelial nanoparticle coverage)/(mean epithelial area)) x 10,000 ± SD. **f**, GBS penetration in mouse vaginal epithelia. Nuclei are stained with DAPI and are shown in blue, GBS are shown in red, and white arrows indicate intraepithelial GBS. Scale bar = 10 μm. Representative images are from one of at least four independent experiments. **g-h** Flow cytometry analysis of surface E Cadherin (**g**) or N Cadherin (**h**) on GBS infected hVECs compared to mock (PBS) (n=3, **p<0.005, two-sided, unpaired t test, mean displayed, error bars ± SEM). **i**, qRT-PCR analysis of classical EMT markers in GBS infected hVECs compared to mock (n=3, **p<0.005, ****p<0.00005, Sidak's multiple comparison test following one-way ANOVA, mean displayed, error bars ± SEM). **j**, E Cadherin immunostaining in murine vaginal tracts at 24 and 96 hours post vaginal inoculation of PBS (i, ii) or WT GBS (iii, iv), respectively. Scale bar = 100 μm.

Representative image from one of three independent experiments is shown. **k**, Flow cytometry of surface E Cadherin on CD326+ murine vaginal epithelial cells at 96 hours after vaginal inoculation of WT GBS or control PBS (6 mice/group, *$p<0.05$, two-sided, unpaired t test, mean displayed).

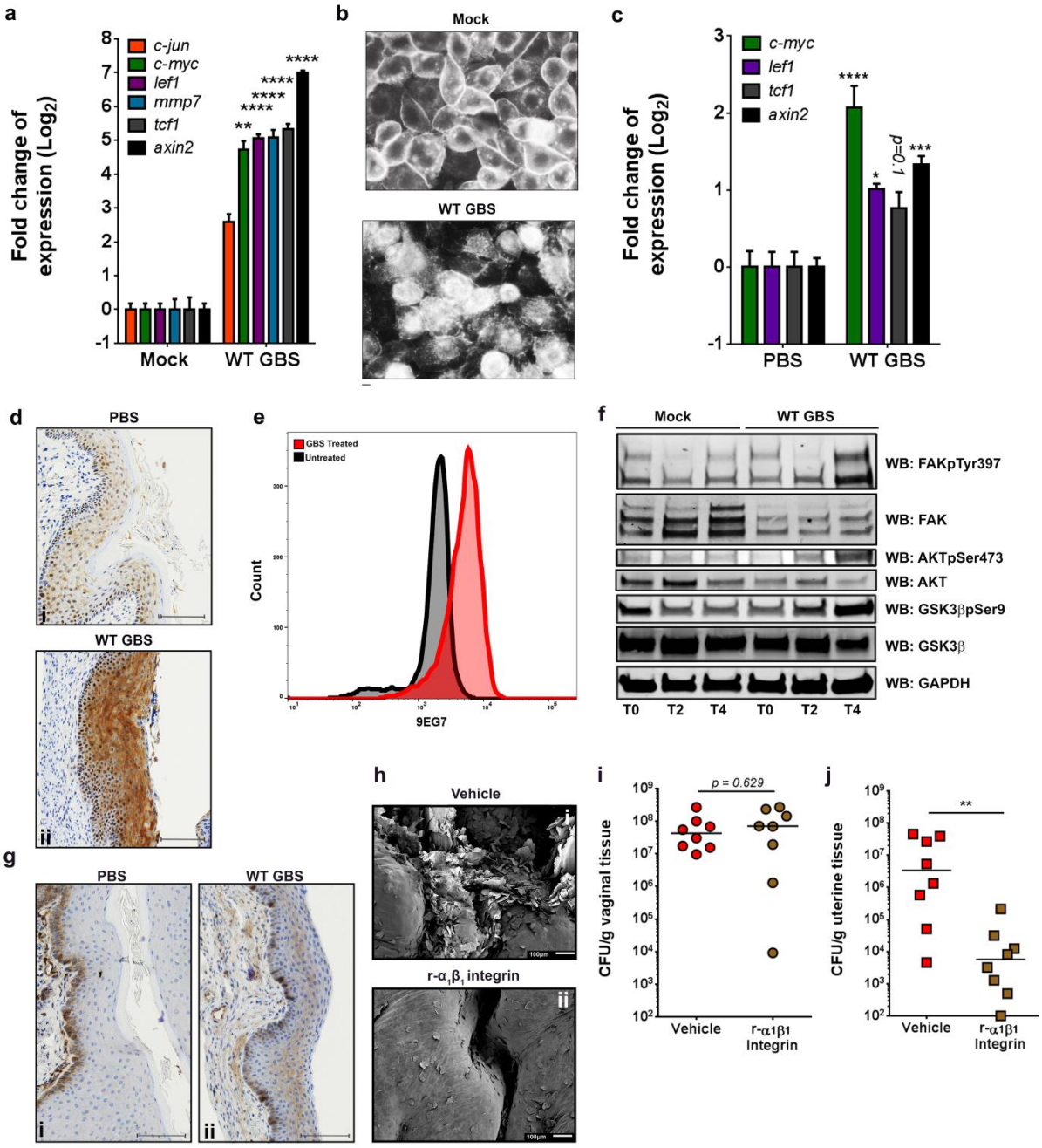

Figure 3-3 – GBS induce β-catenin and integrin signaling in vaginal epithelial cells.

a, Expression of β-catenin target genes in GBS infected hVECs compared to mock controls at 24 hrs post-infection, as measured by qRT-PCR (n=3, **p<0.005, ****p<0.00005, Sidak's multiple comparison test following one-way ANOVA, mean displayed, error bars ± SEM). **b**, Localization of β-catenin in GBS infected hVECs compared to mock controls at 24 hours post-

infection. β-catenin staining is shown in white for ease of visualization. Representative images are from one of three independent experiments. **c**, Expression of β-catenin target genes by qRT-PCR in murine vaginal tissues at 96 hours after vaginal inoculation with WT GBS compared to control PBS (n=4/group, *p<0.05, ***p<0.0005, ****p<0.00005, Sidak's multiple comparison test following one-way ANOVA, mean displayed, error bars ± SEM). **d**, c-Myc immunostaining in murine vaginal tracts at 96 hours post vaginal inoculation with PBS (i) or WT GBS (ii). Scale bar = 100 μm. Representative image from one of three independent experiments is shown. **e**, Flow cytometry of active β_1 integrin (9EG7 antibody) on the surface of GBS infected hVECs compared to mock controls after 24 hours. Representative images are from one of three independent experiments. **f**, Western blots for phosphoproteins FAKpTyr397, AKTpSer473, and GSK3βpSer9 in GBS infected hVECs compared to mock controls at 0, 2, and 4 hours. GAPDH is shown as a loading control. Representative images are from one of three independent experiments. **g**, Active β_1 integrin immunostaining using 9EG7 antibody in murine vaginal tracts at 96 hours post vaginal inoculation with PBS (i) or WT GBS (ii). Scale bar = 100 μm. Representative image from one of three independent experiments is shown. **h**, Vaginal epithelial exfoliation in mice at 96 hours post-vaginal inoculation with WT GBS and treated with control vehicle (i) or recombinant murine $\alpha_1\beta_1$ integrin (ii). Scale bar = 100 μm. **i-j**, Bacterial burden in (**i**) vaginal or (**j**) uterine tissue of mice that were intravaginally treated with recombinant murine $\alpha_1\beta_1$ integrin or control vehicle at 96 hours post vaginal inoculation with WT GBS (**p<0.05, Mann-Whitney test, median displayed).

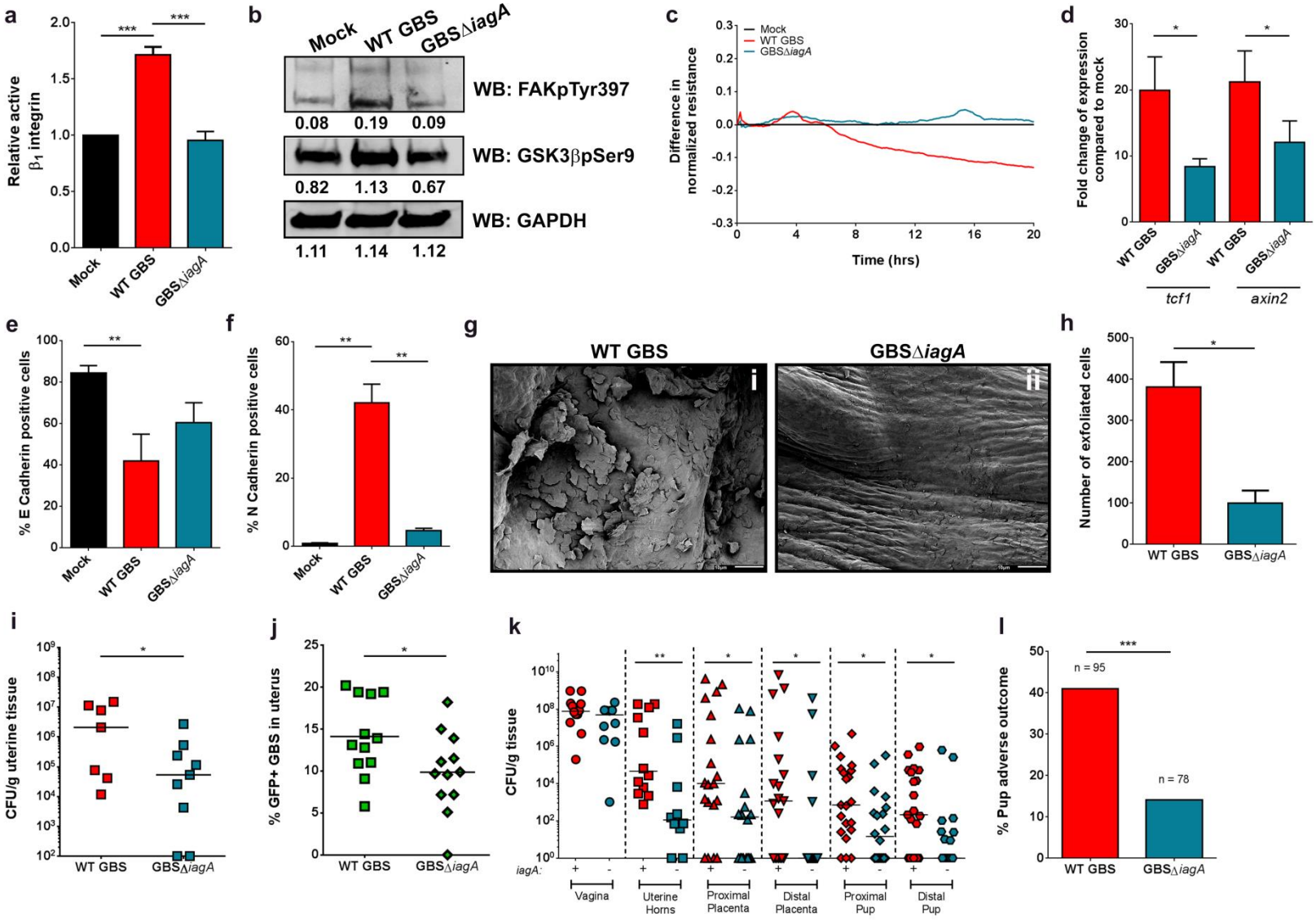
a
Relative active β1 integrin
Mock
WT GBS
GBSΔiagA
b
Mock
WT GBS
GBSΔiagA
WB: FAKpTyr397
0.08 0.19 0.09
WB: GSK3βpSer9
0.82 1.13 0.67
WB: GAPDH
1.11 1.14 1.12
c
Mock
WT GBS
GBSΔiagA
Difference in normalized resistance
Time (hrs)
d
Fold change of expression compared to mock
WT GBS
GBSΔiagA
tcf1
axin2
e
% E Cadherin positive cells
f
% N Cadherin positive cells
g
WT GBS
GBSΔiagA
i
ii
h
Number of exfoliated cells
i
CFU/g uterine tissue
j
% GFP+ GBS in uterus
k
CFU/g tissue
iagA:
Vagina
Uterine Horns
Proximal Placenta
Distal Placenta
Proximal Pup
Distal Pup
l
% Pup adverse outcome
n = 95
n = 78

Figure 3-4 – Reduction of epithelial exfoliation and EMT correlates with decreased ascending infection and preterm birth.

a, Active β_1 integrin on the surface of hVECs infected with either WT GBS, GBSΔ*iagA*, or mock infected (n=3, **p<0.005, Sidak's multiple comparison test following one-way ANOVA, mean displayed with error bars ± SEM). **b**, Western blot for the phosphoproteins FAKpTyr397 and GSK3βpSer9 in hVECs infected with WT GBS, GBSΔ*iagA*, or mock . GAPDH is shown as a loading control. Representative images are from one of three independent experiments. **c**, Barrier function of hVECs infected with WT GBS, GBSΔ*iagA*, or mock control was monitored in real time using ECIS (n=3, mean displayed). **d**, Expression of β-catenin targets (*tcf1*, *axin2*) in hVECs infected with either WT GBS or GBSΔ*iagA* compared to mock controls, as measured by qRT-PCR assay (n=3, *p<0.05, paired t test, mean displayed, error bars ± SEM). **e**-**f**, Flow cytometry of surface E Cadherin (**e**) and N Cadherin (**f**) on hVECs infected with WT GBS, GBSΔ*iagA*, or mock controls for 24 hours (n=3, **p<0.005, Sidak's multiple comparison test following one-way ANOVA, mean displayed with error bars ± SEM). **g**, Vaginal epithelial exfoliation in mice at 96 hours post-vaginal inoculation with WT GBS (i) or GBSΔ*iagA* (ii). Scale bar = 100 μm. Representative images are from one of three independent experiments. **h**, Blinded quantification of exfoliated murine vaginal epithelial cells after 96 hours post-inoculation with WT GBS or GBSΔ*iagA* (n=3 images/3 tissues/group, *p<0.05, two-sided, unpaired t test, mean displayed with error bars ± SEM). **i**, Bacterial burden in the uterine tissue of mice at 72 hours post vaginal inoculation with WT GBS or GBSΔ*iagA* (*p<0.05, Sidak's multiple comparison test following ANOVA, median displayed). **j**, Presence of GFP+ GBS (WT or GBSΔ*iagA*) in uterine tissue at 96 hours post-inoculation, as measured by flow cytometry. (*p<0.05, two-sided, unpaired t test with Welch's correction, mean displayed). **k**, Pregnant female mice were vaginally inoculated with approximately 10^8 CFU of either WT GBS or GBSΔ*iagA*. At 72 hours post-

inoculation or at the first sign of preterm birth (vaginal bleeding and/or pups in cage), mice were euthanized and bacterial burden in vaginal tissue, uterine tissue, placental tissue, or fetal tissue was enumerated (*$p<0.05$, Sidak's multiple comparison test following one-way ANOVA, median displayed). **l**, Pups with adverse birth outcome (either *in utero* fetal demise or premature birth) between pregnant female mice vaginally inoculated with WT GBS (39 of 95 pups) or GBSΔ*iagA* (11 of 78). Data are displayed as percent of pups exhibiting for adverse birth outcomes (***$p<0.0005$, two-sided Fisher's exact test).

3.7 SUPPLEMENTARY FIGURES AND TABLES

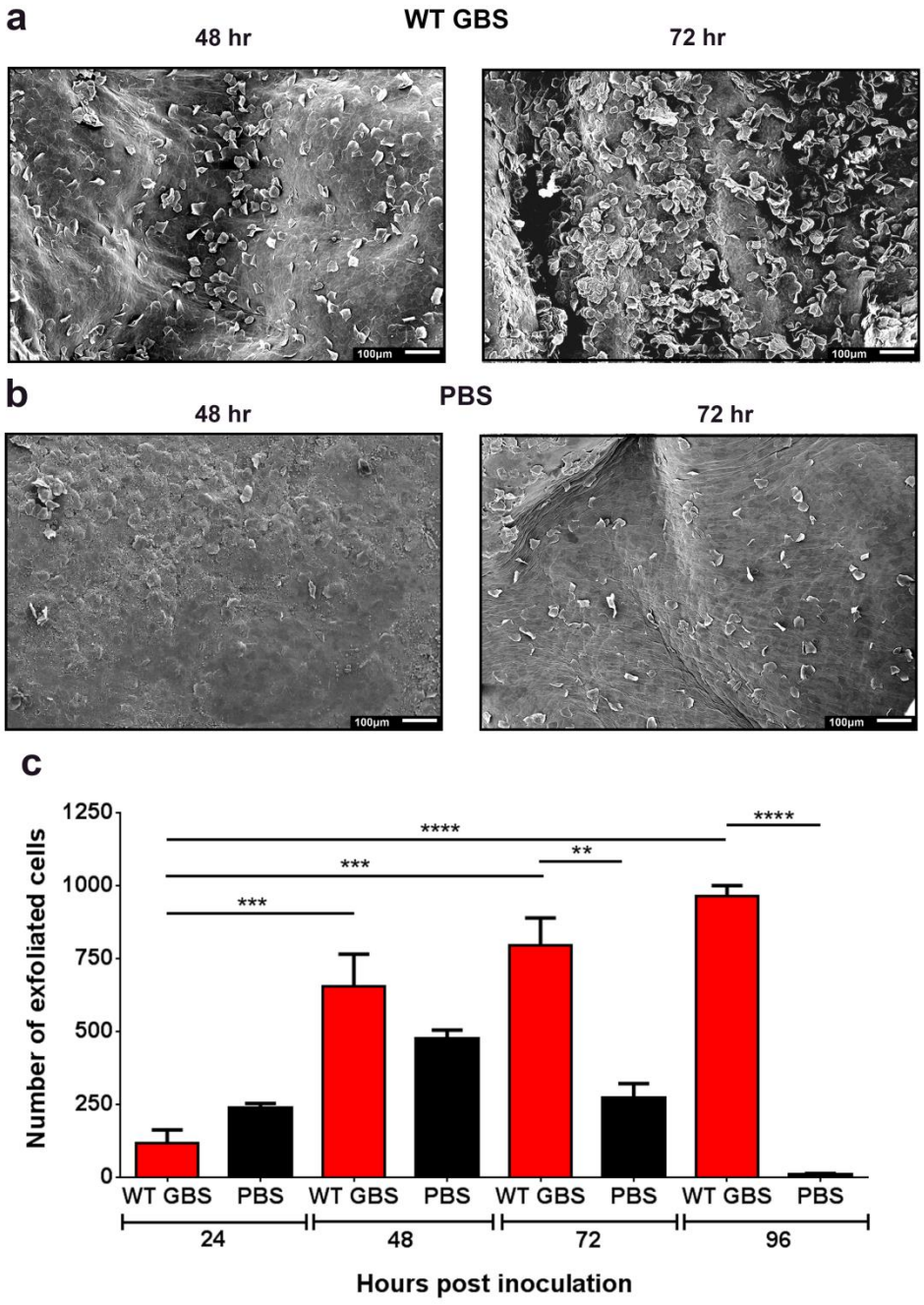

Figure 3-S1 – GBS induces vaginal epithelial exfoliation

a-**b**, Female WT C57BL6/J mice were vaginally inoculated with approximately 10^8 CFU of either WT GBS or an equal volume of control PBS (n=3/group) and analyzed by scanning electron microscopy (SEM). The SEM images show vaginal epithelial exfoliation at 48 and 72 hours post-inoculation with WT GBS (**a**) or control PBS (**b**). Images are representative of one of at least three independent experiments. Scale bar = 100 μm. **c**, Exfoliated vaginal epithelial cells at 24, 48, 72, and 96 hours post-inoculation was quantified in a blinded fashion (n=3 images/2 tissues/group), **p<0.005, ****p<0.00005, Sidak's multiple comparison test following ANOVA, mean displayed, error bars ± SEM).

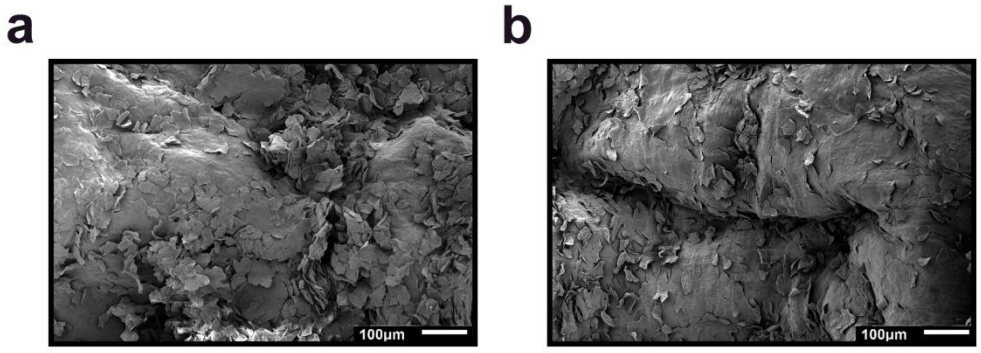

Figure 3-S2 – The GBS strain CJB111 induces vaginal epithelial exfoliation.

a-b, Female WT C57BL6/J mice were vaginally inoculated with approximately 10^8 CFU of the WT GBS strain COH1 or CJB111 and analyzed by scanning electron microscopy (SEM). The SEM image show vaginal epithelial exfoliation at 72 hours post-inoculation with (**a**) COH1 or (**b**) CJB111. Representative image is from one of three independent experiments.

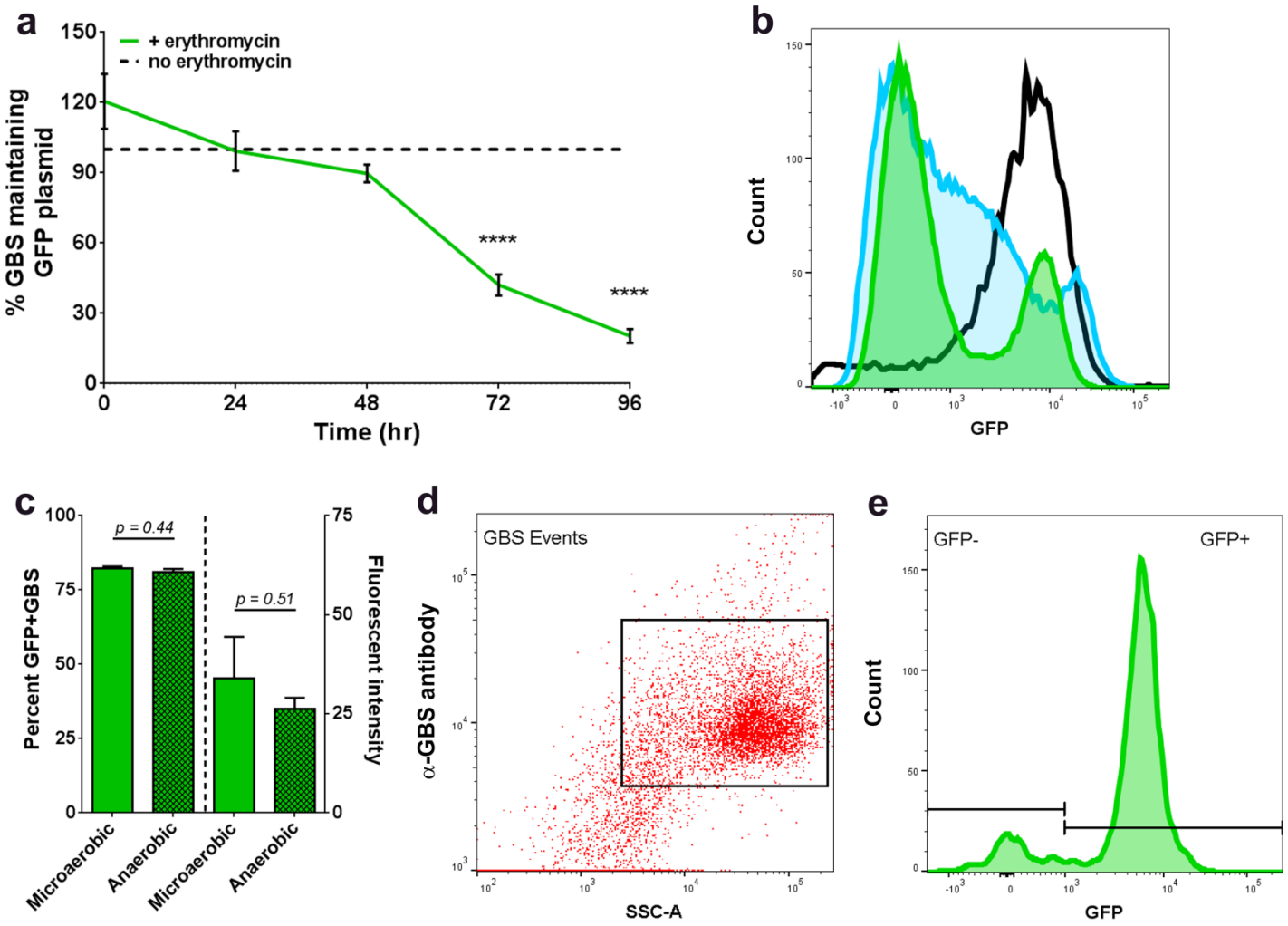
a
+ erythromycin
no erythromycin
% GBS maintaining GFP plasmid
Time (hr)
****
****
b
Count
GFP
c
p = 0.44
p = 0.51
Percent GFP+GBS
Fluorescent intensity
Microaerobic
Anaerobic
Microaerobic
Anaerobic
d
GBS Events
α-GBS antibody
SSC-A
e
GFP-
GFP+
Count
GFP

Figure 3-S3 – Retention of GFP expressing plasmid in the absence of selection pressure *in vitro* and *in vivo*

a, Representative line graph showing maintenance of the GFP-encoding plasmid from GBS with and without selection pressure in culture. Plasmid retention was measured by serial dilution and plating on antibiotic-free and antibiotic-containing media following subculture every 24 hours (n=3, ****p<0.00005, Sidak's multiple comparison test following ANOVA, mean and SEM displayed) **b**, Representative histogram showing flow cytometry analysis of GBS expressing a plasmid-encoded GFP without selection pressure in culture. GFP expression was measured 4 hours (black), 24 hours (blue), and 48 hours (green) after initial removal of selection pressure. Cultures were sub-cultured every 24 hours. Data shown represent images from one of two independent experiments. **c**, GFP expression was measured by flow cytometry under microaerobic and anaerobic growth conditions to represent genitourinary oxygen levels. Data are displayed as total fluorescent GBS (left axis) and fluorescent intensity (right axis, n=3, mean and SEM displayed). **d-e**, Representative scatter plot and histogram of flow cytometry analysis of GBS GFP expression in murine genital tissues. GBS events were gated for size and positive staining with anti-GBS antibody (**d**), and then for GFP expression (**e**). Representative images are from one of sixteen murine tissues obtained from two independent experiments.

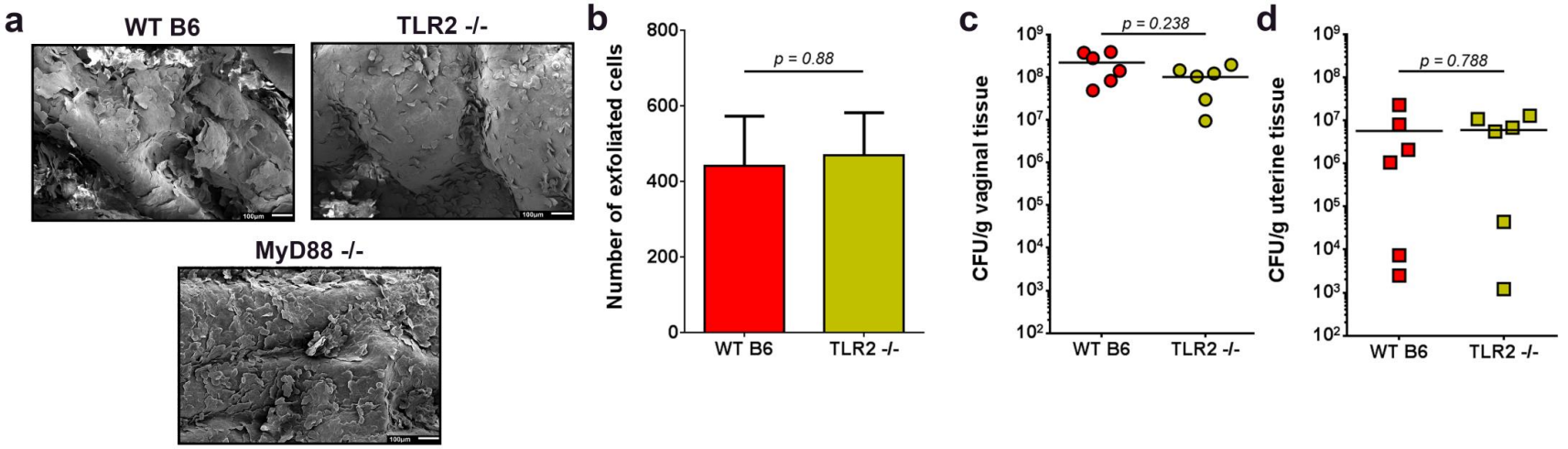

Figure 3-S4 – GBS-induced epithelial exfoliation and ascension is independent of TLR2

a-**d**, Female WT C57BL6/J or B6.129-Tlr2^{tm1Kir}/J (TLR2KO) mice were vaginally inoculated with approximately 10^8 CFU of WT GBS. **a**, Vaginal epithelial exfoliation at 96 hours post-vaginal inoculation of WT GBS in WT C57BL6/J mice (i) or TLR2KO mice (ii). Scale bar = 100 μm. Representative images are from one of three independent experiments. **b**, Blinded quantification of exfoliated murine vaginal epithelial cells at 96 hours post-inoculation of WT GBS in WT C57BL6/J or TLR2 KO mice (n=3 images/3 tissues/group, *p<0.05, two-sided, unpaired t test, mean displayed with error bars ± SEM). **c**-**d**, Bacterial burden in (**c**) vaginal and (**d**) uterine tissue was enumerated at 96 hours post-vaginal inoculation (Mann-Whitney test, median displayed).

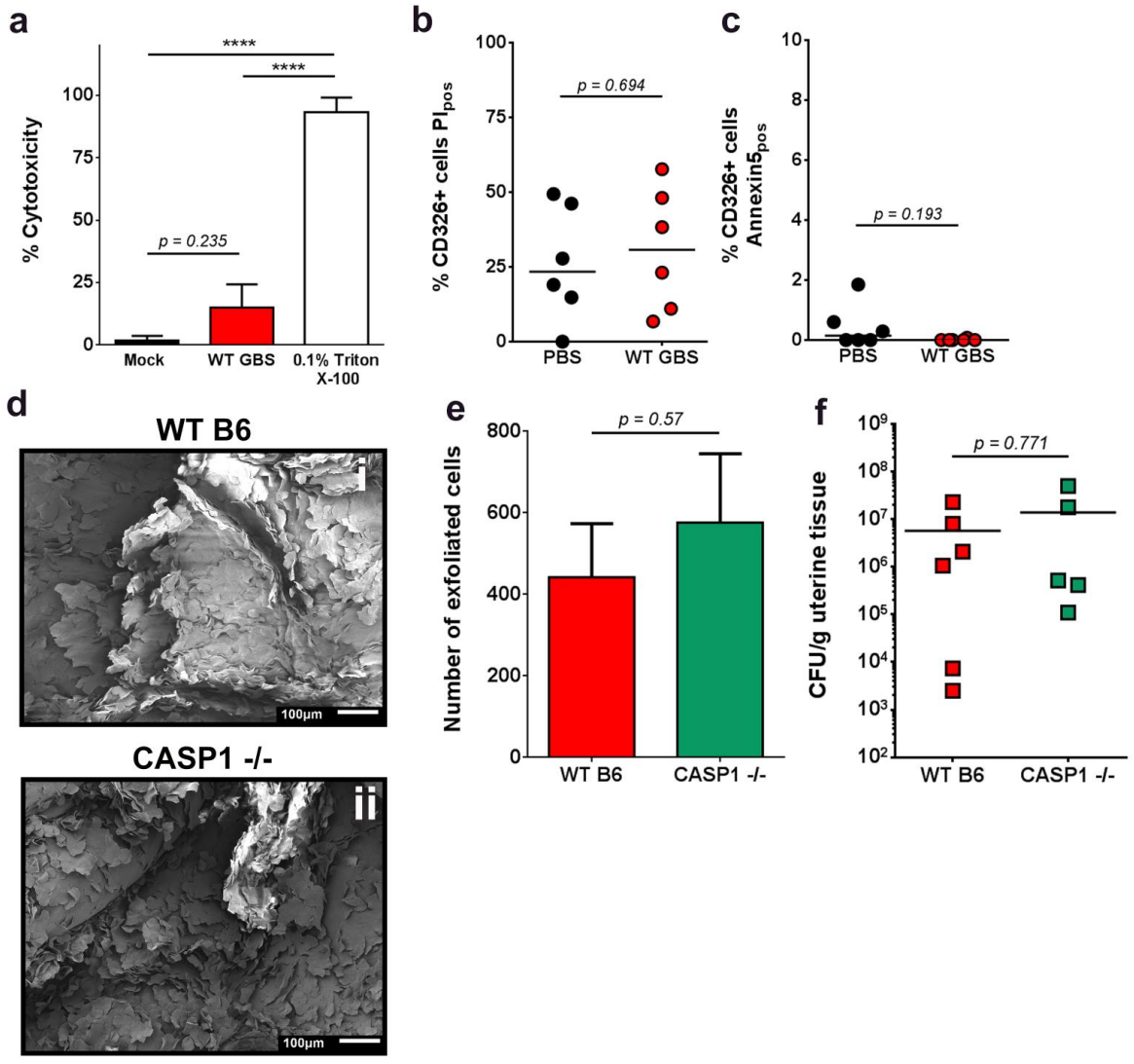

Figure 3-S5 – GBS-induced epithelial exfoliation and ascension are independent of cytotoxicity, apoptosis, and caspase 1.

a, Cytoxoxicty was measured by lactate dehydrogenase (LDH) release assay from hVECs 24 hours after mock infection, infection with WT GBS at an MOI = ~1.0, or treated for 1 hour with 0.1% Triton X-100 (n=4, ****p<0.00005, Sidak's multiple comparison test following ANOVA, mean displayed, error bars ± SEM). **b-f**, Female WT C57BL6/J or B6N.129S2-Casp1^{tm1Flv}/J (Caspase 1 KO) mice were vaginally inoculated with approximately 10^8 CFU of the WT GBS. **b**, Flow cytometric analysis of propidium iodide uptake in vaginal lavage cells recovered from the

mouse vagina at 96 hours post-inoculation (unpaired t test, mean displayed). **c**, Flow cytometric analysis of Annexin 5 in vaginal lavage cells recovered from the mouse vagina at 96 hours post-inoculation (unpaired t test, mean displayed). **d**, Vaginal epithelial exfoliation at 96 hours post-vaginal inoculation of WT GBS in WT C57BL6/J mice (i) or Caspase 1 KO mice (ii). Scale bar = 100 μm. Representative images are from one of three independent experiments. **e**, Blinded quantification of exfoliated vaginal epithelial cells at 96 hours post-inoculation with WT GBS in WT C57BL6/J or Caspase 1 KO mice (n=3 images/3 tissues/group, *$p<0.05$, two-sided, unpaired t test, mean displayed with error bars ± SEM). **f**, Bacterial burden in uterine tissue was enumerated at 96 hours post-vaginal inoculation (Mann-Whitney test, median displayed).

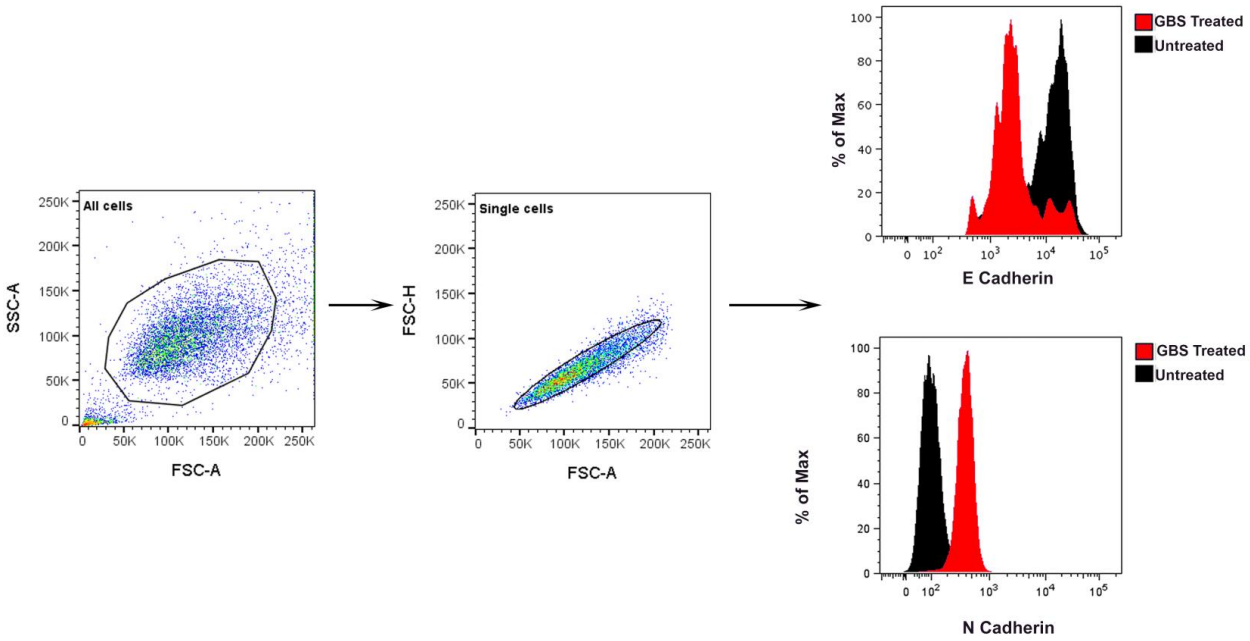

Figure 3-S6 – Human vaginal epithelial cell gating strategy

Representative scatter plots and histograms of flow cytometry analysis of EMT marker expression in hVECs. hVEC's that were untreated or infected with GBS were harvested 24 hrs post infection and were first gated for single cells, then analyzed for E cadherin or N cadherin as shown above.

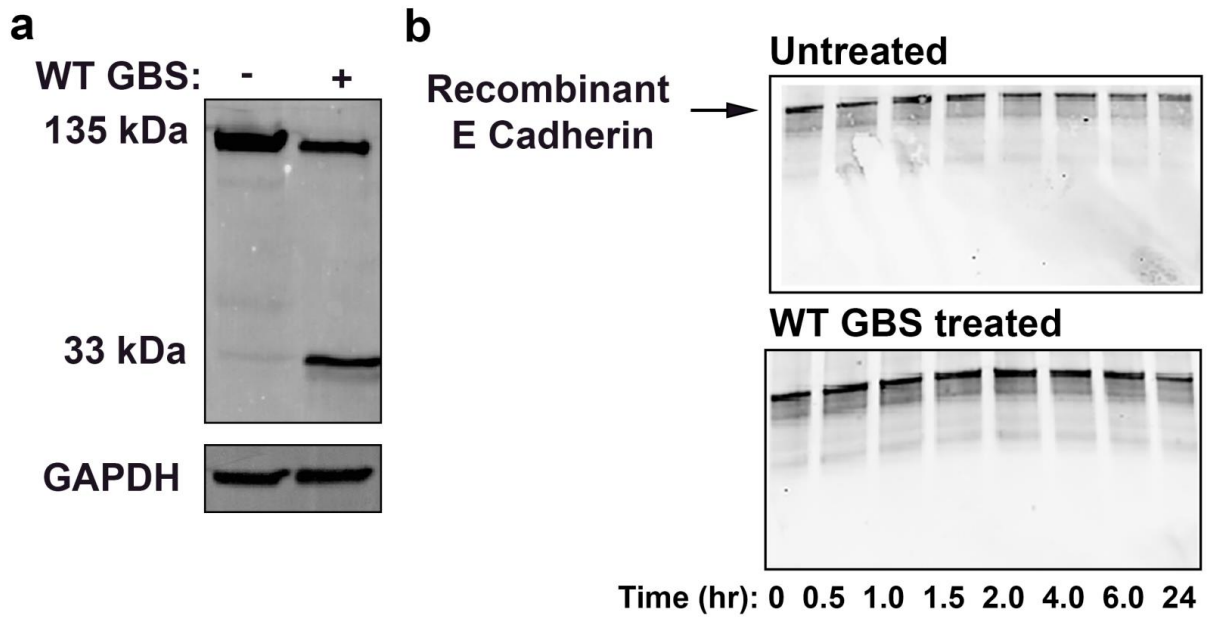

Figure 3-S7 – GBS does not directly cleave E Cadherin

a, E Cadherin western blot on hVECs that were untreated or treated with WT GBS. GAPDH was included as a loading control. Representative image from one of three independent experiments is shown. **b**, E Cadherin western blot showing commercially purified recombinant E Cadherin directly incubated with WT GBS or control media (untreated). Representative images are from one of two independent experiments.

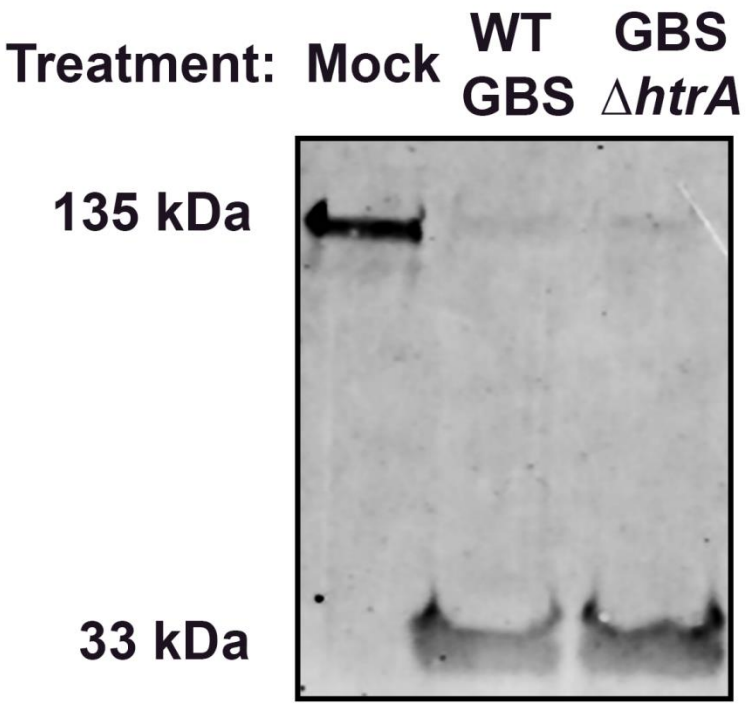

Figure 3-S8 – E Cadherin cleavage is not dependent on the GBS serine protease HtrA

E Cadherin Western blot from hVECs infected with WT GBS, GBSΔ*htrA*, or mock after 24 hours. Representative image is from one of two independent experiments.

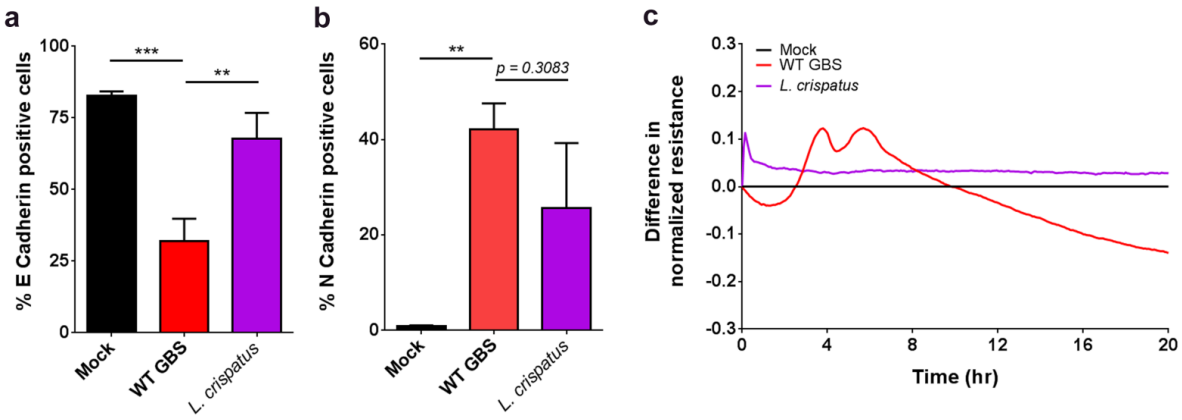

Figure 3-S9 – A common vaginal commensal does not induce EMT or loss of barrier function

a-**b**, Flow cytometry quantification of surface E Cadherin (**a**) or N Cadherin expression (**b**) from hVECs infected for 24 hours with either WT GBS, *Lactobacillus crispatus* (a vaginal commensal/symbiont), or mock control (n=2, **p<0.005, ***p<0.0005, Sidak's multiple comparison test following one-way ANOVA, mean and SEM displayed). **c**, Barrier function of hVEC monolayers was monitored in real time using ECIS. Infection with WT GBS leads to a disruption in barrier function as determined by the decrease in resistance of the infected monolayers compared to mock while *Lactobacillus crispatus* infection does not affect barrier function (uninfected control, n=3, mean displayed).

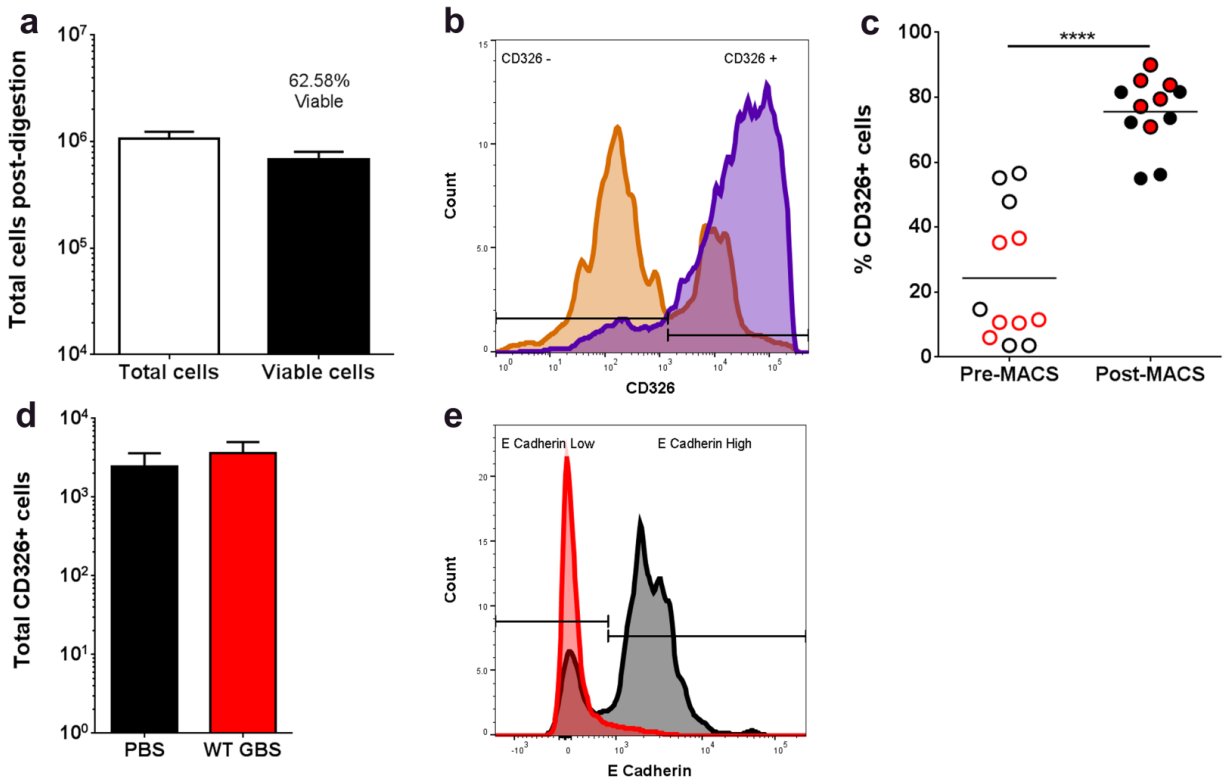

Figure 3-S10 – Validation of CD326+ epithelial cells isolation from murine vaginal tracts

a, Analysis of total and viable cells recovered following enzymatic digestion of murine vaginal tissues prior to CD326 selection. Viability was assessed by trypan blue staining (n=12, mean displayed, error bars ± SEM). **b**, Representative histogram showing flow cytometry analysis of CD326 purity prior to CD326 MACS selection (orange) and following CD326 MACS selection (purple). Representative histogram is from one of twelve tissues obtained. **c**, Compiled flow cytometry analysis of CD326 purity before (pre) and after (pro) MACS selection. Data shown indicate mice inoculated with WT GBS (red) or control PBS (black, ****p<0.00005, two-sided, unpaired t test with Welch's correction, mean displayed). **d**, Flow cytometry analysis of total number of CD326+ cells per sample (n=6, mean displayed, error bars ± SEM). **e**, Surface E Cadherin on CD326+ murine vaginal epithelial cells at 96 hours post-inoculation with WT GBS

(red) or control PBS (black). Representative histogram are from one of twelve tissues from two independent experiments.

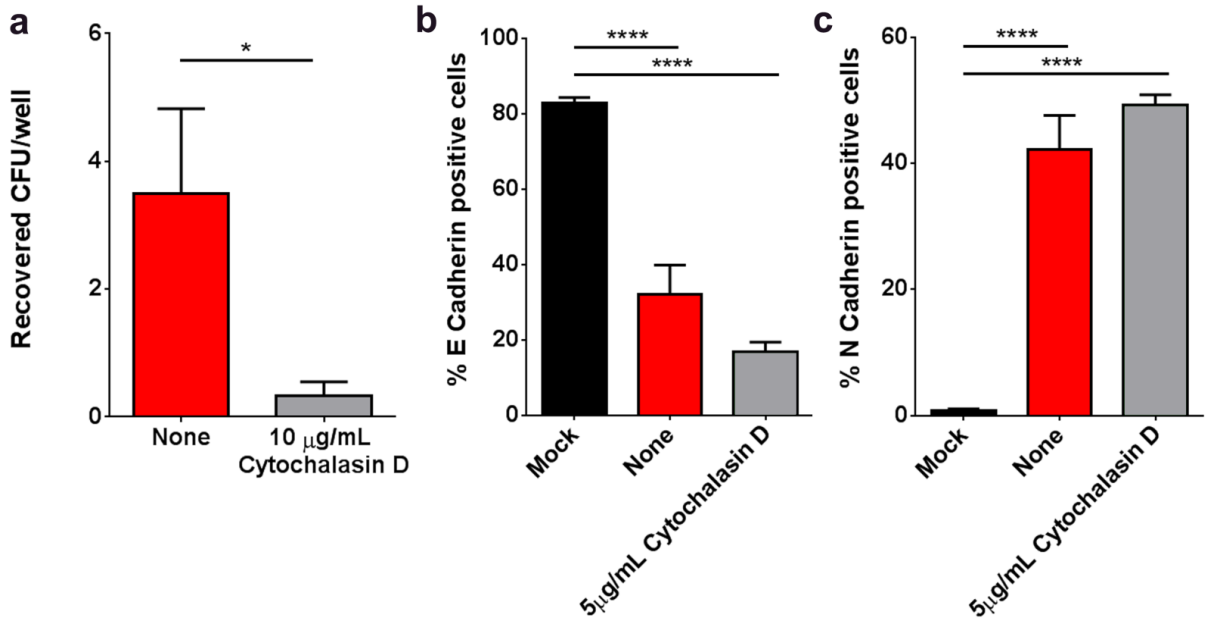

Figure 3-S11 – GBS invasion does not drive EMT

a, GBS invasion of hVECs after one hour of infection in the presence and absence of 10 μg/mL cytochalasin D (n=3, *p<0.05, two-sided, paired t test, mean displayed, error bars ± SEM). **b-c**, Flow cytometry quantification of surface E Cadherin (**b**) or N Cadherin (**c**) in GBS infected hVECs in the presence or absence of 5 μg/mL cytochalasin D (n=3, ****p<0.00005, Sidak's multiple comparison test following one-way ANOVA, mean and SEM displayed).

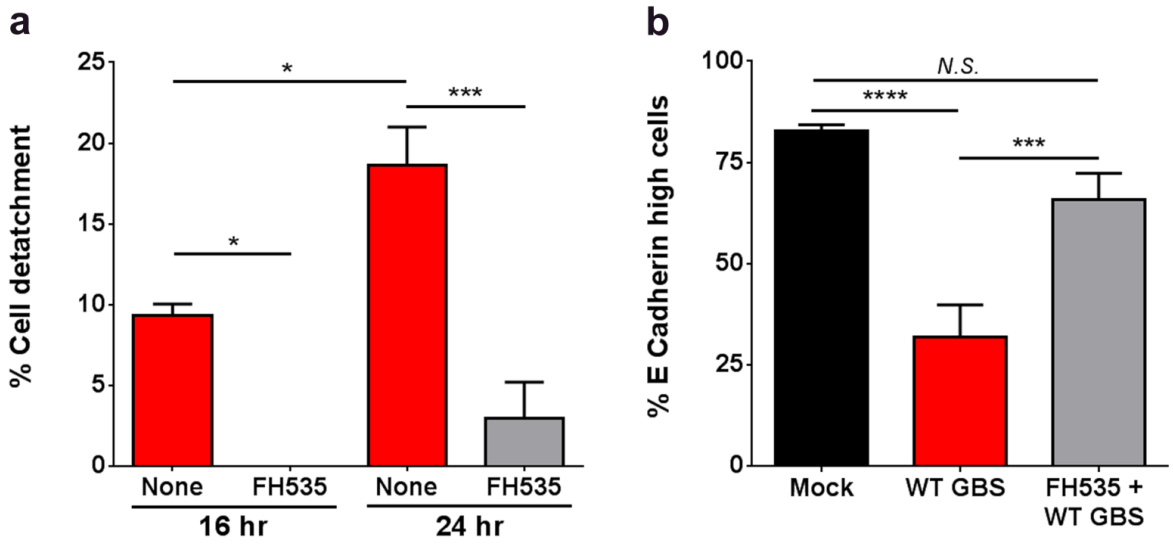

Figure 3-S12 – β-Catenin signaling inhibitor FH535 prevents cell detachment and EMT

a, hVECs were untreated or treated with the β-Catenin signaling inhibitor FH535 (15 µM) for one hour prior to WT GBS infection for 16 or 24 hours; loosely adherent cells were then quantified using 10% crystal violet (see Materials and Methods). Data are normalized to uninfected controls (n=3, *p<0.05, ***p<0.0005, Sidak's multiple comparison test following ANOVA; mean displayed, error bars ± SEM). **b**, Flow cytometry analysis of surface E Cadherin on hVECs that were either untreated (Mock), treated with WT GBS or were pretreated with 15 µM FH535 for one hour prior to infection with WT GBS for 24 hours (n=3, ***p<0.0005, ****p<0.00005, mean displayed, error bars ± SEM).

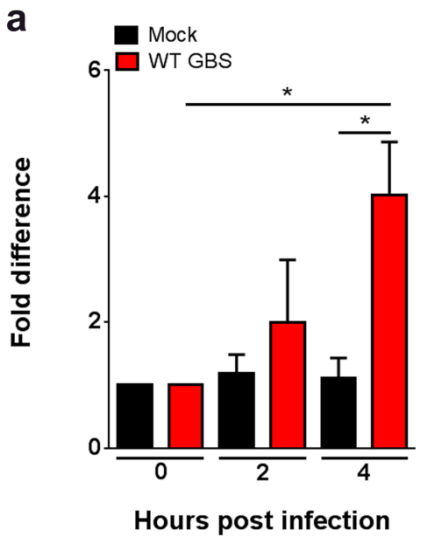
a
Mock
WT GBS
*
*
Fold difference
0
2
4
6
0
2
4
Hours post infection

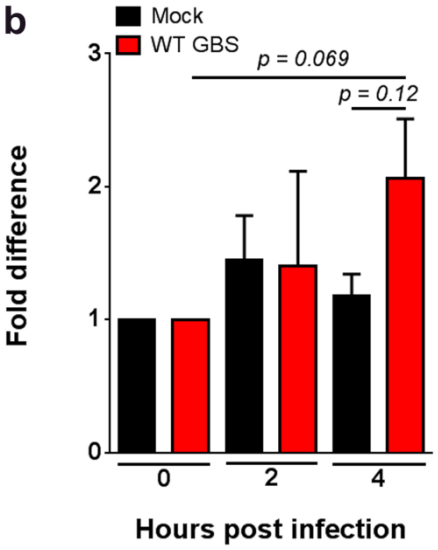
b
Mock
WT GBS
p = 0.069
p = 0.12
Fold difference
0
1
2
3
0
2
4
Hours post infection

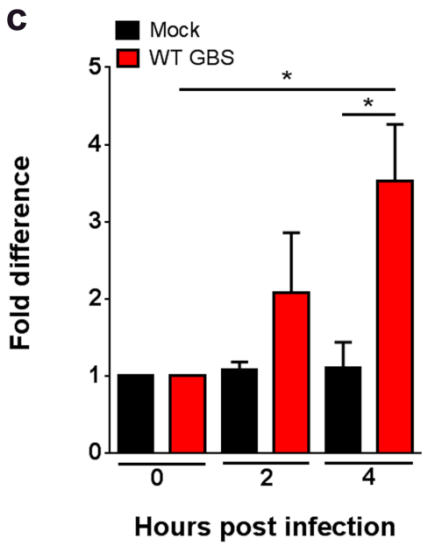
c
Mock
WT GBS
*
*
Fold difference
0
1
2
3
4
5
0
2
4
Hours post infection

Figure 3-S13 – Quantification of western blots for phosphoproteins FAKpTyr397, AKTpSer473, and GSK3βpSer9

a-c, Quantification of band intensity of western blots for phosphoproteins (Figure 4) FAKpTyr397 (**a**), AKTpSer473 (**b**), and GSK3βpSer9 (**c**). Band intensity was first normalized to GAPDH as a load control, then to T0 of the corresponding treatment (n=3/group, *$p<0.05$, Sidak's multiple comparison test following one-way ANOVA, mean displayed with error bars ± SEM).

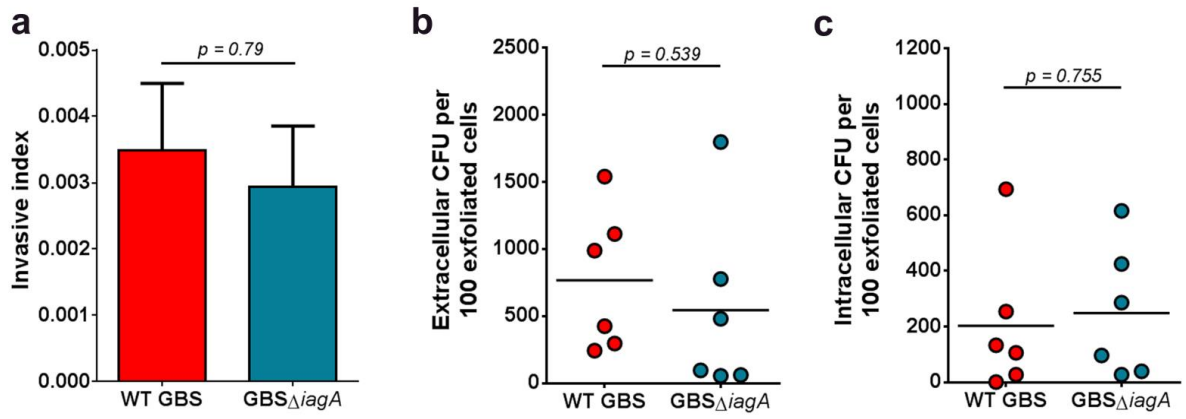

Figure 3-S14 – IagA does not affect invasion of vaginal epithelial cells

a-**c**, Decreased epithelial exfoliation by GBSΔ*iagA in vivo* (Figure 4) does not correlate with decreased invasion. **a**, The invasive index (number of invaded bacterial CFU divided by number adherent bacterial CFU) of WT GBS or GBSΔ*iagA* was measured in hVECs 30 min after infection. **b**-**c**, Female WT C57BL6/J mice were vaginally inoculated with approximately 10^8 CFU of the WT GBS or GBSΔ*iagA*, and exfoliated cells were collected by lavage. Extracellular (**b**) and intracellular (**c**) bacterial burden was enumerated by serial dilution and plating (unpaired t test, mean displayed).

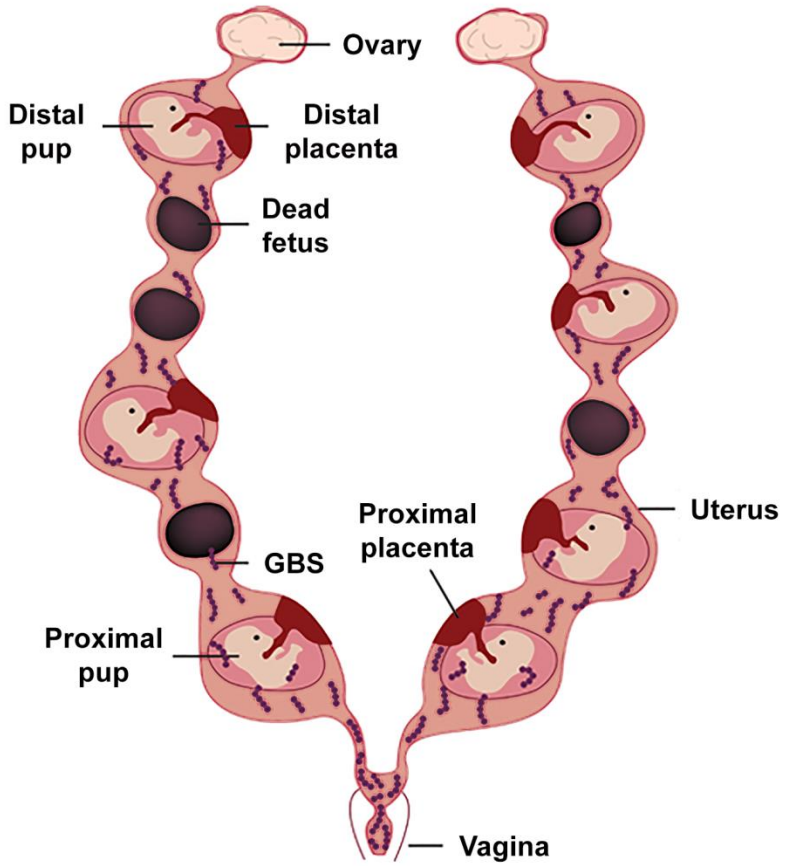

Figure 3-S15 – Diagram of murine female genital tract during pregnancy

The murine female genital tract is comprised of a bifurcated uterus that contains multiple embryonic sacs that contain a single pup and placenta. GBS are inoculated into the vagina, whereupon it ascends into the pregnant uterus where it can infect uterine tissue, placentas, and pups. If fetuses die *in utero*, they can be resorbed or removed through preterm birth. In these studies, "proximal" and "distal" pups and placentas are labeled in reference to the vagina, where "proximal" refers to those closest to the vagina and "distal" refers to those furthest from the vagina.

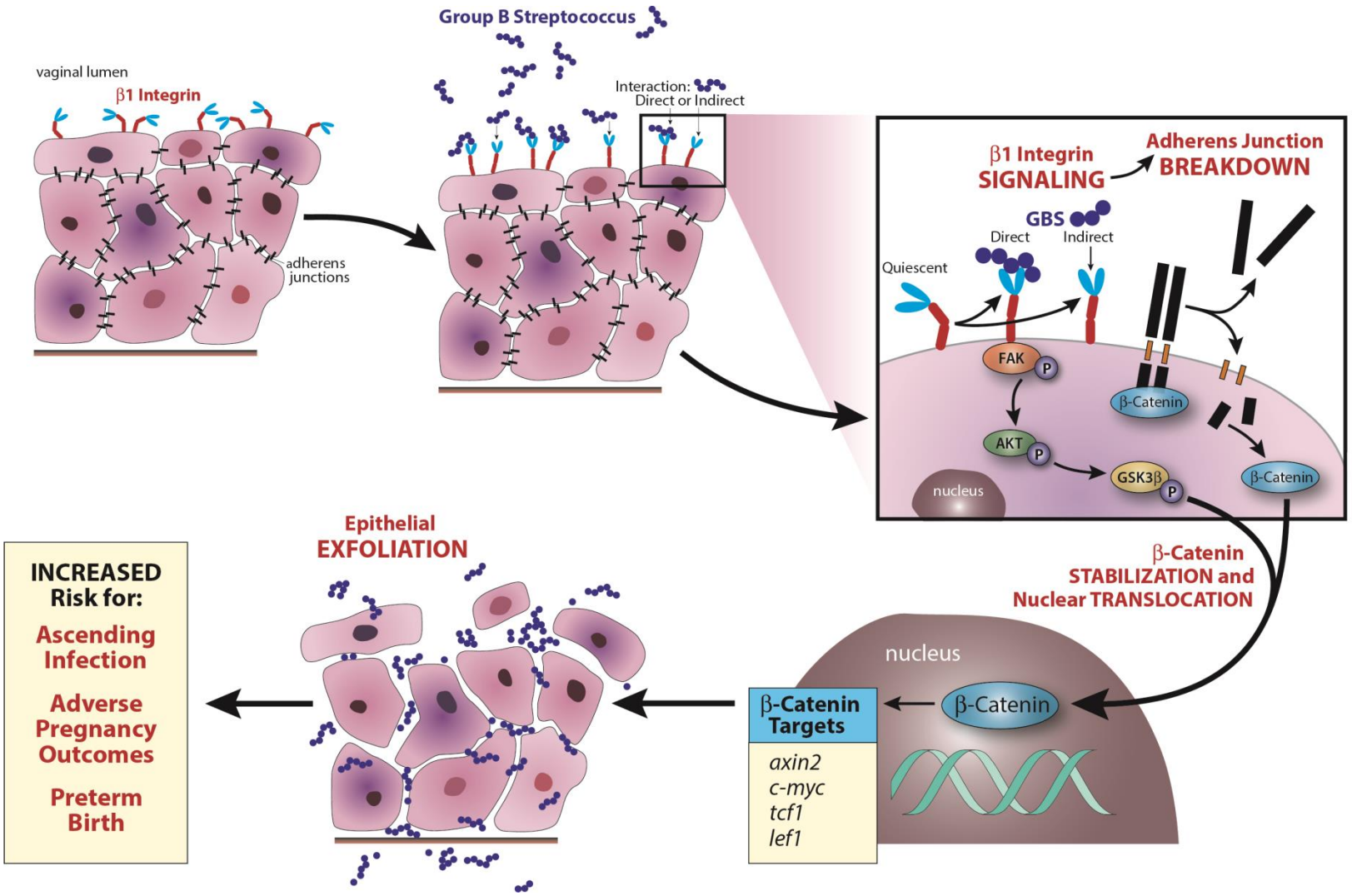
vaginal lumen
β1 Integrin
adherens junctions
Group B Streptococcus
Interaction: Direct or Indirect
β1 Integrin SIGNALING
Adherens Junction BREAKDOWN
GBS
Direct
Indirect
Quiescent
FAK
P
β-Catenin
AKT
P
GSK3β
P
β-Catenin
nucleus
β-Catenin STABILIZATION and Nuclear TRANSLOCATION
nucleus
β-Catenin
β-Catenin Targets
axin2
c-myc
tcf1
lef1
Epithelial EXFOLIATION
INCREASED Risk for:
Ascending Infection
Adverse Pregnancy Outcomes
Preterm Birth

Figure 3-S16 – Model of GBS-induced epithelial exfoliation and ascending infection

Upon GBS colonization, β_1 integrin is either directly or indirectly activated by GBS. Upon β_1 integrin activation, focal adhesion kinase (FAK) is phosphorylated, which in turn phosphorylates AKT, which phosphorylates GSK3β. As adherens junctions breakdown, β-catenin is released into the cytoplasm. In its de-phosphorylated form, GSK3β marks β-catenin for degradation, thus preventing β-catenin stabilization, nuclear translocation, and signaling; however, when it is phosphorylated, it cannot mark β-catenin for degradation, leading to β-catenin stabilization and nuclear translocation. Once in the nucleus, β-catenin stimulates expression of a variety of genes, including those that drive epithelial-to-mesenchymal transition and epithelial exfoliation. Rather than removing colonization GBS, epithelial exfoliation permits bacterial dissemination through loss of barrier function. This leads to increased ascending infection, which increases these rates of adverse pregnancy outcomes and preterm birth.

Chapter 4. Role of the GBS hyaluronidase in ascending infection

The following text is from the article:

Jay Vornhagen, Phoenicia Quach, Erica Boldenow, Sean Merillat, Christopher Whidbey, Lisa Y. Ngo, Kristina Adams Waldorf, Lakshmi Rajagopal. (2016) Bacterial hyaluronidase promotes ascending GBS infection and preterm birth. **mBio**, vol. 7, no. 3, e00781-16.

Figure numbers have been updated to conform to the dissertation. The text remains as published with minor editorial changes.

4.1 ABSTRACT

Preterm birth increases the risk of adverse birth outcomes and is the leading cause of neonatal mortality. A significant cause of preterm birth is *in utero* infection with vaginal microorganisms. These vaginal microorganisms are often recovered from the amniotic fluid of preterm birth cases. A vaginal microorganism frequently associated with preterm birth is Group B Streptococcus (GBS) or *Streptococcus agalactiae*. However, the molecular mechanisms underlying GBS ascension are poorly understood. Here, we describe the role of the GBS hyaluronidase in ascending infection and preterm birth. We show that clinical GBS strains associated with preterm labor or neonatal infections have increased hyaluronidase activity compared to commensal strains obtained from rectovaginal swabs of healthy women. Using a murine model of ascending infection we show that hyaluronidase activity was associated with increased ascending GBS infection, preterm birth and fetal demise. Interestingly, hyaluronidase activity reduced uterine inflammation, but did not impact placental or fetal inflammation. Our study shows that hyaluronidase activity enables GBS to subvert uterine immune responses leading to increased rates of ascending infection and preterm birth. These findings have important implications for the development of therapies to prevent *in utero* infection and preterm birth.

4.2 INTRODUCTION

Preterm birth is a major indicator for neonatal morbidity and mortality[2,3]. Approximately 6-15% of all deliveries are preterm, resulting in an estimated 4 million neonatal deaths per year, making preterm birth the leading cause of mortality in neonates and in children under 5 years of age[4,235-238]. The largest burden of neonatal and under-5 mortality due to preterm birth is

concentrated in Sub-Saharan Africa and Southern Asia, where healthcare systems are often too weak to effectively manage high preterm birth rates[9]. Preterm birth rates are also alarmingly high in the developed world, including North America, where it has an annual healthcare cost in the tens-of-billions of dollars[3,239]. In order to reduce the burden and subsequent cost of preterm birth, we need a better understanding of the causes and physiology of its biological processes.

Although the clinical events associated with preterm birth have been well-studied, its underlying causes remain ill-defined. An estimated 25-40% of preterm births are a result of *in utero* bacterial infection[240]. Bacteria can be recovered from the amniotic fluid of preterm birth cases[42,241,242]. Bacteria reach the amniotic fluid by means of ascending infection, which occurs when bacteria penetrate the cervical barrier and enter the uterus[3]. Once in the uterine space, bacteria cause multiple physiological events associated with preterm birth, including increased levels of pro-inflammatory cytokines, chorioamniotic membrane rupture, cervical ripening, and uterine contraction[3,96,241,243,244]. One group of bacteria associated with these physiological events that has been recovered from amniotic fluid is Group B Streptococcus (GBS) or *Streptococcus agalactiae*[42,96,243,245,246]. GBS are a leading cause of neonatal morbidity and mortality, and approximately 30% of healthy women are recto-vaginally colonized with GBS[4,235,236,238]. Heavy vaginal GBS colonization is the primary risk factor for GBS-associated preterm birth[43,247]. Despite the large number of women at risk for GBS-associated preterm birth, little is known about the bacterial and host factors involved in GBS colonization and ascending infection.

Multiple host and bacterial factors play a role in ascending infection and preterm birth. One such factor is the high-molecular weight polymer hyaluronic acid, which is cleaved by hyaluronidases. Hyaluronic acid polymers have multiple roles, including a structural role in epithelial cell extracellular matrix (ECM) formation, aiding in cell migration, cell-cell signaling,

and induction of ECM remodeling enzymes and inflammation[109]. Recently, it has been shown that cervical hyaluronic acid protects against ascending infection and preterm birth due to its role in epithelial barrier function, and that lipopolysaccharide-induced murine cervical hyaluronidase expression increases the risk of preterm birth[110,111,248]. These studies highlight the importance of hyaluronic acid and hyaluronidases during pathogen colonization and preterm birth, but a mechanistic connection between pathogen hyaluronidase activity during vaginal colonization and preterm birth is not known.

Interestingly, GBS produces a hyaluronidase (hereafter referred to as "HylB"), encoded by the *hylB* gene. HylB was first identified in the 1950s and is well-characterized as a specific exolytic enzyme[108,249,250]. It was recently determined that HylB plays an important role in GBS evasion of the host immune system[65]. These studies show that GBS degrades hyaluronic acid into disaccharide fragments, which blocks toll-like receptors (TLRs) 2 and 4, preventing GBS ligands from activating pro-inflammatory signaling cascades[65]. Despite these exciting advances, it is unknown if HylB is important for ascending GBS infection and/or preterm birth.

In this chapter, we show that clinical GBS strains isolated from women in preterm labor had increased levels of HylB activity when compared to commensal strains isolated from rectogvaginal swabs of non-laboring pregnant women. Using a mouse model of ascending GBS infection, we observed that genetic ablation of *hylB* in GBS leads to decreased rates of bacterial ascension and fetal demise. Finally, we show that maternal uterine cells infected with wild type (WT) GBS exhibition lower level of inflammation compared to GBS lacking HylB. These data are the first to describe a role for the GBS hyaluronidase in ascending infection and preterm birth.

4.3 RESULTS

4.3.1 *Clinical GBS Isolated Associated with Invasive Disease Exhibit Increased Hyaluronidase Activity*

We hypothesized that GBS encoded hyaluronidase activity may be critical for ascending infection and preterm birth. To measure HylB activity in various GBS isolates, we adapted a hyaluronidase activity assay that was previously described[251]. Amongst our laboratory collection of GBS strains representing each capsular serotype, we observed that strains showed varying levels of hyaluronidase activity. GBS strain A909 (serotype Ia) and NEM316 (serotype III) showing little to no activity whereas the strains NCTC 01/82 (serotype IV), CBJ111 (serotype V), and JM9 (serotype XIII) showed highest levels of activity (Figure 4-1a). Interestingly, strains belonging to the same capsular serotype exhibited varying levels of hyaluronidase activity (compare COH1to NEM316 and NCTC 10/84 to CBJ111). These data suggest that while hyaluronidase activity varied amongst GBS strains, it is not correlated to capsular serotype.

We next sought to compare hyaluronidase activity in clinical GBS strains isolated from amniotic fluid or neonatal blood (invasive infection, n = 23) to those obtained from women who were rectovaginally colonized with GBS without symptoms of invasive infection (n = 48). Overall hyaluronidase activity was higher in GBS strains obtained from invasive settings when compared to that of commensal settings (Figure 4-1b). Finally, we stratified invasive GBS strains into those isolated from neonatal disease without preterm birth (n = 15) and GBS-associated preterm birth (n = 8). Interestingly, isolates from cases of GBS-associated preterm birth displayed modestly higher levels of hyaluronidase activity compared to isolates from neonatal disease and much higher levels of activity compared to isolates from vaginal swabs (Figure 4-

1c). Taken together, these data suggest a role for HylB in invasive GBS disease and preterm birth.

4.3.2 *HylB Promotes Ascending GBS Infection and Adverse Birth Outcomes*

Given the higher levels of hyaluronidase activity in GBS strains isolated from women in preterm labor, we examined if HylB activity is important for ascending infection and preterm birth. We adapted a pregnant murine model of ascending GBS infection, recently developed by Randis and colleagues[39], with the modification that we omitted the use of gelatin during vaginal inoculation of pregnant mice. We constructed a *hylB* mutant (hereafter referred to as GBSΔ*hylB*) in WT GBS COH1 (serotype III, ST17 clone associated with increased virulence[193]) and confirmed the loss of hyaluronidase activity in the GBSΔ*hylB* mutant by gel electrophoresis. The results shown in Figure 4-2 indicate that WT GBS COH1 displays high hyaluronidase activity (indicated by the lower hyaluronic acid band, (Figure 4-2a, lane 2), the GBSΔ*hylB* strain displays no hyaluronidase activity (Figure 4-2a, lane 3).

Next, we vaginally inoculated pregnant C57BL/6J mice on day E15 of pregnancy with approximately 10^8 colony-forming units (CFUs) of WT GBS or isogenic GBSΔ*hylB* (Figure 4-2a). The mice were then monitored for signs of preterm birth (defined as vaginal bleeding or pups in cage) for up to 72 hours post inoculation. Upon signs of preterm birth or at 72 hours post-inoculation (whichever occurred first), the mice were euthanized, a midline laparotomy was performed, and *in utero* fetal death (IUFD) was recorded prior to subsequent analysis. Intriguingly, mice inoculated with WT GBS showed significantly higher rates of ascending infection and adverse pregnancy outcomes (preterm birth and/or IUFD) when compared to mice

inoculated with GBSΔ*hylB* (Figure 4-2c-e). Consistent with these findings, pregnant mice inoculated with WT GBS also exhibited significantly higher bacterial load in the uterine horns compared to mice inoculated with GBSΔ*hylB* (Figure 4-3). Placentas and pups most proximal to the vaginal tract showed significantly more bacterial CFUs in mice inoculated with WT GBS when compared to mice inoculated with GBSΔ*hylB*. Similar trends were also seen in the distal pups and placenta but these data did not reach statistical significance. Notably, vaginal colonization did not appear to be significantly different between mice inoculated with WT GBS and GBSΔ*hylB*, suggesting that the differences in infection outcomes cannot be attributed to differences in vaginal colonization. Additionally, there is a weak, but statistically significant, correlation between the amount of ascended GBS load (average of uterine horn, pup, and placental CFUs) and the percentage of pups with an adverse birth outcome (Figure 4-S1). Together, these data show that HylB plays an important role in ascending GBS infection leading to adverse birth outcomes.

4.3.3 *Hyaluronidase (HylB) Activity Dampens Uterine Immune Responses during Ascending GBS Infection*

Previous studies by Kolar *et al.* have shown that GBS utilizes the *hylB*-encoded hyaluronidase to degrade hyaluronic acid into disaccharide fragments, which blocks TLR2/4 signaling to prevent inflammation[65]. Uterine epithelial cells express high levels of TLRs 1, 2, and 6, which are more responsive to Gram-positive bacteria than to other types of pathogens[252]. Additionally, uterine TLR2 expression in mice increases as gestation progresses, whereas placental and fetal TLR2 expression decreases during gestational progression[253]. To determine if the GBS hyaluronidase mediates uterine immune responses during ascending infection, we performed luminex assays to measure levels of inflammatory cytokines in uterine tissues from

pregnant mice vaginally inoculated with WT GBS or GBSΔ*hylB*. (Figure 4-4a-d, panel i). We found that inflammatory cytokines from mice inoculated with GBSΔ*hylB* clustered into discrete low and high groups that correlated with the presence or absence of bacteria. Therefore, we stratified the uterine samples to those with bacteria and noted significantly higher levels of TNFα and MIP2 (Figure 4-4a-b, panel ii) and modestly higher levels of IL-6 and MIP1β (Figure 4-4c-d, panel ii) in the uterine tissues of mice inoculated with GBSΔ*hylB* compared to that of mice inoculated with WT GBS. Levels of inflammatory markers in the bacteria-free uterine tissues (all from mice inoculated with GBSΔ*hylB*) were similar to that of mice inoculated with PBS (Figure 4-4a-d, panel ii). No differences were observed in levels of IL-10, IL-1β, or GROα in uterine tissues (Figure 4-S2), nor were there differences in the levels of TNFα, MIP2, IL-6, MIP1β, IL-10, IL-1β, or GROα in placental or fetal tissues (Figure 4-S3). These data suggest that immune responses in uterine tissues, rather than placental or fetal tissues, are responsible for decreasing the incidence of ascending GBS infection and that GBS circumvents this response by blocking TLRs through HylB activity.

4.3.4 *Hyaluronidase Activity Dampens Uterine Immune Responses, but not Placental Immune Responses, in Human Tissues*

Given our *in vivo* findings, we set out to determine if HylB modulates inflammatory responses in human tissues. We first used an *ex vivo* model of GBS infection of chorioamniotic/placental membranes. Intact choriomaniotic membranes were collected from healthy non-laboring women undergoing cesarean sections at term and were mounted on transwells as previously described[96]. Membranes were then inoculated with approximately 10^7 CFUs on the choriodecidual/maternal side, which was supplemented with 1.25 mg/mL hyaluronic acid. At 4 and 24 hours post-infection, media was collected from both the chorionic

and amniotic side of the membranes TNFα, IL-6, and IL-8 concentrations were measured by enzyme-linked immune absorbance assay (ELISA). As was observed *in vivo*, GBS induced significant cytokine expression from the gestational membranes, but this inflammation was not decreased by HylB (Figure 4-S4). These data indicate that HylB does not play a role in dampening the inflammatory response from the placenta, and suggest that another tissue is responsible for preventing ascending infection.

We then tested the impact of HylB in uterine tissue using an immortalized human endometrial cell (HEC-1-B) model of infection. HEC-1-B cells were infected with GBS at an MOI of 0.01 in media supplemented with 1.25 mg/mL hyaluronic acid. Cell culture supernatant was collected at 48 hours post-infection and levels of TNFα, IL-6, and IL-8 were measured by ELISA. Interestingly, HEC-1-B cells infected with GBS lacking *hylB* display significantly higher levels of inflammatory cytokines TNFα, IL-6, and IL-8 than WT GBS, which corroborates our *in vivo* findings (Figure 4-5). These data suggest a role for uterine immune responses in preventing ascending infection by clearing GBS that have entered the uterine space. GBS that are able to block uterine immune responses through HylB appear to be able to disseminate into deeper tissues, such as placental and fetal tissues, leading to adverse pregnancy outcomes such as *in utero* fetal demise and/or preterm birth. Collectively, our studies indicate the importance of GBS encoded hyaluronidase in suppression of uterine immune responses during ascending infection and preterm birth.

4.4 DISCUSSION

This work establishes a novel role for the GBS hyaluronidase, HylB, as a critical virulence factor in ascending GBS infection and resulting preterm birth. We have shown that

GBS strains isolated from women undergoing preterm labor show higher levels of hyaluronidase activity and that this activity permits ascending infection by reducing anti-bacterial inflammation in uterine tissue. Recent work has described the role of HylB in tissue dissemination and immune evasion during septic GBS infection, but the role of HylB in ascending infection has heretofore been unstudied[65,254]. Our data indicates that HylB is important for pathogensis during ascending infection. GBSΔ*hylB* showed decreased bacterial ascension, fetal demise and induced more inflammation in both human and murine uterine tissues. Moreover, as hyaluronidases encoded by other bacterial pathogens, such as *S. pyogenes* and *Staphylococcus aureus*, are critical for virulence[255,256], our work will be relevant to understanding the role of microbial hyaluronidases during disease pathogenesis.

Hyaluronic acid plays a pivotal role in the progression of pregnancy and labor[110,111,248,257,258]. During parturition, hyaluronic acid production drastically increases in cervical tissue until it comprises approximately 1.0% of the dry weight of the cervix[248]. For a successful vaginal birth, the cervix must undergo a softening process (referred to as cervical ripening) in order to allow cervical distention[259]. Cleavage of hyaluronic acid is vital for proper cervical ripening. Humans and mice produce multiple hyaluronidases to cleave the abundance of hyaluronic acid present in the cervix, and application of exogenous hyaluronidase is one method used to induce cervical ripening and labor[260]. Interestingly, vaginal inoculation with hyaluronidase-encoding *E. coli* leads to increased preterm birth rates in mice[111]. These data suggest that microbial hyaluronidases can induce cervical ripening and labor, and our data supports this hypothesis. While we do not know that the GBS hyaluronidase specifically induces cervical ripening, we show that it is crucial in increasing GBS infection associated preterm birth (Figure 4-2d-e). The ability of the GBS hyaluronidase, and other microbial hyaluronidases, to

induce cervical ripening needs to be explored further. Inhibition of microbial hyaluronidases may be a possible avenue for developing therapeutics to reduce preterm birth rates.

Traditionally, inflammation is thought to be a driver of preterm labor, so it is counterintuitive that genetic ablation of *hylB* leads to more uterine inflammation but less preterm birth. We speculate that this is due to the temporal nature of uterine inflammation. The uterine epithelium expresses high levels of the bacteria-responsive TLRs 1, 2, and 6[252]. Moreover, TLR2 expression increases in the uterine tissue during gestational progression, while TLR2 expression declines in other gestational tissues, such as placental tissue and chorionic membranes[253]. We reason that the uterus is the primary immunological barrier that prevents Gram-positive bacterial invasion of gestational tissues. If this immunological barrier fails due to inhibited TLR signaling, ascended bacteria may avoid detection by the host. This may allow dissemination into placental and fetal tissues and preterm birth, as was observed in pregnant mice inoculated with WT GBS (Figure 4-2c. Figure 4-3). Conversely, if TLR signaling is not inhibited, an increase in uterine inflammation may lead to bacterial clearance, such as what we observed in pregnant mice inoculated with GBSΔ*hylB* (Figure 4-2c, Figure 4-3a, Figure 4-4a-d). The timing and magnitude of inflammation may also play important roles in preterm labor as an outcome of ascending bacterial infection. If the increase in uterine inflammation is a transient event, rather than a sustained event, the host may be able to clear the infection without the induction of labor. It is interesting that mice inoculated with GBSΔ*hylB* that did not show ascending infection also had lower levels of inflammation than those that did show ascending infection (Figure 4-4). We hypothesize that ascended bacteria caused a large spike in inflammation early in infection, leading to their clearance from the uterine space. Once the bacteria are cleared, the inflammation may rapidly dissipate, promoting healthy pregnancy (Figure 4-6). These results imply a need for

earlier GBS screening during pregnancy, but additional research is needed to fully address this hypothesis.

Preterm birth is the leading cause of adverse pregnancy outcomes for both the mother and fetus, and a significant number of preterm births are due to *in utero* infection with vaginal flora, such as GBS[2-4,9,237,238,243]. Understanding the virulence factors that allow vaginal flora to switch from commensal colonizers to ascending pathogens is crucial for developing successful interventions to prevent *in utero* infection and resulting preterm birth. While studies have characterized the role of the GBS hemolytic pigment in vaginal colonization, ascending infection, induction of inflammation, and fetal damage[39,66,119], we know little about the role of other GBS virulence factors involved in these processes. By defining the mechainism underlying these different virulence factors, it may be possible to develop strategies for intervention. Interestingly, multiple compounds are able to inhibit microbial hyaluronidase activity[256,261]. To our knowledge, little attention has been given to finding a hyaluronidase inhibitor specific to GBS, but such an inhibitor may be an effective means of combatting multiple types of GBS infections.

We have described a novel role for the GBS hyaluronidase in ascending infection and preterm birth. First, we draw a strong association between GBS hyaluronidase activity and serious disease outcomes in clinical isolates derived from human samples. Next, we show that presence of the GBS hyaluronidase permits increased bacterial ascension from the vaginal tract to the uterine space, which is associated with a reduction in uterine inflammation and leukocyte invasion compared to GBS lacking the hyaluronidase. Finally, we are suggesting a more refined role for uterine inflammation during pregnancy, wherein inflammation can potentially lead to the elimination of ascended bacteria without inducing preterm labor. Future research should focus on

further defining the role of the GBS hyaluronidase in these processes and developing a hyaluronidase inhibitor to prevent ascending GBS infections.

4.5 MATERIALS AND METHODS

4.5.1 *Ethics Statement*

All animal experiments were approved by the Seattle Children's Research Institutional Animal Care and Use Committee (protocol #13907) and performed in strict accordance with the recommendations in the Guide for the Care and Use of Laboratory Animals of the National Institutes of Health (8th Edition).

4.5.2 *Bacterial Strains*

Chemicals in this study were purchased from Sigma Aldrich unless stated otherwise. The WT GBS strain COH1 used in these studies is a serotype III (ST17 clone) clinical isolate from an infected human newborn[262]. GBS cultures were grown in Tryptic Soy Broth (TSB) or on Tryptic Soy Agar (TSA, Difco Laboratories) at 30° or 37°C in 5% CO_2, and monitored at 600nm. The *hylB* allelic replacement mutant was generated using methods previously described [229]. Briefly, 1.0 kb regions flanking either side of the *hylB* gene (*hylB* 3' Forward CCA AGG AGC CTA AAG AGG CCT GAC CCA AGA GAT TAA C, *hylB* 3' Reverse TTT AGC CAT TTT TAC TCC TTA GGT TTT AAA ATT GTA AAC, *hylB* 5' Forward ATT GTT TTA GCT AAC CGT ACA TAA AAA ACC TAT C, *hylB* 5' Reverse GTA GGC GCT AGG GAC AAC TGT CCT TGA TAA ATT GAC) and a kanamycin resistance cassette (kan^R Forward GGA GTA AAA AAT GGC TAA AAT GAG AAT ATC AC, kan^R Reverse ACG GTT AGC TAA AAC AAT

TCA TCC AGT AAA ATA TAA TAT TTT ATT TTC) were PCR amplified from genomic DNA (for flanking regions) or from the plasmid pCIV2 (for kan^R cassette). Each primer contained a short (15-25 bp) region of homology that corresponded to either the temperature sensitive cloning vector pHY304 or the next corresponding region. The pHY304 cloning vector was PCR linearized (pHY304 Forward GTC CCT AGC GCC TAC GGG, pHY304 Reverse CTC TTT AGC TCC TTG GAA GCT GTC), and all four fragments (2 flanking regions, kanR cassette, and linear pHY304) were ligated using the Gibson Assembly Cloning Kit (New England BioLabs). This plasmid was then electroporated into the WT GBS strain COH1, and selection for allelic replacement was performed as previously described[229].

4.5.3 *Clinical Isolates*

GBS clinical isolates were collected as previously described[96,119]. Briefly, rectovaginal swabs were obtained from women in their third trimester of pregnancy at the University of Washington Medical Center and Harborview Medical Center in 2007 under University of Washington IRB# 30308; samples were collected without any identifiers or clinical information and a waiver for written informed consent was obtained for testing anonymous samples. GBS clinical isolates from amniotic fluid, chorioamnion and/or cord blood were obtained from women enrolled with preterm labor and intact membranes at less than or equal to 34 weeks gestation at the University of Washington Medical Center, Swedish Medical Center and Virginia Mason Medical Center, Seattle, Washington between June 25, 1991 to June 30, 1997. This cohort was previously described and the University of Washington Institutional Review Board approved the study protocol and all participants provided written informed consent[263]. Fifteen GBS isolates from infected newborns were kindly provided by Dr. Sharon Hillier, University of Pittsburgh.

4.5.4 *Human Cell Culture*

Human HEC-1-B endometrial cells (ATCC strain HTB-113) were grown at 37°C in 5% CO_2. Cells were maintained in Eagle's Minimal Essential Media (MEM, Corning), supplemented with 10% heat-inactivated fetal bovine serum (Corning) and 50 to 100 I.U./mL penicillin and 50 to 100 µg/mL streptomycin (Corning). Cells were split every 3-4 days and passaged at a 1:4 dilution. 24 hours prior to infection, antibiotic containing media was aspirated, cells were washed with sterile PBS, and media was replaced with antibiotic-free, serum free MEM. At the time of infection the media was aspirated and replaced with fresh antibiotic-free, serum free media supplemented with or without 1.25 mg/mL hyaluronic acid. All GBS infections were performed at an approximate MOI = 0.01 for 48 hours between passages 7-14.

4.5.5 *Hyaluronidase Activity Assay*

GBS strains were grown overnight in TSB at 30° C with 5.0% CO_2. Overnight cultures were pelleted at 4000 rpm for 8 min, and resulting supernatants were collected for analysis. 50 µL of spent supernatants were pre-warmed for 5-10 min at 37° C with 5.0% CO_2, and were then added to 200 µL hyaluronic acid solution (1.25 mg Hyaluronic Acid Sodium Salt from Rooster Comb (Sigma) dissolved in 36.0 mg/mL monobasic sodium phosphate, pH = 5.35 at 37° C) and incubated at 37° C with 5.0% CO_2 for 45 min. After incubation 50 µL of 0.8 M sodium tetraborate (pH = 9.1) pre-heated to 95° C was added, and the sample was boiled at 95° C for 3 min. Following boiling, 1.5 mL of 1.0% (w/v) 4-methylaminobenzaldehyde dissolved in 15.3 M acetic acid and 1.25 M HCl was added to the sample, and 200 µL were removed and read on a plate reader at 585 nm. To calculate the amount of hyaluronidase activity, standard curves of

commercial hyaluronidase (Hyaluronidase from Bovine Testes, Sigma) dissolved in TSB were created and included in conjunction with every assay. Hyaluronidase activity values from unknown samples were interpolated from the standard curve, which was fit to a 4-parameter logistic curve using GraphPad Prism 6 (La Jolla, CA). If sample reads exceeded the standard curve, the initial spent supernatant was diluted in TSB as necessary to fit within the standard curve range.

4.5.6 *Hyaluronic Acid Gel Electrophoresis*

For hyaluronic gel electrophoresis, overnight cultures of GBS wild type and GBSΔ*hylB* were pelleted at 4000 rpm for 8 min and then 50 µL of supernatant was incubated with 200ul of hyaluronic acid solution (see above) for 45 min at 37°C with 5.0% CO_2. After incubation, samples were boiled at 95° C for 3 min, frozen, and lyophilized until completely dry. Samples were then mixed with 17 µL of loading buffer (0.02% (w/v) bromophenol blue, 2 M sucrose in 1x TBE) and resolved on a 0.8% agarose gel. Electrophoresis was carried out at a voltage of 100 V for approximately 2.5 hr. Once the run was completed, the gel was placed in 500 mL of 0.005% Stains-All (Sigma) solution dissolved in 50% ethanol overnight under light-protected cover at room temperature and de-stained in water for ~1 hr until background was photobleached.

4.5.7 *Murine Model of Ascending Infection*

Six-to-eight week old female C57BL/6J mice were obtained from The Jackson Laboratory and used for ascending infection studies. Female mice were individually paired with male C57BL/6J mice for 2 days, then separated and monitored for 14 days post-separation.

Pregnancy was confirmed by observable weight gain and palpation for the presence of pups. Mice were inoculated on day E15 of pregnancy. Overnight GBS cultures were sub-cultured 1:20, grown to OD_{600} = 0.3, pelleted at 4000 rpm for 8 min, washed once with sterile PBS, and re-suspended in sterile PBS to final concentration of 10^{10} CFU/mL. Mice were anesthetized using 4% isoflurane and 10 µL (~10^8 CFU) of inoculum was administered into the vaginal tract using a micropipette. Mice were left inverted for 5 additional minutes under anesthesia, then returned to their cages and monitored until ambulatory. Mice were monitored twice daily up to 72 hr post-inoculation for signs of preterm birth (vaginal bleeding and/or pups in cage). At 72 hrs post infection or earlier if preterm birth was observed, mothers were euthanized and a mid-line laparotomy was performed to identify fetal injury, loss of pregnancy, and to collect maternal and fetal tissues. Tissues were excised, homogenized and serially plated on TSB to determine the number of CFUs associated with maternal and fetal tissues. All data were normalized to total tissue weight in grams. Homogenized tissue was then incubated overnight at 4° C in lysis buffer (0.15 M NH_4Cl, 1 mM $NaHCO_3$, pH 7.2), pelleted, and supernatants were collected for further analysis as described below.

4.5.8 *Luminex Analysis of Murine Tissues*

Tissue lysates from the mouse ascending infection model (see Materials and Methods, "Ascending Infection Model") were thawed and centrifuged at 10,000 x g for 5 minutes at 4^0C to remove residual cell debris. Fifty microliters of the supernatants were then used for cytokine analysis (IL-10, IL-1β, IL-6, GROα, TNF-α, MIP-2, MIP-1β) by Luminex assay (Procartaplex™ Multiplex Immunoassay, eBioscience) as per the manufacturer's instructions. Expected cytokine concentrations for the standard curve were translated into logarithmic scale, fit to a 5-parameter

logistic curve, and median fluorescence intensity readings from unknown samples were then interpolated from this standard curve using GraphPad Prism 6 (La Jolla, CA). These data were translated out of logarithmic scale back into concentration values (pg/mL) and were then normalized to total tissue weight in milligrams.

4.5.9 *Cytokine Analysis in GBS-Infected Human Chorioamnion*

Human chorioamniotic/placental membranes were collected from de-identified healthy term pregnancies undergoing scheduled Cesearan sections at the University of Washington Hospital. Since identifiable information was not collected, this research is exempt from IRB review (see letter from UW IRB: Determination Form #44282, "Use of Discarded Placentas"). Chorioamniotic membranes were cultured on transwells as previously described[96]. Briefly, membranes were dissected from placenta immediately following delivery and transported on ice. Membranes were rinsed in PBS and mounted on transwell inserts (12 mm) lacking the synthetic filter membrane. Gestational membranes were held in place with sterile latex bands. Transwells were placed in 12-well plates with 0.5 mL medium (DMEM with L-glutamine supplemented with 1% FBS and pen/strep) in the upper chamber and 1.5 mL medium in the lower chamber at 37 C. Following overnight acclimation, membranes on transwell inserts were washed and inoculated with approximately 10^7 CFU in the upper (choriodecidual/maternal) chamber in DMEM supplemented with or without 1.25 mg/mL hyaluronic acid. Media was sampled at 4 and 24 hours from both the apical and basal compartments and stored at -20° C until analysis. ELISA assays for cytokine levels were purchased from R and D Systems and performed as per manufacturer's instruction. Media from infected tissue was diluted 1:50 (TNFα) or 1:100 (IL-6, IL-8, CCL4), and media from control tissue was diluted 1:4.

4.5.10 *Statistical Analysis*

Mann-Whitney test, Fisher's Exact test, or Tukey's multiple comparison test following ANOVA was used to estimate differences as appropriate and p value <0.05 was considered significant. Statistics were performed using GraphPad Prism version 5.0 for Windows, GraphPad Software, USA, www.graphpad.com.

4.6 Acknowledgements, Author Contributions, and Conflict of Interest

4.6.1 *Acknowledgements*

We would like to gratefully acknowledge Dr. Sharon Hillier and Lorna Rabe for the generous gift of clinical GBS isolates from infected patients. We thank Jan Hamanishi and Gina Heidel for their help in preparing the figures. We thank Verónica Santana-Ufret and Leticia Campos for experimental assistance.

4.6.2 *Author Contributions*

J.V. and L.R. designed the experiments, J.V., P.Q., S.M., E.B., and C.W. performed the experiments, K.A.W. collected the clinical samples, and J.V., P.Q., S.M., and L.R. wrote and edited the manuscript.

4.6.3 *Conflict of Interest*

The authors declare no competing financial interests.

4.7 FIGURES

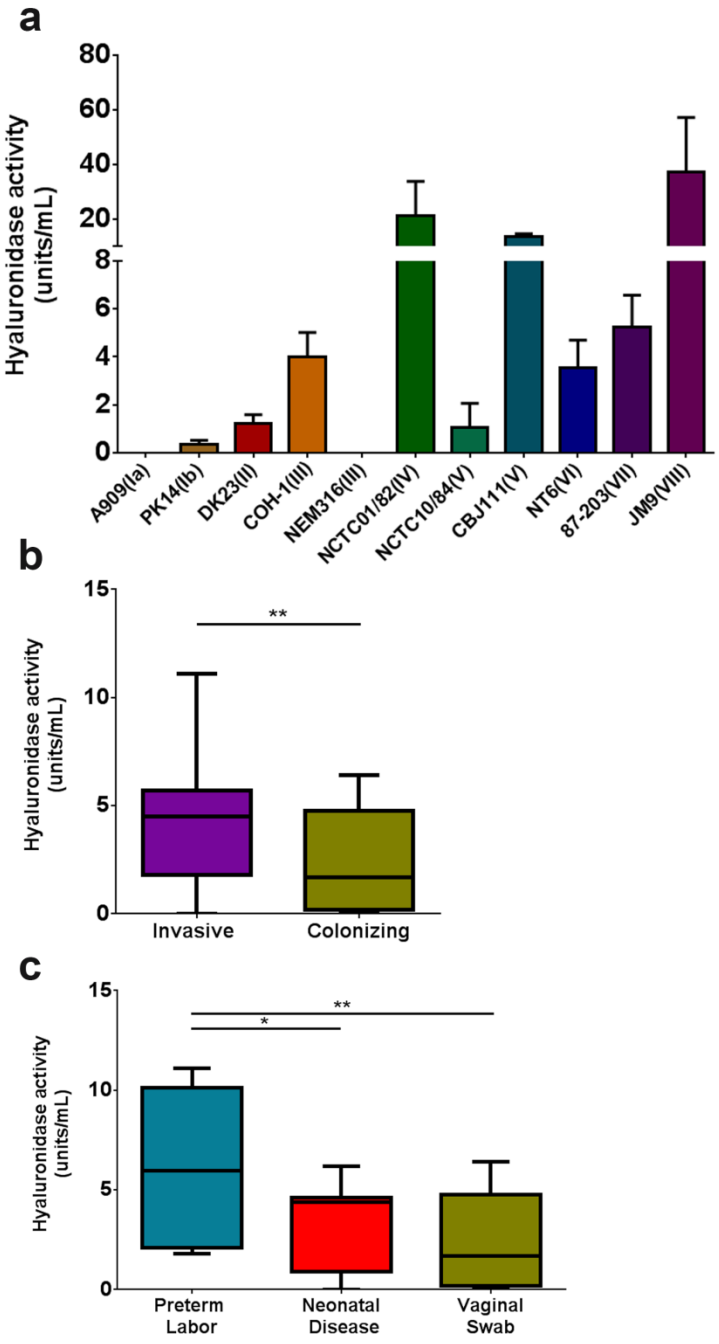
a
Hyaluronidase activity (units/mL)
80
60
40
20
8
6
4
2
0
A909(Ia)
PK14(Ib)
DK23(II)
COH-1(III)
NEM316(III)
NCTC01/82(IV)
NCTC10/84(V)
CBJ111(V)
NT6(VI)
87-203(VII)
JM9(VIII)
b
Hyaluronidase activity (units/mL)
15
10
5
0
**
Invasive
Colonizing
c
Hyaluronidase activity (units/mL)
15
10
5
0
**
*
Preterm Labor
Neonatal Disease
Vaginal Swab

Figure 4-1 - Disease-associated clinical GBS isolates display increased hyaluronidase activity

a-c, GBS strains representative of each capsular serotype (**a**) and clinical GBS strains from invasive disease (n = 23) or from rectovaginal swabs (n = 48, **b**) were grown overnight and assessed for their hyaluronidase activity. Invasive clinical GBS strains were also stratified into those isolated from women undergoing preterm labor (n = 8) or those isolates from neonatal disease (n = 15, **c**). All experiments were performed three independent times in triplicate. Unpaired Student's t-test was used to assess statistical significance between single groups (**b**, ** $p > 0.01$). Data bars are displaying mean displayed with error bars ± SEM (**a**) or box plots with mean, 25% percentile, 75% percentile, and errors bars indicating minimum and maximum values (**b-c**). Tukey's multiple comparison test following one-way ANOVA was used to assess statistical significance between multiple groups (**c**, * $p < 0.05$, ** $p < 0.01$).

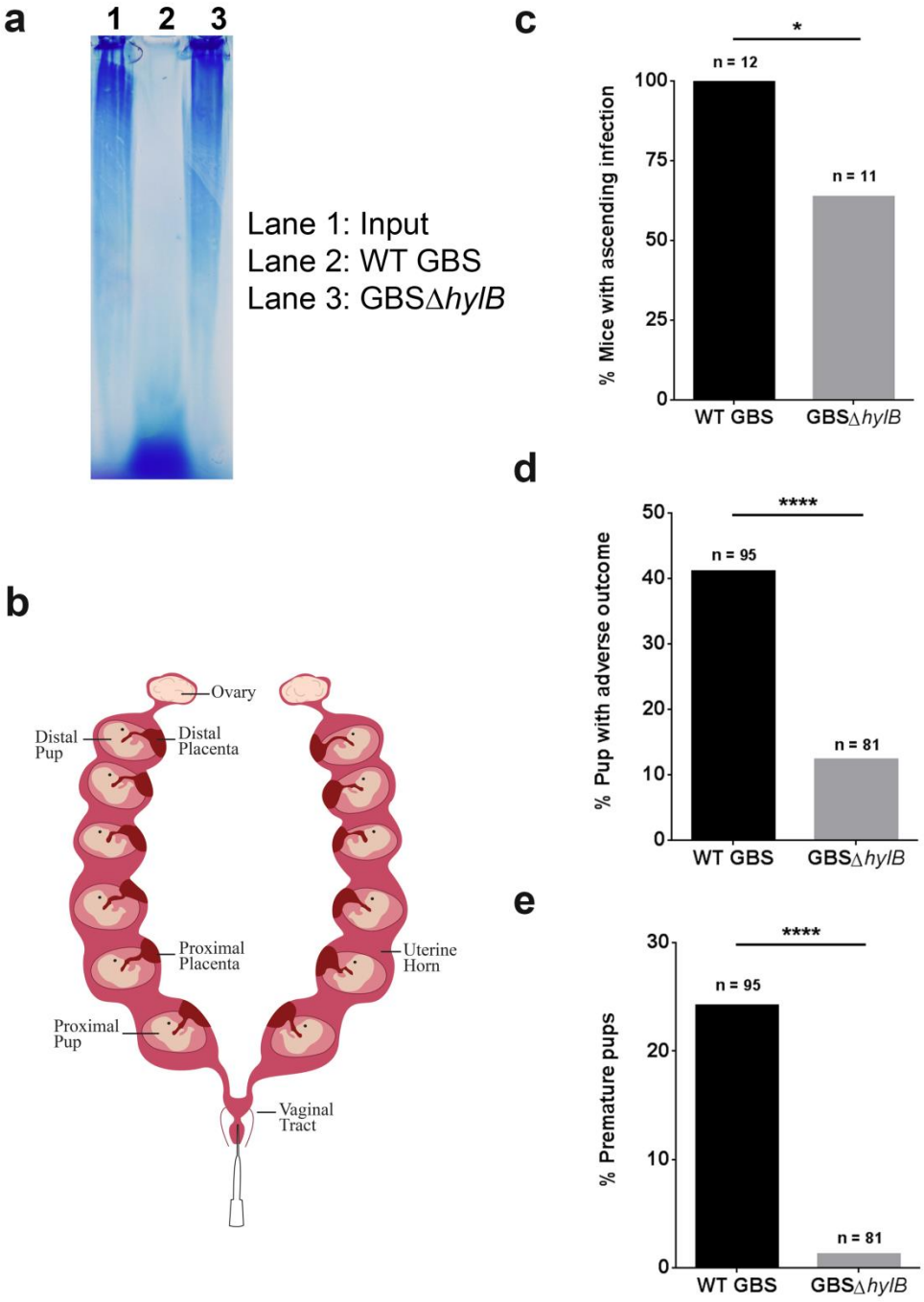

Figure 4-2 - HylB activity leads to increased rates of ascending infection and adverse pregnancy outcomes including preterm birth

a, Hyaluronic acid incubated with or without GBS was analyzed by agarose gel electrophoresis. The WT GBS strain COH1 shows increased hyaluronidase activity (Lane 2: WT GBS) compared

to the isogenic *hylB* mutant (Lane 3: GBSΔ*hylB*), which shows no hyaluronidase activity (Compare to Lane 1: Input). **b-e**, Pregnant female C57BL/6J mice (a schematic can be found in panel **b**) were inoculated with approximately 10^8 CFU of WT GBS (n = 12) or GBSΔ*hylB* (n = 11). Contingency analyses were performed on observed outcomes of these mice. Observed outcomes were ascending bacterial infection (**c**), pups with adverse outcome (either born prematurely or *in utero* fetal death, **d**), and pups born prematurely (**e**). Fisher's exact test was used to assess statistical significance between groups (A-C, * $p < 0.05$, **** $p < 0.00005$).

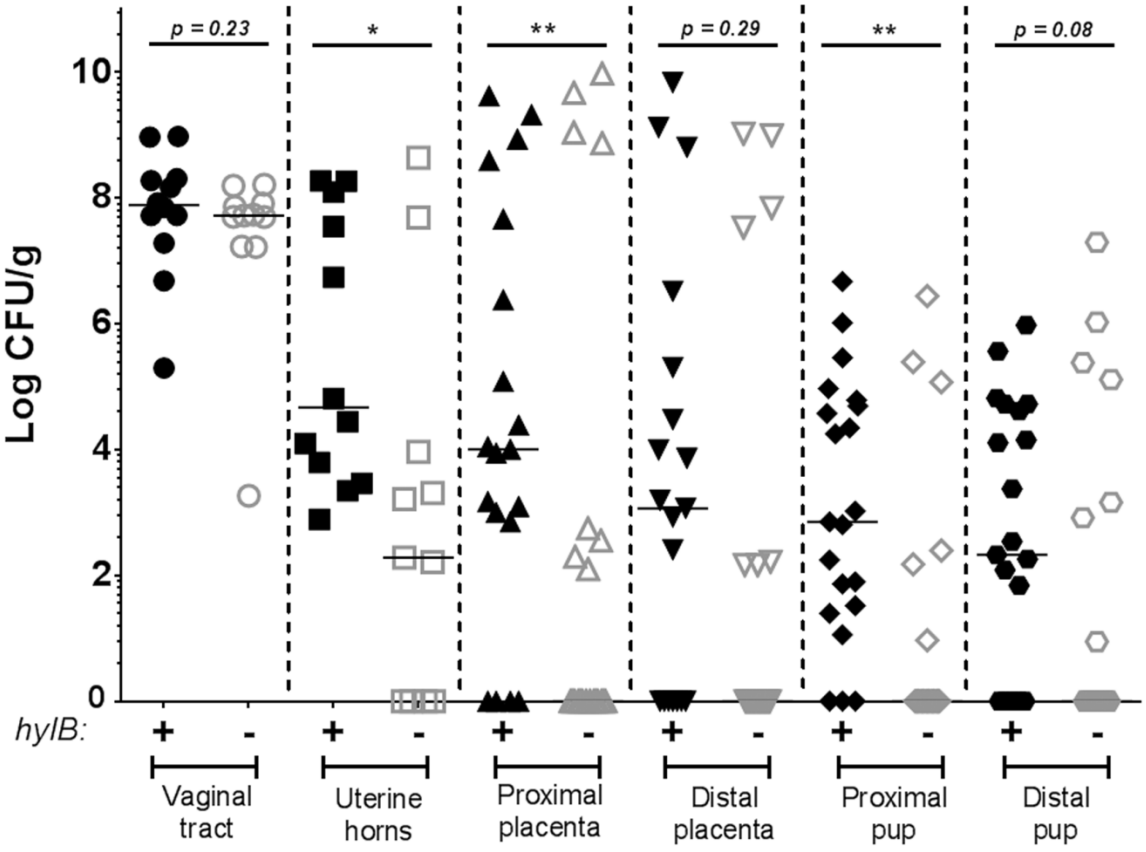

Figure 4-3 – HylB activity leads to increased bacterial ascension

Pregnant female C57BL/6J mice were inoculated with approximately 10^8 CFU of WT GBS (n = 12) or GBSΔ*hylB* (n = 11). The vaginal tract, uterine horns, distal and proximal placentas, and distal and proximal pups of these mice were removed and assessed for bacterial load by serial dilution plating. Data are displayed as individual data points with median bar. Mann-Whitney U test was used to assess statistical significance between groups (* $p < 0.05$, ** $p < 0.01$).

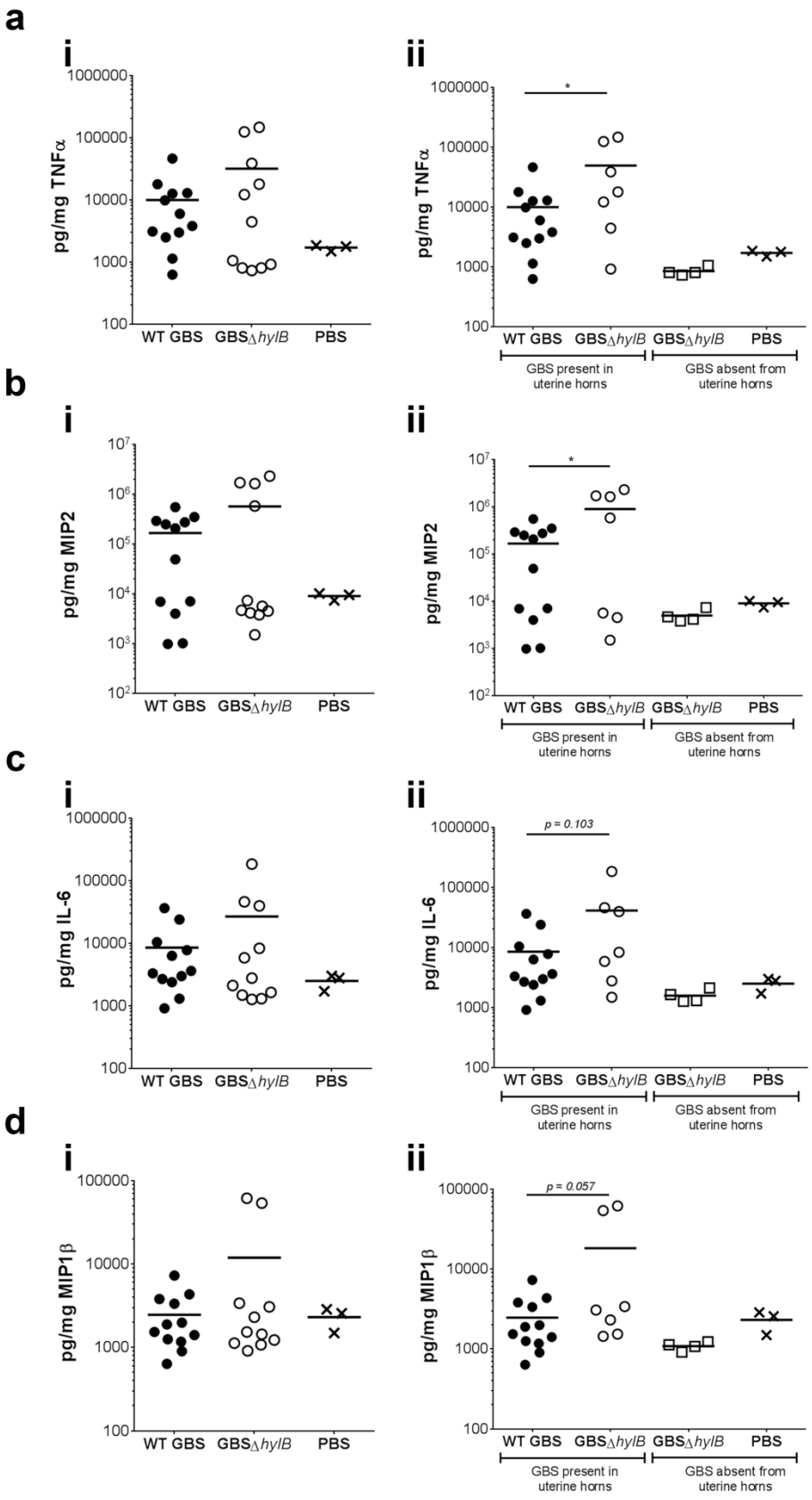
a
i
ii
pg/mg TNFα
1000000
100000
10000
1000
100
WT GBS
GBSΔhylB
PBS
*
GBS present in uterine horns
GBS absent from uterine horns
b
pg/mg MIP2
10^7
10^6
10^5
10^4
10^3
10^2
c
pg/mg IL-6
p = 0.103
d
pg/mg MIP1β
p = 0.057

Figure 4-4 – GBS HylB activity blocks uterine inflammation in vivo

a-d, Luminex assays were used to assess the levels of the inflammatory markers TNFα (**a**), MIP2 (**b**), IL-6 (**c**), and MIP1β (**d**) in the uterine tissues of pregnant female C57BL/6J mice inoculated with approximately 10^8 CFU of WT GBS strain COH1 (n = 12), GBSΔ*hylB* (n = 11), or PBS (n=3). Data are represented as immune responses in uterine samples irrespective of bacteria (see **a-d**, panel i) or as uterine samples with GBS to those without GBS (either inoculated with GBS or PBS, **a-d**, panel ii). Unpaired Student's t-test was used to assess statistical significance between groups (**a-d**, data bars are displaying mean, * $p < 0.05$).

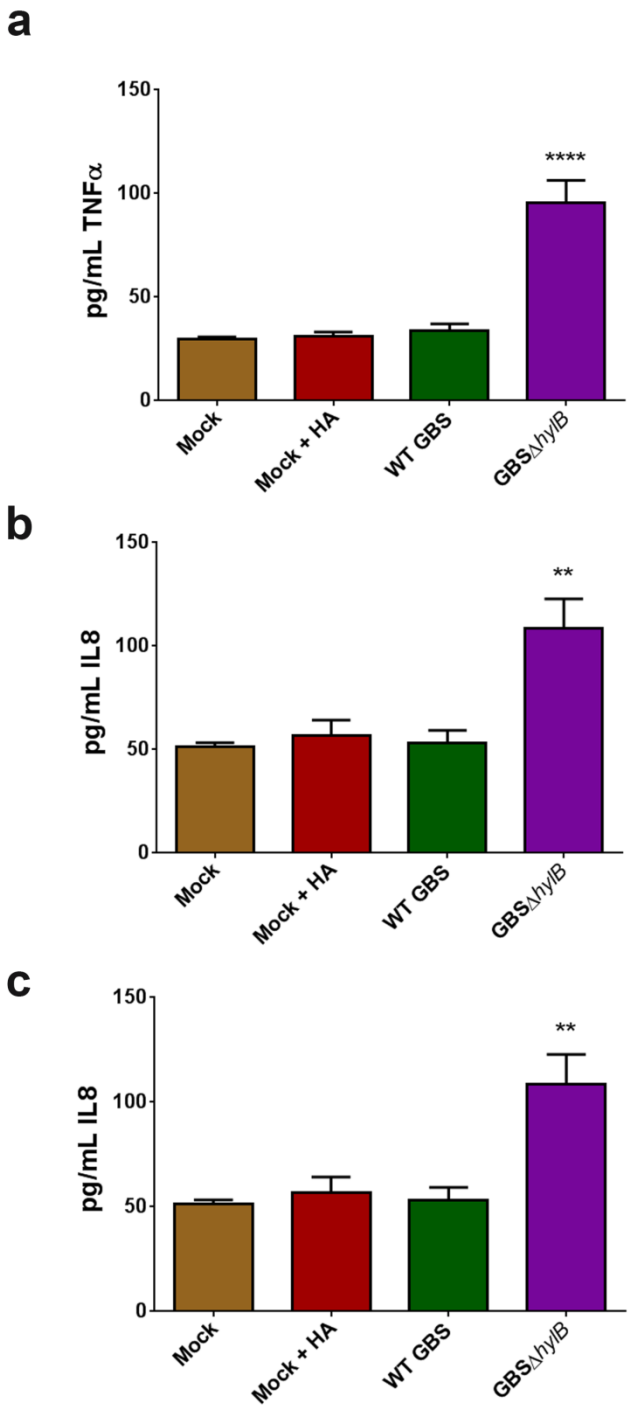

Figure 4-5 – HylB activity dampens immune responses in immortalized endometrial cells

a-c, ELISA assays used to assess the levels of TNFα (**a**), IL-8 (**b**), IL-6 (**c**) in immportalized endometrial HEC-1-B cells that were infected for 48 hours with WT GBS or GBSΔ*hylB* at an

MOI = 0.01 in media supplemented with 1.25 mg/mL hyaluronic acid (HA). Experiments were performed in triplicate and repeated six times. One-way ANOVA with Tukey's multiple correction test was used to assess statistical significance between groups (**a-c**, ** $p < 0.005$, **** $p < 0.00005$, stars over single bars indicate significant compared to all other groups).

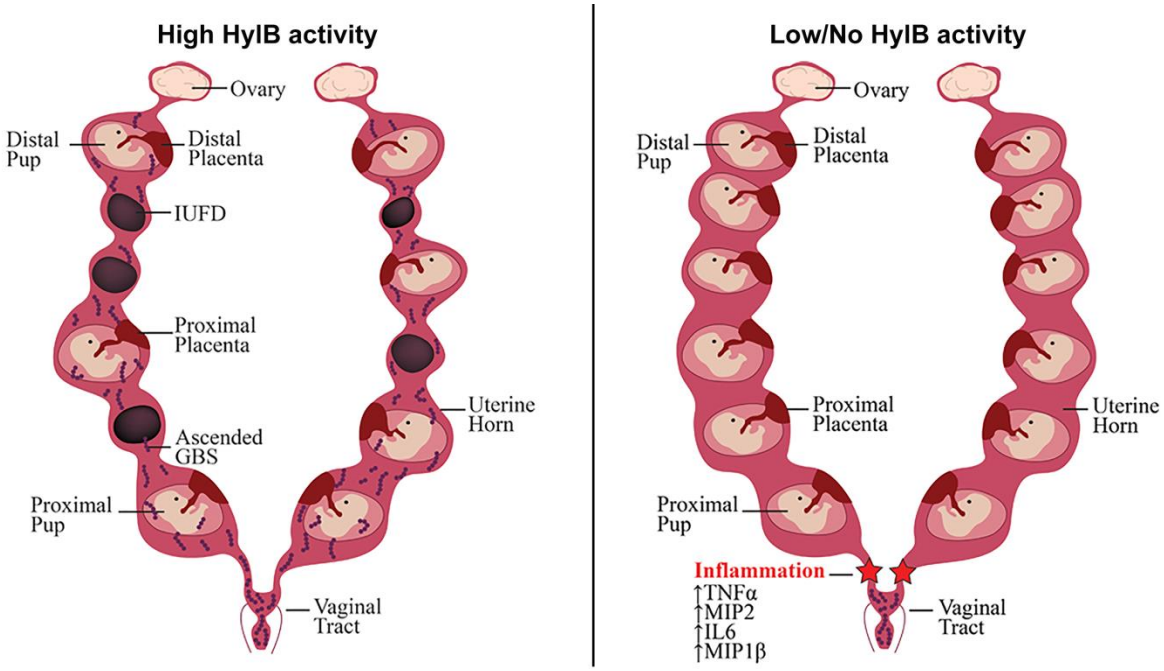

Figure 4-6 – Proposed model of HylB-mediated preterm birth

GBS colonizes the rectovaginal tract of 20-40% of women, where it behaves as a commensal organism. GBS strains with high hyaluronidase (HylB) activity are able to ascend into the uterine space by blocking uterine TLR signaling and avoiding immune detection. Once in the uterine space, ascended GBS are able to invade placental and fetal tissues, leading to *in utero* fetal demise and/or preterm birth. GBS strains with low HylB activity levels are not able to subvert immune detection and are either unable to ascend into the uterine space or conversely are cleared by immune cells soon after ascension. These strains are relegated to the vaginal tract, and thus are not able to infect fetal and placental tissues or induce preterm birth.

4.8 SUPPLEMENTARY FIGURES

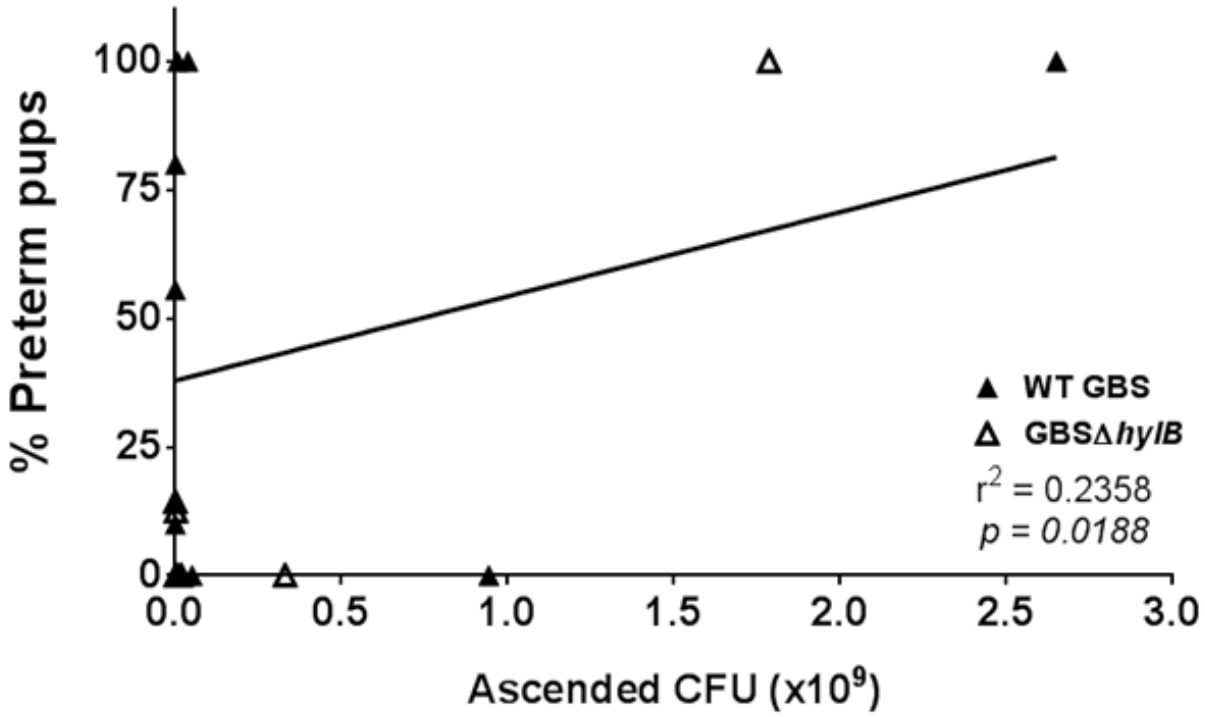

Figure 4-S1 – Correlation between ascended GBS and preterm birth

Spearman correlation between the number of ascended GBS (average CFU in uterine space, placentas, and pups) and the percentage of preterm pups (either in cage or IUFD).

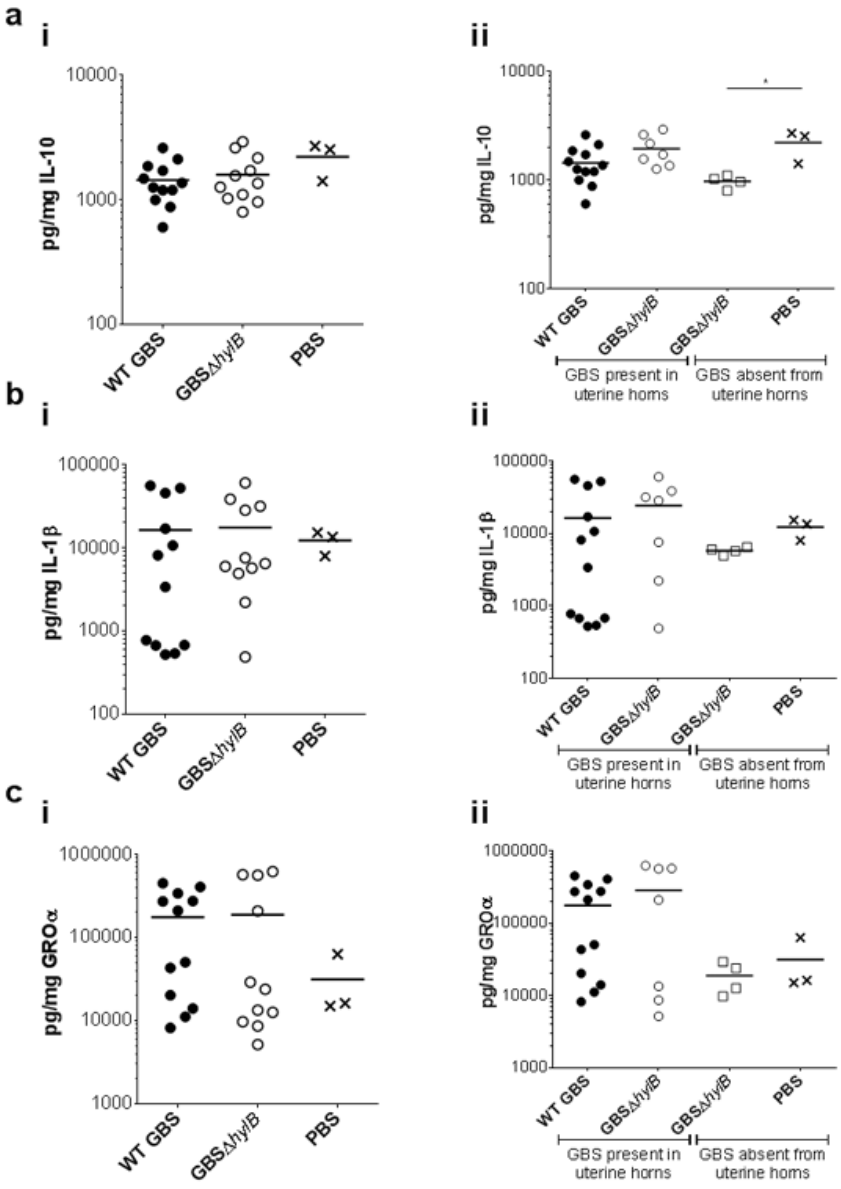

Figure 4-S2 – Inflammatory markers not affected by HylB in the uterine space

a-c, Luminex assays were used to assess the levels of the inflammatory markers IL-10 (**a**), IL-1β (**b**), and GROα (**c**) in the uterine tissues of pregnant female C57BL/6J mice inoculated with approximately 10^8 CFU of COH1 (n = 12), COH1Δ*hylB* (n = 11), or PBS (n=3). Data are shown as all 3 groups of uterine samples (**a-c**, panel i), as uterine samples with GBS present or as

uterine samples without GBS (either inoculated with GBS or PBS, **a-c**, panel ii). Unpaired Student's t-test was used to assess statistical significance between groups (**a-c**, * $p < 0.05$).

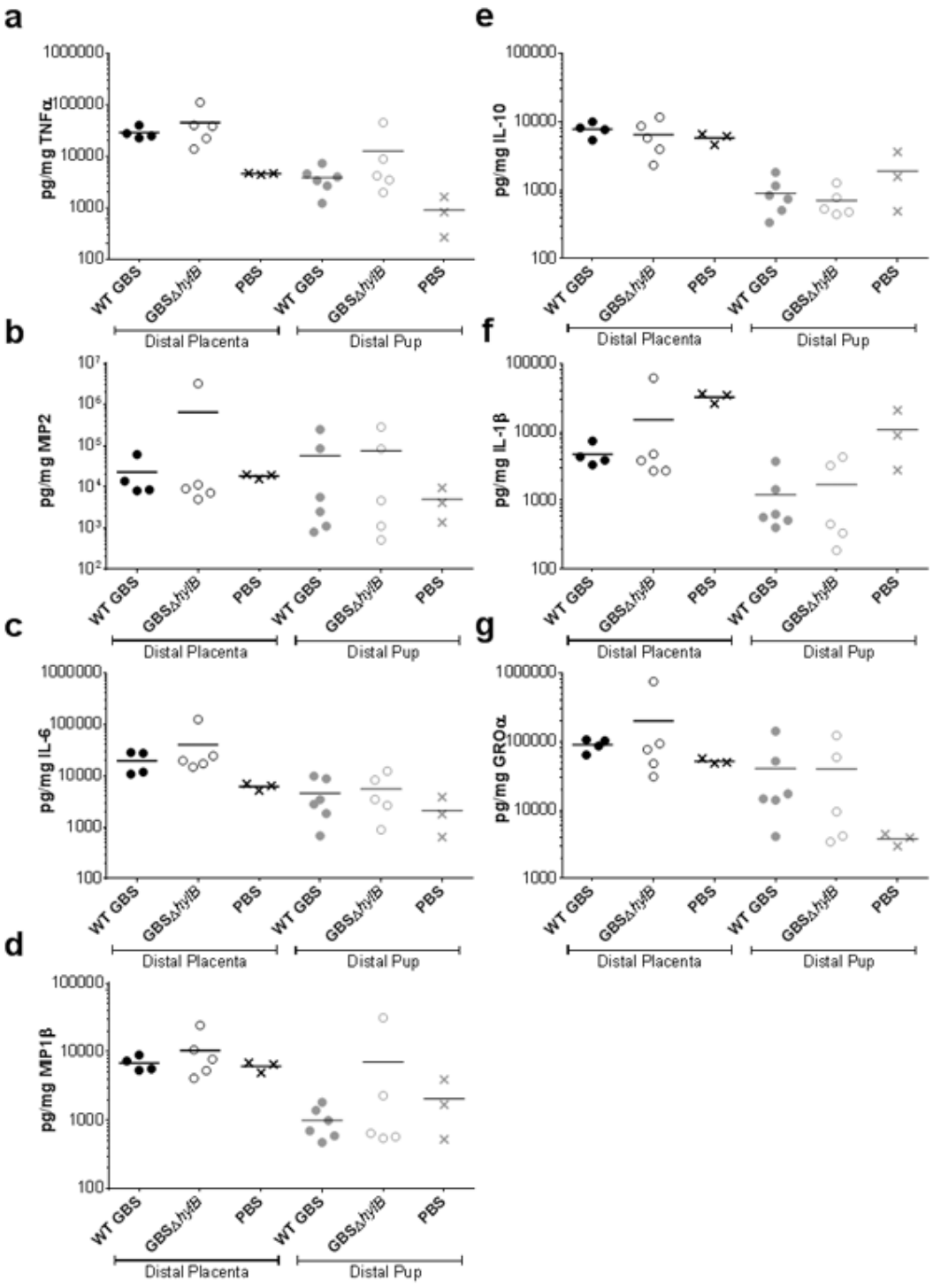

Figure 4-S3 – Inflammation not affected by HylB in distal placental or distal pup tissues

a-g, Luminex assays were used to assess the levels of the inflammatory markers TNFα (**a**), MIP2 (**b**), IL-6 (**c**), MIP1β (**d**), IL-10 (**e**), IL-1β (**f**), and GROα (**g**) in the distal placental tissues (see

Figure 4-2**b** for schematic) of pregnant female C57BL/6J mice inoculated with approximately 10^8 CFU of COH1 (n = 5), COH1Δ*hylB* (n = 5), or PBS (n=3).

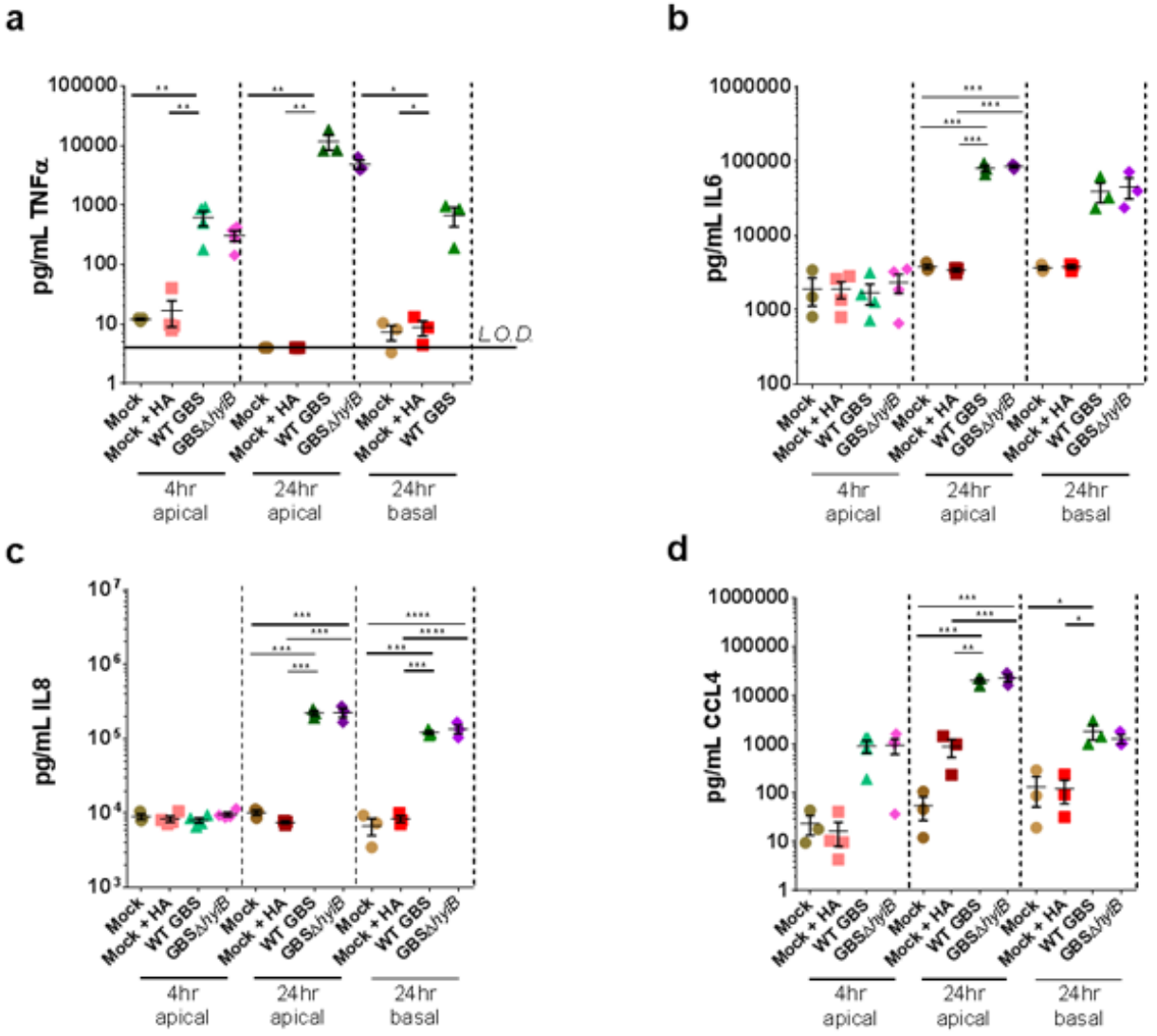

Figure 4-S4 – Inflammation not affected by HylB in ex vivo gestational membranes

a-d, ELISAs were used to assess the levels of the inflammatory markers TNFα (**a**), IL-6 (**b**), IL-8 (**c**), CCL4 (**d**) in the gestational tissues inoculated with approximately 10^7 CFU of COH1 or COH1Δ*hylB*. Culture media was supplemented with 1.25 mg/mL hyaluronic acid (HA). Experiments were performed in duplicate on at least 3 gestational tissues. One-way ANOVA with Tukey's multiple correction test was used to assess statistical significance between groups (**a-d**, * $p < 0.05$, ** $p < 0.005$, *** $p < 0.0005$, **** $p < 0.00005$, L.O.D. = limit of detection).

Chapter 5. Conclusions and final thoughts

The figures and figure legends in this chapter have been adapted from the following articles:

Jay Vornhagen, Kristina Adams Waldorf, and Lakshmi Rajagopal. (2017) Perinatal Group B Streptococcal infections: virulence factors, immunity and prevention strategies. Trends in Microbiology, accepted.

Figure numbers have been updated to conform to the dissertation. Adapted text remains as published with minor editorial changes.

5.1 SUMMARY OF FINDINGS

The work presented in this dissertation attempts to address several outstanding questions about the mechanisms of GBS colonization and ascending infection and provide insight into the complexity of the host-pathogen interactions that occur during these processes.

The role of the hemolytic pigment in GBS pathogenesis has been well-studied[66,96,103,147,182], yet its role in vaginal colonization was not clear. The data presented in Chapter 2 indicate that a delicate balance of pigment expression is needed for successful vaginal colonization. Abrogation of pigment expression leads to diminished colonization, whereas overexpression of pigment leads to bacterial clearance from the vagina. Bacterial clearance is mediated through the activation and degranulation of a specific subset of tissue-resident immune cells in the vagina known as mast cells. Mast cells degranulate in response to the GBS pigment, leading to release of pre-formed inflammatory mediators. Removal of mast cells from the vagina prolongs vaginal colonization of hyper-pigmented GBS strains, which are normally not present in the vagina, but are highly associated with preterm birth and neonatal infection. If hyper-pigmented GBS strains are able to bypass vaginal immunity and infect the placenta, then they are able to resistance clearance by the host immune system.

Despite significant advances in our understanding of vaginal colonization, the process by which GBS ascends from the vagina to the uterus remained unknown. The work in Chapter 3 are the first to demonstrate a mechanism of how GBS ascends from the vagina into the uterus and causes preterm birth. We show that GBS induces epithelial exfoliation of vaginal epithelial cells, which was previously considered to be a means by which the host clears infectious bacteria from the vagina. Instead, we show that rather than being removed from the vagina, GBS mediated epithelial exfoliation leads to ascending infection through the disruption of epithelial barrier

function and increased bacterial dissemination. Loss of epithelial barrier function occurs when GBS activates β_1 integrin and β-catenin signaling which lead to epithelial-to-mesenchymal transition. Consistent with this mechanism, reduction of epithelial exfoliation diminished ascending infection and improved pregnancy outcomes in a murine model of ascending infection.

Once GBS enters the uterus, mechanisms of how GBS evades the host immune response were not completely understood. In Chapter 4, we show that the HylB hyaluronidase secreted by GBS plays a critical role in preventing immune recognition. Previous reports have shown that HylB degrades the host ECM molecule hyaluronic acid into disaccharide units, which block TLR signaling and diminish the host immune response to GBS. Our data shows that GBS strains isolated from women undergoing preterm birth display higher levels of hyaluronidase activity than rectovaginal GBS isolates. Deletion of *hylB* in GBS leads to reduction of bacterial load in uterine, placental, and fetal tissues, and reduced rates of adverse pregnancy outcomes. Despite fewer bacteria, uterine tissues displayed higher levels of inflammation, indicating a role for HylB in controlling the uterine immune response, and therefore GBS access to placental and fetal tissues.

Taken as a whole, these chapters represent the first attempt to comprehensively understand the natural course of GBS colonization and ascending infection in settings that closely replicate human disease. Additional discussions of the future research are presented below.

5.2 Next Steps for Vaginal Colonization Research

Despite recent advances, there are many limitations in our understanding of GBS vaginal colonization. Importantly, the complete repertoire of GBS virulence factors, host factors, and

environmental factors that determine the extent and duration of vaginal colonization remain unknown. This point is key given that the dynamics of colonization during pregnancy are highly variable[79,264]. Frequently, women are transiently colonized during pregnancy[264], and colonization densities can vary[79]. Interestingly, even in cases of transient colonization, the GBS clonal population remains homogenous[79], which is consistent with findings that relatively few clonal types cause a significant portion of human disease[193,265]; however, the means by which vaginal populations of GBS can be both transient and stable remains unexplained. More studies are needed to explore the dynamics of colonization during pregnancy, as current studies have been limited to the use of non-pregnant models of colonization[85,105]. Understanding the temporal dynamics of GBS colonization will lead to more effective interventions to prevent transmission to the fetus or newborn.

A major limitation of colonization studies performed in laboratory settings is the use of animal models that do not perfectly model the human vaginal environment. The most genetically tractable animal model is the mouse which, unfortunately, has many differences in their genitourinary tract compared to humans. While other animal models are limited by their biology, expense, and available resources[40], advances in the mouse model have been made to better recapitulate human biology. For example, the use of gnotobiotic mice with reconstituted human vaginal microbiomes has recently been used to study the prenatal environment[266,267]. Additionally, the use of humanized mice that more closely resemble humans in the study of vaginal infections is becoming more common[199,268]. Adaptation of models such as these to murine models of GBS colonization could reveal novels aspects of its biology and host genetic factors that lead to successful vaginal colonization.

Finally, significant questions about both vertical and horizontal GBS transmission remain. It is often assumed that neonates contract GBS from contaminated vaginal fluids during the birthing process; however, given the kinetics of neonatal disease (frequently displaying clinical symptoms within 0-24 hours of birth[51]), many cases are thought to be a result of *in utero* infections caused by ascended GBS. This idea is also supported by the frequent recovery of GBS from the amniotic fluid and chorioamniotic membranes in cases of infection-associated preterm birth[12,42,269]. While Chapters 3 and 4 of this dissertation help establish a model of ascending infection, no model of vertical GBS transmission during delivery exists. Moreover, how GBS is transmitted from person to person is unknown. Some studies have observed cases of sexual transmission of GBS[80-84]; however, no consensus on the exact route exists, nor does a model of horizontal GBS transmission. The bacterial factors involved in transmission from the mother to the perinate during delivery or in horizontal transmission may be different than those that are important for colonization, yet these fields remains completely unexplored. Given its important implication for understanding GBS disease, colonization is an area of active research.

5.3 Next Steps for Ascending Infection Research

While studies have provided some insight into virulence factors that enable GBS to gain access to the uterine space from the lower genital tract and host factors involved in this process, significant research is required to fully understand ascending GBS infection. Currently, little is known about host factors that prevent ascending infection, such as the role of the cervical barrier, endocrine signaling, and cellular immunity. Further, host specific factors and genetics that may influence ascending GBS infection are unknown. The murine model of ascending GBS infection has only recently been established[39,60], and there is significant opportunity to use this model in future studies. Much of our insight into host-GBS interactions occurs in models that are not

directly relevant to GBS infections, such as intraperitoneal, retro-orbital, and intravenous routes of infection. Moreover, *in vitro* models of infection are not appropriate in the study of ascending infection. Our understanding of the role of GBS and host factors in ascending infection could be greatly expanded through the use of the murine ascending GBS infection model. Additionally, the use of other animal models, such as guinea pigs or non-human primates, could result in an expansion in our knowledge of ascending infection. The choice of animal model is key in answering some of these questions due to important differences in pregnancy physiology, mechanism of labor and placental structure between humans and mice[270]. Nonhuman primates are the closest animal model to fully recapitulate important aspects of human pregnancy[270] but are limited in their use by ethical constraints, availability and cost. Ideally, a combination of lower animal and nonhuman primate models should be used in order to delineate relevant aspects of disease.

Clinical studies should be planned to delineate the epidemiology of ascending GBS infection. It is known that ascending GBS infection and infection-associated preterm birth occur in humans[12,42,269], yet nothing is known about the rates of ascending infection in these settings. Moreover, little is known about the specific etiology of preterm birth and stillbirth, or the environmental factors that contribute to these etiologies. As our knowledge of the host and bacterial factors involved in ascending infection increase, more information about the presence of these factors in nature is needed. If clinical samples are collected more frequently from preterm births and stillbirths they could be used to define the role of GBS and GBS factors in clinical settings.

Finally, clinical studies should be designed to identify biomarkers for ascending infection. Viral infection of the cervix[38] and diminished cervical hyaluronic acid levels[111] have

been associated with increased ascending infection, however, little is known about the clinical relevance of these or other factors in the context of ascending GBS infection. Initiatives such as the Global Alliance to Prevent Prematurity and Stillbirth (GAPPS, http://gapps.org/) and Child Health and Mortality Prevention Surveillance program (CHAMPS, http://www.ianphi.org/whatwedo/champs/index.html) can provide novel tools and insight into the study of ascending infection. Understanding the epidemiology of ascending GBS infection is vital for directing future research in this area, and filling these knowledge gaps could lead to the development of therapeutics for preventing ascending infection.

5.4 Expansion of GBS Screening Programs

Unlike the United States, some countries have not adopted the GBS screening program but instead administer antibiotics upon the development of a risk factor for GBS neonatal disease (e.g. prolonged rupture of membranes)[55]. However, neither the GBS screening program nor the risk factor assessment approaches have fully eliminated neonatal GBS infections. This is because these prevention strategies do not address the risk of ascending infection, which can potentially occur anytime during pregnancy leading to preterm birth or stillbirth, and they also do not prevent late onset GBS infections (observed in neonates who are older than one week of age) where vertical transmission is not the only mode of acquisition[271]. Also, these preventive measures do not consider the complexity of GBS infections wherein a pregnancy maybe at increased risk due to increased pathogenicity of GBS (high expression of certain virulence factors), host factors that can affect the outcome of infection, influence of the vaginal/rectal microbiome, false negative screening results, or changes in GBS antibiotic resistance. As current interventions targeting GBS infections is limited to antibiotic therapy, and given that antibiotic resistance is on the rise[272], a deeper understanding of how GBS are able to colonize the vagina

and cause neonatal disease is critical for the development of new therapeutics. Ultimately, universal screening programs are needed in more countries to measure the burden of GBS colonization and successfully prevent disease.

5.5 Therapeutics Strategies for the Prevention of Group B Streptococcus Colonization and Ascending Infection

Currently, strategies focus on the prevention of GBS transmission during labor and delivery through the use of antibiotics. This strategy does not fully capture the biology of GBS infection, nor does it completely address the full burden of GBS disease. Moreover, antibiotic resistance is increasing[272], and use of antibiotics during pregnancy has consequential effects for neonatal health that are only now being appreciated[273,274]. To successfully eradicate the burden of disease, interventions need to be specifically targeted, have minimal detrimental effects on the microbiome and target processes upstream of vertical transmission, such as colonization and ascending infection.

Multiple studies have focused on a probiotic approach to reducing vaginal GBS colonization. Recent studies using probiotic *Lactobacillus* species have shown that pretreatment of the vagina prior to GBS colonization can block GBS adherence to vaginal epithelial cells[275], and reduce colonization[276,277]. Probiotic administration of the oral colonizer *Streptococcus salivarius* has also been shown to have the ability to reduce vaginal GBS burden through a yet unidentified anti-microbial activity[278]. It is important to note that frequent doses (3-7) of probiotic bacteria were required for a protective effect *in vivo*[276,277], raising the question as to the feasibility of probiotic intervention in humans, and highlighting the need to continue to explore this field to identify an efficient and feasible probiotic therapy to prevent GBS colonization. Moreover, little is known about the interactions between GBS and the vaginal microbiome, and

whether those interactions have any positive benefits to human health. Further studies that aim to understand these interactions would shed much needed light on this topic.

A vaccine to prevent GBS colonization would be the most effective intervention; however, development of a vaccine has proven to be challenging. Recent work has shown that vaccination of mice with killed bacteria reduces preterm birth rates[279] and that mucosal vaccine delivery is more effective than intramuscular delivery[280]. Multiple studies have identified maternal antibody levels to the GBS capsule as being protective against GBS infection[281-284], and it has long been known that anti-capsular antibodies can confer protection to infection[47]. Unfortunately, vaccines targeting the GBS capsule alone are ineffective due to their poor immunogenicity and thus, conjugate-capsule vaccines and a vaccine that targets the alpha C/Rib protein family are now being tested in clinical trials (Reviewed in[285-287]). Despite the promise of these vaccine candidates, challenges to the eradication of GBS disease will exist even after the implementation of a vaccine. While ten GBS capsular serotypes have been identified, serotypes Ia, Ib, II, III, and V are predominantly responsible for GBS disease[287]. Consequently, current vaccine candidates target serotypes Ia, Ib, and III[285], and a pentavalent vaccine targeting serotypes Ia, Ib, II, III, and V is in pre-clinical development[286]. The development of vaccines targeting various antigens such as Alpha C/Rib may prove to be vital, as non-typeable GBS strains can cause disease[288]. Additionally, GBS strains can switch capsular serotypes[289], thereby evading host immunity conferred by vaccination.

It is possible that if these vaccines are developed, serotypes or strains that are not typically a significant cause of GBS disease may emerge in vaccinated populations. Indeed, this phenomenon has been observed with implementation of conjugate vaccines against *Streptococcus pneumoniae*[231,290]. Thus, GBS surveillance programs would need to remain

vigilant even after a vaccine becomes widely used. There are also significant challenges in resource-limited settings to consider prior to implementation (Reviewed in[291]). Regardless, it is clear that a vaccine would be the most effective means of reducing the global GBS burden of disease[292].

5.6 Final Thoughts

GBS has long been recognized as a significant human pathogen[48], yet we are only now, beginning to fully understand its pathogenesis almost a century later. It is clear that understanding the interplay between the host and bacteria is vital for understanding how to effectively prevent GBS disease while having minimal adverse effects on the human host. Research in this field has revealed novel insights into the bacterial virulence factors necessary for successfully establishing disease and an appropriate host response to prevent ascending infection and preterm birth. Any disturbance in this balance can lead to serious and lasting outcomes for the host, or disadvantageous pressures for the bacteria. Several examples of how this balance can be perturbed to benefit human health have described above, but more research is needed to fully understand what triggers ascending GBS infection, the host immune response to colonization and ascending infection, and the physiological drivers of fetal damage and preterm. Additionally, more epidemiological data are required to describe the global burden of GBS colonization and disease. As GBS colonization during pregnancy is intermittent and variable[79], the current screening methodology likely misses a significant portion of colonization during pregnancy. This issue results in a measurable risk for ascending GBS infection during pregnancy that could lead to stillbirth, preterm birth, and early term birth. An evaluation of earlier and more frequent GBS screening during pregnancy may shed light on these issues. With these data, effective and feasible interventions to prevent GBS disease can be developed. Ultimately, vaccination will

prove to be the most effect intervention. A combination of rational vaccine design, intelligent implementation and monitoring strategies, and strong advocacy[55] may lead to the eradication of GBS as a human pathogen.

References

1 Mokdad, A. H. *et al.* Global burden of diseases, injuries, and risk factors for young people's health during 1990-2013: a systematic analysis for the Global Burden of Disease Study 2013. *Lancet* **387**, 2383-2401, doi:10.1016/S0140-6736(16)00648-6 (2016).

2 Liu, L. *et al.* Global, regional, and national causes of child mortality: an updated systematic analysis for 2010 with time trends since 2000. *Lancet* **379**, 2151-2161, doi:10.1016/S0140-6736(12)60560-1 (2012).

3 Romero, R., Dey, S. K. & Fisher, S. J. Preterm labor: one syndrome, many causes. *Science* **345**, 760-765, doi:10.1126/science.1251816 (2014).

4 Lawn, J. E., Gravett, M. G., Nunes, T. M., Rubens, C. E. & Stanton, C. Global report on preterm birth and stillbirth (1 of 7): definitions, description of the burden and opportunities to improve data. *BMC Pregnancy Childbirth* **10 Suppl 1**, S1, doi:10.1186/1471-2393-10-S1-S1 [pii] (2010).

5 Liu, L. *et al.* Global, regional, and national causes of child mortality in 2000-13, with projections to inform post-2015 priorities: an updated systematic analysis. *Lancet* **385**, 430-440, doi:10.1016/S0140-6736(14)61698-6 (2015).

6 Marlow, N., Wolke, D., Bracewell, M. A., Samara, M. & Group, E. P. S. Neurologic and developmental disability at six years of age after extremely preterm birth. *N Engl J Med* **352**, 9-19, doi:10.1056/NEJMoa041367 (2005).

7 O'Connor, A. R., Wilson, C. M. & Fielder, A. R. Ophthalmological problems associated with preterm birth. *Eye (Lond)* **21**, 1254-1260, doi:10.1038/sj.eye.6702838 (2007).

8 Greenough, A. Long term respiratory outcomes of very premature birth (<32 weeks). *Semin Fetal Neonatal Med* **17**, 73-76, doi:10.1016/j.siny.2012.01.009 (2012).

9 Blencowe, H. *et al.* Born too soon: the global epidemiology of 15 million preterm births. *Reprod Health* **10 Suppl 1**, S2, doi:10.1186/1742-4755-10-S1-S2 (2013).

10 in *Preterm Birth: Causes, Consequences, and Prevention* (ed RE Behrman, Butler, AS) 398-429 (National Academies Press, 2007).

11 Martin, J. A., Hamilton, B. E., Osterman, M. J., Driscoll, A. K. & Mathews, T. J. Births: Final Data for 2015. *Natl Vital Stat Rep* **66**, 1 (2017).

12 Romero, R. *et al.* The role of infection in preterm labour and delivery. *Paediatr Perinat Epidemiol* **15 Suppl 2**, 41-56 (2001).

13 Han, Y. W., Shen, T., Chung, P., Buhimschi, I. A. & Buhimschi, C. S. Uncultivated bacteria as etiologic agents of intra-amniotic inflammation leading to preterm birth. *J Clin Microbiol* **47**, 38-47, doi:10.1128/JCM.01206-08 (2009).

14 DiGiulio, D. B. *et al.* Microbial prevalence, diversity and abundance in amniotic fluid during preterm labor: a molecular and culture-based investigation. *PLoS One* **3**, e3056, doi:10.1371/journal.pone.0003056 (2008).

15 Marconi, C., de Andrade Ramos, B. R., Peracoli, J. C., Donders, G. G. & da Silva, M. G. Amniotic fluid interleukin-1 beta and interleukin-6, but not interleukin-8 correlate with microbial invasion of the amniotic cavity in preterm labor. *Am J Reprod Immunol* **65**, 549-556, doi:10.1111/j.1600-0897.2010.00940.x (2011).

16 Markenson, G. R. *et al.* The use of the polymerase chain reaction to detect bacteria in amniotic fluid in pregnancies complicated by preterm labor. *Am J Obstet Gynecol* **177**, 1471-1477 (1997).

17 Mann, J. R., McDermott, S. & Gill, T. Sexually transmitted infection is associated with increased risk of preterm birth in South Carolina women insured by Medicaid. *J Matern Fetal Neonatal Med* **23**, 563-568, doi:10.3109/14767050903214574 (2010).
18 De Santis, M. *et al.* Syphilis Infection during pregnancy: fetal risks and clinical management. *Infect Dis Obstet Gynecol* **2012**, 430585, doi:10.1155/2012/430585 (2012).
19 Peltier, M. R. *et al.* Amniotic fluid and maternal race influence responsiveness of fetal membranes to bacteria. *J Reprod Immunol* **96**, 68-78, doi:10.1016/j.jri.2012.07.006 (2012).
20 Bourgeois-Nicolaos, N. *et al.* Evaluation of the Cepheid Xpert GBS assay for rapid detection of group B Streptococci in amniotic fluids from pregnant women with premature rupture of membranes. *J Clin Microbiol* **51**, 1305-1306, doi:10.1128/JCM.03356-12 (2013).
21 Parry, S. & Strauss, J. F., 3rd. Premature rupture of the fetal membranes. *N Engl J Med* **338**, 663-670, doi:10.1056/NEJM199803053381006 (1998).
22 Lannon, S. M., Vanderhoeven, J. P., Eschenbach, D. A., Gravett, M. G. & Adams Waldorf, K. M. Synergy and interactions among biological pathways leading to preterm premature rupture of membranes. *Reprod Sci* **21**, 1215-1227, doi:10.1177/1933719114534535 (2014).
23 Sadowsky, D. W., Adams, K. M., Gravett, M. G., Witkin, S. S. & Novy, M. J. Preterm labor is induced by intraamniotic infusions of interleukin-1beta and tumor necrosis factor-alpha but not by interleukin-6 or interleukin-8 in a nonhuman primate model. *Am J Obstet Gynecol* **195**, 1578-1589, doi:10.1016/j.ajog.2006.06.072 (2006).
24 Cappelletti, M., Della Bella, S., Ferrazzi, E., Mavilio, D. & Divanovic, S. Inflammation and preterm birth. *J Leukoc Biol* **99**, 67-78, doi:10.1189/jlb.3MR0615-272RR (2016).
25 Gomez-Lopez, N., Olson, D. M. & Robertson, S. A. Interleukin-6 controls uterine Th9 cells and CD8(+) T regulatory cells to accelerate parturition in mice. *Immunol Cell Biol* **94**, 79-89, doi:10.1038/icb.2015.63 (2016).
26 Robertson, S. A. *et al.* Interleukin-6 is an essential determinant of on-time parturition in the mouse. *Endocrinology* **151**, 3996-4006, doi:10.1210/en.2010-0063 (2010).
27 Martinez de Tejada, B. Antibiotic use and misuse during pregnancy and delivery: benefits and risks. *Int J Environ Res Public Health* **11**, 7993-8009, doi:10.3390/ijerph110807993 (2014).
28 Hutzal, C. E. *et al.* Use of antibiotics for the treatment of preterm parturition and prevention of neonatal morbidity: a metaanalysis. *Am J Obstet Gynecol* **199**, 620 e621-628, doi:10.1016/j.ajog.2008.07.008 (2008).
29 Kenyon, S. *et al.* Childhood outcomes after prescription of antibiotics to pregnant women with spontaneous preterm labour: 7-year follow-up of the ORACLE II trial. *Lancet* **372**, 1319-1327, doi:10.1016/S0140-6736(08)61203-9 (2008).
30 Kenyon, S. *et al.* Childhood outcomes after prescription of antibiotics to pregnant women with preterm rupture of the membranes: 7-year follow-up of the ORACLE I trial. *Lancet* **372**, 1310-1318, doi:10.1016/S0140-6736(08)61202-7 (2008).
31 Adams Waldorf, K., Gibbs, R., Gravett, M. in *Infectious Diseases of the Fetus and Newborn* Ch. 3, 51-80 (Elsevier Saunders, 2015).
32 Thinkhamrop, J., Hofmeyr, G. J., Adetoro, O., Lumbiganon, P. & Ota, E. Antibiotic prophylaxis during the second and third trimester to reduce adverse pregnancy outcomes

and morbidity. *Cochrane Database Syst Rev* **1**, CD002250, doi:10.1002/14651858.CD002250.pub2 (2015).
33 Brown, E. D. & Wright, G. D. Antibacterial drug discovery in the resistance era. *Nature* **529**, 336-343, doi:10.1038/nature17042 (2016).
34 Hussey, S. *et al.* Parenteral antibiotics reduce bifidobacteria colonization and diversity in neonates. *Int J Microbiol* **2011**, doi:10.1155/2011/130574 (2011).
35 Favier, C. F., de Vos, W. M. & Akkermans, A. D. Development of bacterial and bifidobacterial communities in feces of newborn babies. *Anaerobe* **9**, 219-229, doi:10.1016/j.anaerobe.2003.07.001 (2003).
36 Mendz, G. L., Kaakoush, N. O. & Quinlivan, J. A. Bacterial aetiological agents of intra-amniotic infections and preterm birth in pregnant women. *Front Cell Infect Microbiol* **3**, 58, doi:10.3389/fcimb.2013.00058 (2013).
37 Hansen, L. K. *et al.* The cervical mucus plug inhibits, but does not block, the passage of ascending bacteria from the vagina during pregnancy. *Acta Obstet Gynecol Scand* **93**, 102-108, doi:10.1111/aogs.12296 (2014).
38 Racicot, K. *et al.* Viral infection of the pregnant cervix predisposes to ascending bacterial infection. *J Immunol* **191**, 934-941, doi:10.4049/jimmunol.1300661 (2013).
39 Randis, T. M. *et al.* Group B Streptococcus beta-hemolysin/cytolysin breaches maternal-fetal barriers to cause preterm birth and intrauterine fetal demise in vivo. *J Infect Dis* **210**, 265-273, doi:10.1093/infdis/jiu067 (2014).
40 De Clercq, E., Kalmar, I. & Vanrompay, D. Animal models for studying female genital tract infection with Chlamydia trachomatis. *Infect Immun* **81**, 3060-3067, doi:10.1128/IAI.00357-13 (2013).
41 McDuffie, R. S. & Gibbs, R. S. Animal models of ascending genital-tract infection in pregnancy. *Infect Dis Obstet Gynecol* **2**, 60-70, doi:10.1155/S1064744994000414 (1994).
42 Hillier, S. L., Krohn, M. A., Kiviat, N. B., Watts, D. H. & Eschenbach, D. A. Microbiologic causes and neonatal outcomes associated with chorioamnion infection. *Am J Obstet Gynecol* **165**, 955-961 (1991).
43 Allen, U. *et al.* Relationship between antenatal group B streptococcal vaginal colonization and premature labour. *Paediatr Child Health* **4**, 465-469 (1999).
44 Edwards, M. S. & Baker, C. J. Group B streptococcal infections in elderly adults. *Clin Infect Dis* **41**, 839-847, doi:10.1086/432804 (2005).
45 Sendi, P., Johansson, L. & Norrby-Teglund, A. Invasive group B Streptococcal disease in non-pregnant adults : a review with emphasis on skin and soft-tissue infections. *Infection* **36**, 100-111, doi:10.1007/s15010-007-7251-0 (2008).
46 Norcard, N. & Mollereau, R. Sur une mammite contagieuse des vaches laitieres. *Ann Inst Pasteur* **1**, 109-126 (1887).
47 Lancefield, R. C. & Hare, R. The Serological Differentiation of Pathogenic and Non-Pathogenic Strains of Hemolytic Streptococci from Parturient Women. *J Exp Med* **61**, 335-349 (1935).
48 Fry, R. M. Fatal infections by hemolytic streptococcus group B. *Lancet* **1**, 199-201 (1938).
49 Le Doare, K. & Heath, P. T. An overview of global GBS epidemiology. *Vaccine* **31 Suppl 4**, D7-12, doi:10.1016/j.vaccine.2013.01.009 (2013).
50 Stoll, B. J. *et al.* Early Onset Neonatal Sepsis: The Burden of Group B Streptococcal and E. coli Disease Continues. *Pediatrics* **127**, 817-826, doi:10.1542/peds.2010-2217 (2011).

51 Schrag, S. J. *et al.* Epidemiology of Invasive Early-Onset Neonatal Sepsis, 2005 to 2014. *Pediatrics* **138**, e20162013, doi:10.1542/peds.2016-2013 (2016).

52 Weston, E. J. *et al.* The burden of invasive early-onset neonatal sepsis in the United States, 2005-2008. *Pediatr Infect Dis J* **30**, 937-941, doi:10.1097/INF.0b013e318223bad2 (2011).

53 Kalliola, S., Vuopio-Varkila, J., Takala, A. K. & Eskola, J. Neonatal group B streptococcal disease in Finland: a ten-year nationwide study. *Pediatr Infect Dis J* **18**, 806-810 (1999).

54 *Group B Strep (GBS)*, <https://www.cdc.gov/groupbstrep/clinicians/clinical-overview.html> (2016).

55 Burns, G. & Plumb, J. GBS public awareness, advocacy, and prevention--what's working, what's not and why we need a maternal GBS vaccine. *Vaccine* **31 Suppl 4**, D58-65, doi:10.1016/j.vaccine.2013.02.039 (2013).

56 Hoogkamp-Korstanje, J. A., Gerards, L. J. & Cats, B. P. Maternal carriage and neonatal acquisition of group B streptococci. *J Infect Dis* **145**, 800-803 (1982).

57 Cheng, P. J. *et al.* Risk factors for recurrence of group B streptococcus colonization in a subsequent pregnancy. *Obstet Gynecol* **111**, 704-709, doi:10.1097/AOG.0b013e318163cd6b (2008).

58 Mitchell, K. *et al.* Group B Streptococcus colonization and higher maternal IL-1beta concentrations are associated with early term births. *J Matern Fetal Neonatal Med* **26**, 56-61, doi:10.3109/14767058.2012.725789 (2013).

59 Monari, F. *et al.* Fetal bacterial infections in antepartum stillbirth: a case series. *Early Hum Dev* **89**, 1049-1054, doi:10.1016/j.earlhumdev.2013.08.010 (2013).

60 Vornhagen, J. *et al.* Bacterial Hyaluronidase Promotes Ascending GBS Infection and Preterm Birth. *MBio* **7**, pii: e00781-00716, doi:10.1128/mBio.00781-16 (2016).

61 Adams Waldorf, K. M. *et al.* Choriodecidual group B streptococcal inoculation induces fetal lung injury without intra-amniotic infection and preterm labor in Macaca nemestrina. *PLoS One* **6**, e28972, doi:10.1371/journal.pone.0028972 (2011).

62 Boldenow, E. *et al.* Group B Streptococcus circumvents neutrophils and neutrophil extracellular traps during amniotic cavity invasion and preterm labor. *Science Immunology* **1**, doi:10.1126/sciimmunol.aah4576 (2016).

63 Ancona, R. J. & Ferrieri, P. Experimental vaginal colonization and mother-infant transmission of group B streptococci in rats. *Infect Immun* **26**, 599-603 (1979).

64 Kothary, V. *et al.* Group B Streptococcus Induces Neutrophil Recruitment to Gestational Tissues and Elaboration of Extracellular Traps and Nutritional Immunity. *Frontiers in Cellular and Infection Microbiology* **7**, fcimb.2017.00019, doi:10.3389/fcimb.2017.00019 (2017).

65 Kolar, S. L. *et al.* Group B Streptococcus Evades Host Immunity by Degrading Hyaluronan. *Cell Host Microbe* **18**, 694-704, doi:10.1016/j.chom.2015.11.001 (2015).

66 Whidbey, C. *et al.* A streptococcal lipid toxin induces membrane permeabilization and pyroptosis leading to fetal injury. *EMBO molecular medicine* **7**, 488-505, doi:10.15252/emmm.201404883 (2015).

67 Singh, U. *et al.* Immunological properties of human decidual macrophages--a possible role in intrauterine immunity. *Reproduction* **129**, 631-637, doi:10.1530/rep.1.00331 (2005).

68 Boldenow, E. *et al.* Role of cytokine signaling in group B Streptococcus-stimulated expression of human beta defensin-2 in human extraplacental membranes. *Am J Reprod Immunol* **73**, 263-272, doi:10.1111/aji.12325 (2015).
69 Duriez, M. *et al.* Human decidual macrophages and NK cells differentially express Toll-like receptors and display distinct cytokine profiles upon TLR stimulation. *Front Microbiol* **5**, 316, doi:10.3389/fmicb.2014.00316 (2014).
70 Ali, S. R. *et al.* Siglec-5 and Siglec-14 are polymorphic paired receptors that modulate neutrophil and amnion signaling responses to group B Streptococcus. *J Exp Med* **211**, 1231-1242, doi:10.1084/jem.20131853 (2014).
71 Kwatra, G. *et al.* Prevalence of maternal colonisation with group B streptococcus: a systematic review and meta-analysis. *Lancet Infect Dis*, doi:10.1016/S1473-3099(16)30055-X (2016).
72 Barcaite, E. *et al.* Prevalence of maternal group B streptococcal colonisation in European countries. *Acta Obstet Gynecol Scand* **87**, 260-271, doi:10.1080/00016340801908759 (2008).
73 Nan, C. *et al.* Maternal group B Streptococcus-related stillbirth: a systematic review. *BJOG* **122**, 1437-1445, doi:10.1111/1471-0528.13527 (2015).
74 Petersen, K. B. *et al.* Increasing prevalence of group B streptococcal infection among pregnant women. *Dan Med J* **61**, A4908 (2014).
75 Kleweis, S. M., Cahill, A. G., Odibo, A. O. & Tuuli, M. G. Maternal Obesity and Rectovaginal Group B Streptococcus Colonization at Term. *Infect Dis Obstet Gynecol* **2015**, 586767, doi:10.1155/2015/586767 (2015).
76 Colicchia, L. C., Lauderdale, D. S., Du, H., Adams, M. & Hirsch, E. Recurrence of group B streptococcus colonization in successive pregnancies. *J Perinatol* **35**, 173-176, doi:10.1038/jp.2014.185 (2015).
77 Dahan-Saal, J. *et al.* [Determinants of group B streptococcus maternal colonization and factors related to its vertical perinatal transmission: case-control study]. *Gynecol Obstet Fertil* **39**, 281-288, doi:10.1016/j.gyobfe.2011.02.014 (2011).
78 Bryant, A. S., Cheng, Y. W. & Caughey, A. B. Equality in obstetrical care: racial/ethnic variation in group B streptococcus screening. *Matern Child Health J* **15**, 1160-1165, doi:10.1007/s10995-010-0682-8 (2011).
79 Hansen, S. M., Uldbjerg, N., Kilian, M. & Sorensen, U. B. Dynamics of Streptococcus agalactiae colonization in women during and after pregnancy and in their infants. *J Clin Microbiol* **42**, 83-89 (2004).
80 Bliss, S. J. *et al.* Group B Streptococcus colonization in male and nonpregnant female university students: a cross-sectional prevalence study. *Clin Infect Dis* **34**, 184-190, doi:10.1086/338258 (2002).
81 Foxman, B. *et al.* Acquisition and transmission of group B Streptococcus during pregnancy. *J Infect Dis* **198**, 1375-1378, doi:10.1086/592221 (2008).
82 Foxman, B. *et al.* Incidence and duration of group B Streptococcus by serotype among male and female college students living in a single dormitory. *Am J Epidemiol* **163**, 544-551, doi:10.1093/aje/kwj075 (2006).
83 Manning, S. D. *et al.* Prevalence of group B streptococcus colonization and potential for transmission by casual contact in healthy young men and women. *Clin Infect Dis* **39**, 380-388, doi:10.1086/422321 (2004).

84 Manning, S. D. *et al.* Determinants of co-colonization with group B streptococcus among heterosexual college couples. *Epidemiology* **13**, 533-539, doi:10.1097/01.EDE.0000023328.94610.49 (2002).
85 Patras, K. A., Rosler, B., Thoman, M. L. & Doran, K. S. Characterization of host immunity during persistent vaginal colonization by Group B Streptococcus. *Mucosal Immunol* **8**, 1339-1348, doi:10.1038/mi.2015.23 (2015).
86 Soriani, M. *et al.* Group B Streptococcus crosses human epithelial cells by a paracellular route. *J Infect Dis* **193**, 241-250, doi:10.1086/498982 (2006).
87 Jiang, S. & Wessels, M. R. BsaB, a novel adherence factor of group B Streptococcus. *Infect Immun* **82**, 1007-1016, doi:10.1128/IAI.01014-13 (2014).
88 Seo, H. S. *et al.* Characterization of fibrinogen binding by glycoproteins Srr1 and Srr2 of Streptococcus agalactiae. *J Biol Chem* **288**, 35982-35996, doi:10.1074/jbc.M113.513358 (2013).
89 Sheen, T. R. *et al.* Serine-rich repeat proteins and pili promote Streptococcus agalactiae colonization of the vaginal tract. *J Bacteriol* **193**, 6834-6842, doi:10.1128/JB.00094-11 [pii] (2011).
90 Wang, N. Y. *et al.* Group B streptococcal serine-rich repeat proteins promote interaction with fibrinogen and vaginal colonization. *J Infect Dis* **210**, 982-991, doi:10.1093/infdis/jiu151 (2014).
91 Banerjee, A. *et al.* Bacterial Pili exploit integrin machinery to promote immune activation and efficient blood-brain barrier penetration. *Nat Commun* **2**, 462, doi:10.1038/ncomms1474 (2011).
92 Bolduc, G. R., Baron, M. J., Gravekamp, C., Lachenauer, C. S. & Madoff, L. C. The alpha C protein mediates internalization of group B Streptococcus within human cervical epithelial cells. *Cell Microbiol* **4**, 751-758 (2002).
93 Baron, M. J., Filman, D. J., Prophete, G. A., Hogle, J. M. & Madoff, L. C. Identification of a glycosaminoglycan binding region of the alpha C protein that mediates entry of group B Streptococci into host cells. *J Biol Chem* **282**, 10526-10536, doi:10.1074/jbc.M608279200 (2007).
94 Goluszko, P., Popov, V., Wen, J., Jones, A. & Yallampalli, C. Group B streptococcus exploits lipid rafts and phosphoinositide 3-kinase/Akt signaling pathway to invade human endometrial cells. *Am J Obstet Gynecol* **199**, 548 e541-549, doi:10.1016/j.ajog.2008.03.051 (2008).
95 Winram, S. B., Jonas, M., Chi, E. & Rubens, C. E. Characterization of group B streptococcal invasion of human chorion and amnion epithelial cells In vitro. *Infect Immun* **66**, 4932-4941 (1998).
96 Whidbey, C. *et al.* A hemolytic pigment of Group B Streptococcus allows bacterial penetration of human placenta. *J Exp Med* **210**, 1265-1281, doi:10.1084/jem.20122753 (2013).
97 Doran, K. S. *et al.* Blood-brain barrier invasion by group B Streptococcus depends upon proper cell-surface anchoring of lipoteichoic acid. *J Clin Invest* **115**, 2499-2507, doi:10.1172/JCI23829 (2005).
98 Parker, R. E., Knupp, D., Al Safadi, R., Rosenau, A. & Manning, S. D. Contribution of the RgfD Quorum Sensing Peptide to rgf Regulation and Host Cell Association in Group B Streptococcus. *Genes (Basel)* **8**, 10.3390/genes8010023, doi:10.3390/genes8010023 (2017).

99 Dramsi, S., Morello, E., Poyart, C. & Trieu-Cuot, P. Epidemiologically and clinically relevant Group B Streptococcus isolates do not bind collagen but display enhanced binding to human fibrinogen. *Microbes Infect* **14**, 1044-1048, doi:10.1016/j.micinf.2012.07.004 (2012).
100 Sherman, J. M. The Streptococci. *Bacteriol Rev* **1**, 3-97 (1937).
101 Marchlewicz, B. A. & Duncan, J. L. Properties of a hemolysin produced by group B streptococci. *Infect Immun* **30**, 805-813 (1980).
102 Pritzlaff, C. A. *et al.* Genetic basis for the beta-haemolytic/cytolytic activity of group B Streptococcus. *Mol Microbiol* **39**, 236-247 (2001).
103 Liu, G. Y. *et al.* Sword and shield: linked group B streptococcal beta-hemolysin/cytolysin and carotenoid pigment function to subvert host phagocyte defense. *Proc Natl Acad Sci U S A* **101**, 14491-14496, doi:10.1073/pnas.0406143101 (2004).
104 Leclercq, S. Y. *et al.* Pathogenesis of Streptococcus urinary tract infection depends on bacterial strain and beta-hemolysin/cytolysin that mediates cytotoxicity, cytokine synthesis, inflammation and virulence. *Sci Rep* **6**, 29000, doi:10.1038/srep29000 (2016).
105 Carey, A. J. *et al.* Infection and cellular defense dynamics in a novel 17beta-estradiol murine model of chronic human group B streptococcus genital tract colonization reveal a role for hemolysin in persistence and neutrophil accumulation. *J Immunol* **192**, 1718-1731, doi:10.4049/jimmunol.1202811 (2014).
106 Patras, K. A. *et al.* Group B Streptococcus CovR regulation modulates host immune signalling pathways to promote vaginal colonization. *Cell Microbiol* **15**, 1154-1167, doi:10.1111/cmi.12105 (2013).
107 Gochnauer, T. A. & Wilson, J. B. The production of hyaluronidase by Lancefield's Group B streptococci. *J Bacteriol* **62**, 405-414 (1951).
108 Baker, J. R. & Pritchard, D. G. Action pattern and substrate specificity of the hyaluronan lyase from group B streptococci. *Biochem J* **348 Pt 2**, 465-471 (2000).
109 Stern, R., Asari, A. A. & Sugahara, K. N. Hyaluronan fragments: an information-rich system. *Eur J Cell Biol* **85**, 699-715, doi:10.1016/j.ejcb.2006.05.009 (2006).
110 Mahendroo, M. Cervical remodeling in term and preterm birth: insights from an animal model. *Reproduction* **143**, 429-438, doi:10.1530/REP-11-0466 (2012).
111 Akgul, Y. *et al.* Hyaluronan in cervical epithelia protects against infection-mediated preterm birth. *J Clin Invest* **124**, 5481-5489, doi:10.1172/JCI78765 (2014).
112 Surve, M. V. *et al.* Membrane Vesicles of Group B Streptococcus Disrupt Feto-Maternal Barrier Leading to Preterm Birth. *PLoS Pathog* **12**, e1005816, doi:10.1371/journal.ppat.1005816 (2016).
113 Christie, R., Atkins, N.E. , Munch-Petersen, E. A note on a lytic phenomenon shown by group B streptococci. *Aust J Exp Biol Med Sci* **22**, 197–200 (1944).
114 Lang, S. & Palmer, M. Characterization of Streptococcus agalactiae CAMP factor as a pore-forming toxin. *J Biol Chem* **278**, 38167-38173, doi:10.1074/jbc.M303544200 (2003).
115 Jurgens, D., Sterzik, B. & Fehrenbach, F. J. Unspecific binding of group B streptococcal cocytolysin (CAMP factor) to immunoglobulins and its possible role in pathogenicity. *J Exp Med* **165**, 720-732 (1987).
116 Hensler, M. E., Quach, D., Hsieh, C. J., Doran, K. S. & Nizet, V. CAMP factor is not essential for systemic virulence of Group B Streptococcus. *Microb Pathog* **44**, 84-88, doi:10.1016/j.micpath.2007.08.005 (2008).

117 Kvam, A. I., Iversen, O. J. & Bevanger, L. Binding of human IgA to HCl-extracted c protein from group B streptococci (GBS). *APMIS* **100**, 1129-1132 (1992).
118 Nordstrom, T. *et al.* Human Siglec-5 inhibitory receptor and immunoglobulin A (IgA) have separate binding sites in streptococcal beta protein. *J Biol Chem* **286**, 33981-33991, doi:10.1074/jbc.M111.251728 (2011).
119 Gendrin, C. *et al.* Mast cell degranulation by a hemolytic lipid toxin decreases GBS colonization and infection. *Sci Adv* **1**, e1400225, doi:10.1126/sciadv.1400225 (2015).
120 Thomson, A. J. *et al.* Leukocytes infiltrate the myometrium during human parturition: further evidence that labour is an inflammatory process. *Hum Reprod* **14**, 229-236 (1999).
121 Bollapragada, S. *et al.* Term labor is associated with a core inflammatory response in human fetal membranes, myometrium, and cervix. *Am J Obstet Gynecol* **200**, 104 e101-111, doi:10.1016/j.ajog.2008.08.032 (2009).
122 Yuan, M., Jordan, F., McInnes, I. B., Harnett, M. M. & Norman, J. E. Leukocytes are primed in peripheral blood for activation during term and preterm labour. *Mol Hum Reprod* **15**, 713-724, doi:10.1093/molehr/gap054 (2009).
123 Lee, S. K., Kim, C. J., Kim, D. J. & Kang, J. H. Immune cells in the female reproductive tract. *Immune Netw* **15**, 16-26, doi:10.4110/in.2015.15.1.16 (2015).
124 Gomez-Lopez, N., StLouis, D., Lehr, M. A., Sanchez-Rodriguez, E. N. & Arenas-Hernandez, M. Immune cells in term and preterm labor. *Cell Mol Immunol* **11**, 571-581, doi:10.1038/cmi.2014.46 (2014).
125 Hamilton, S. *et al.* Macrophages infiltrate the human and rat decidua during term and preterm labor: evidence that decidual inflammation precedes labor. *Biol Reprod* **86**, 39, doi:10.1095/biolreprod.111.095505 (2012).
126 Gupta, R. *et al.* RNA and beta-hemolysin of group B Streptococcus induce interleukin-1beta (IL-1beta) by activating NLRP3 inflammasomes in mouse macrophages. *J Biol Chem* **289**, 13701-13705, doi:10.1074/jbc.C114.548982 (2014).
127 Boldenow, E., Hassan, I., Chames, M. C., Xi, C. & Loch-Caruso, R. The trichloroethylene metabolite S-(1,2-dichlorovinyl)-l-cysteine but not trichloroacetate inhibits pathogen-stimulated TNF-alpha in human extraplacental membranes in vitro. *Reprod Toxicol* **52**, 1-6, doi:10.1016/j.reprotox.2015.01.007 (2015).
128 Boldenow, E. *et al.* Antimicrobial peptide response to group B Streptococcus in human extraplacental membranes in culture. *Placenta* **34**, 480-485, doi:10.1016/j.placenta.2013.02.010 (2013).
129 Flores-Herrera, H. *et al.* An experimental mixed bacterial infection induced differential secretion of proinflammatory cytokines (IL-1beta, TNFalpha) and proMMP-9 in human fetal membranes. *Placenta* **33**, 271-277, doi:10.1016/j.placenta.2012.01.007 (2012).
130 Gilbert, N. M., Lewis, W. G. & Lewis, A. L. Clinical features of bacterial vaginosis in a murine model of vaginal infection with Gardnerella vaginalis. *PLoS One* **8**, e59539, doi:10.1371/journal.pone.0059539 (2013).
131 Berg, T. G., Philpot, K. L., Welsh, M. S., Sanger, W. G. & Smith, C. V. Ureaplasma/Mycoplasma-infected amniotic fluid: pregnancy outcome in treated and nontreated patients. *J Perinatol* **19**, 275-277 (1999).
132 Jones, H. E. *et al.* Differing prevalence and diversity of bacterial species in fetal membranes from very preterm and term labor. *PLoS One* **4**, e8205, doi:10.1371/journal.pone.0008205 (2009).

133 Miralles, R. *et al.* Relationship between antenatal inflammation and antenatal infection identified by detection of microbial genes by polymerase chain reaction. *Pediatr Res* **57**, 570-577, doi:10.1203/01.PDR.0000155944.48195.97 (2005).
134 Lu, B. *et al.* First molecular evidence of intrauterine and surgical-site infections caused by Streptococcus dysgalactiae subsp. equisimilis. *J Infect Dev Ctries* **10**, 673-677, doi:10.3855/jidc.7914 (2016).
135 Horowitz, S., Mazor, M., Romero, R., Horowitz, J. & Glezerman, M. Infection of the amniotic cavity with Ureaplasma urealyticum in the midtrimester of pregnancy. *J Reprod Med* **40**, 375-379 (1995).
136 Jalava, J. *et al.* Bacterial 16S rDNA polymerase chain reaction in the detection of intra-amniotic infection. *Br J Obstet Gynaecol* **103**, 664-669 (1996).
137 de Jonge, M. I. *et al.* A novel guinea pig model of Chlamydia trachomatis genital tract infection. *Vaccine* **29**, 5994-6001, doi:10.1016/j.vaccine.2011.06.037 (2011).
138 Pal, S., Hui, W., Peterson, E. M. & de la Maza, L. M. Factors influencing the induction of infertility in a mouse model of Chlamydia trachomatis ascending genital tract infection. *J Med Microbiol* **47**, 599-605, doi:10.1099/00222615-47-7-599 (1998).
139 Russell, A. N. *et al.* Analysis of Factors Driving Incident and Ascending Infection and the Role of Serum Antibody in Chlamydia trachomatis Genital Tract Infection. *J Infect Dis* **213**, 523-531, doi:10.1093/infdis/jiv438 (2016).
140 Han, Y. W. *et al.* Fusobacterium nucleatum induces premature and term stillbirths in pregnant mice: implication of oral bacteria in preterm birth. *Infect Immun* **72**, 2272-2279 (2004).
141 Gardella, C. *et al.* Identification and sequencing of bacterial rDNAs in culture-negative amniotic fluid from women in premature labor. *Am J Perinatol* **21**, 319-323, doi:10.1055/s-2004-831884 (2004).
142 Fidel, P. I., Jr., Romero, R., Maymon, E. & Hertelendy, F. Bacteria-induced or bacterial product-induced preterm parturition in mice and rabbits is preceded by a significant fall in serum progesterone concentrations. *J Matern Fetal Med* **7**, 222-226, doi:10.1002/(SICI)1520-6661(199809/10)7:5<222::AID-MFM2>3.0.CO;2-# (1998).
143 Cumley, N. J., Smith, L. M., Anthony, M. & May, R. C. The CovS/CovR acid response regulator is required for intracellular survival of group B Streptococcus in macrophages. *Infect Immun* **80**, 1650-1661, doi:10.1128/IAI.05443-11 (2012).
144 Park, S. E., Jiang, S. & Wessels, M. R. CsrRS and environmental pH regulate group B streptococcus adherence to human epithelial cells and extracellular matrix. *Infect Immun* **80**, 3975-3984, doi:10.1128/IAI.00699-12 (2012).
145 Faralla, C. *et al.* Analysis of two-component systems in group B Streptococcus shows that RgfAC and the novel FspSR modulate virulence and bacterial fitness. *MBio* **5**, e00870-00814, doi:10.1128/mBio.00870-14 (2014).
146 Lamy, M. C. *et al.* CovS/CovR of group B streptococcus: a two-component global regulatory system involved in virulence. *Mol Microbiol* **54**, 1250-1268, doi:10.1111/j.1365-2958.2004.04365.x (2004).
147 Noble, M. A., Bent, J. M. & West, A. B. Detection and identification of group B streptococci by use of pigment production. *J Clin Pathol* **36**, 350-352 (1983).
148 Hooven, T. A. *et al.* Complete Genome Sequence of Streptococcus agalactiae CNCTC 10/84, a Hypervirulent Sequence Type 26 Strain. *Genome Announc* **2**, doi:10.1128/genomeA.01338-14 e01338-14 [pii] (2014).

149 Wilkinson, H. W. & Eagon, R. G. Type-specific antigens of group B type Ic streptococci. *Infect Immun* **4**, 596-604 (1971).
150 Johnzon, C. F., Ronnberg, E. & Pejler, G. The Role of Mast Cells in Bacterial Infection. *Am J Pathol* **186**, 4-14, doi:10.1016/j.ajpath.2015.06.024 (2016).
151 Matsui, H. *et al.* Dermal mast cells reduce progressive tissue necrosis caused by subcutaneous infection with Streptococcus pyogenes in mice. *J Med Microbiol* **60**, 128-134, doi:10.1099/jmm.0.020495-0 (2011).
152 Nakamura, Y. *et al.* Staphylococcus delta-toxin induces allergic skin disease by activating mast cells. *Nature* **503**, 397-401, doi:10.1038/nature12655 (2013).
153 Malbec, O. *et al.* Peritoneal cell-derived mast cells: an in vitro model of mature serosal-type mouse mast cells. *Journal of Immunology* **178**, 6465-6475, doi:178/10/6465 [pii] (2007).
154 Brinkmann, V. & Zychlinsky, A. Beneficial suicide: why neutrophils die to make NETs. *Nat Rev Microbiol* **5**, 577-582, doi:10.1038/nrmicro1710 (2007).
155 Gupta, A. K., Hasler, P., Holzgreve, W., Gebhardt, S. & Hahn, S. Induction of neutrophil extracellular DNA lattices by placental microparticles and IL-8 and their presence in preeclampsia. *Hum Immunol* **66**, 1146-1154, doi:10.1016/j.humimm.2005.11.003 (2005).
156 Brinkmann, V. *et al.* Neutrophil extracellular traps kill bacteria. *Science* **303**, 1532-1535, doi:10.1126/science.1092385 (2004).
157 Carlin, A. F. *et al.* Molecular mimicry of host sialylated glycans allows a bacterial pathogen to engage neutrophil Siglec-9 and dampen the innate immune response. *Blood* **113**, 3333-3336, doi:10.1182/blood-2008-11-187302 (2009).
158 Chaffin, D. O., Mentele, L. M. & Rubens, C. E. Sialylation of group B streptococcal capsular polysaccharide is mediated by cpsK and is required for optimal capsule polymerization and expression. *Journal of Bacteriology* **187**, 4615-4626, doi:187/13/4615 [pii] 10.1128/JB.187.13.4615-4626.2005 (2005).
159 Lupo, A., Ruppen, C., Hemphill, A., Spellerberg, B. & Sendi, P. Phenotypic and molecular characterization of hyperpigmented group B Streptococci. *Int J Med Microbiol* **304**, 717-724, doi:10.1016/j.ijmm.2014.05.003 (2014).
160 Sullivan, M. J. *et al.* The Streptococcus agalactiae virulence regulator CovR affects the pathogenesis of urinary tract infection. *J Infect Dis*, doi:10.1093/infdis/jiw589 (2016).
161 Tamura, G. S., Kuypers, J. M., Smith, S., Raff, H. & Rubens, C. E. Adherence of group B streptococci to cultured epithelial cells: roles of environmental factors and bacterial surface components. *Infect Immun* **62**, 2450-2458 (1994).
162 D'Urzo, N. *et al.* Acidic pH strongly enhances in vitro biofilm formation by a subset of hypervirulent ST-17 Streptococcus agalactiae strains. *Appl Environ Microbiol* **80**, 2176-2185, doi:10.1128/AEM.03627-13 (2014).
163 Ho, Y. R. *et al.* The enhancement of biofilm formation in Group B streptococcal isolates at vaginal pH. *Med Microbiol Immunol* **202**, 105-115, doi:10.1007/s00430-012-0255-0 (2013).
164 Borges, S., Silva, J. & Teixeira, P. Survival and biofilm formation by Group B streptococci in simulated vaginal fluid at different pHs. *Antonie Van Leeuwenhoek* **101**, 677-682, doi:10.1007/s10482-011-9666-y (2012).
165 Ravel, J. *et al.* Vaginal microbiome of reproductive-age women. *Proc Natl Acad Sci U S A* **108 Suppl 1**, 4680-4687, doi:10.1073/pnas.1002611107 (2011).

166 Hickman, M. E., Rench, M. A., Ferrieri, P. & Baker, C. J. Changing epidemiology of group B streptococcal colonization. *Pediatrics* **104**, 203-209 (1999).
167 Taylor, J. K., Hall, R. W. & Dupre, A. R. The incidence of group B streptococcus in the vaginal tracts of pregnant women in central Alabama. *Clin Lab Sci* **15**, 16-17 (2002).
168 Lin, F. Y., Weisman, L. E., Troendle, J. & Adams, K. Prematurity is the major risk factor for late-onset group B streptococcus disease. *J Infect Dis* **188**, 267-271, doi:10.1086/376457 (2003).
169 Oh, H. Y., Seo, S. S., Kong, J. S., Lee, J. K. & Kim, M. K. Association between Obesity and Cervical Microflora Dominated by Lactobacillus iners in Korean Women. *J Clin Microbiol* **53**, 3304-3309, doi:10.1128/JCM.01387-15 (2015).
170 Poston, L. *et al.* Preconceptional and maternal obesity: epidemiology and health consequences. *Lancet Diabetes Endocrinol* **4**, 1025-1036, doi:10.1016/S2213-8587(16)30217-0 (2016).
171 Sagar, A. *et al.* The beta-hemolysin and intracellular survival of Streptococcus agalactiae in human macrophages. *PLoS One* **8**, e60160, doi:10.1371/journal.pone.0060160 (2013).
172 Martin, T. R., Rubens, C. E. & Wilson, C. B. Lung antibacterial defense mechanisms in infant and adult rats: implications for the pathogenesis of group B streptococcal infections in the neonatal lung. *J Infect Dis* **157**, 91-100 (1988).
173 Mohammadi, N. *et al.* Neutrophils Directly Recognize Group B Streptococci and Contribute to Interleukin-1beta Production during Infection. *PLoS One* **11**, e0160249, doi:10.1371/journal.pone.0160249 (2016).
174 Derre-Bobillot, A. *et al.* Nuclease A (Gbs0661), an extracellular nuclease of Streptococcus agalactiae, attacks the neutrophil extracellular traps and is needed for full virulence. *Mol Microbiol* **89**, 518-531, doi:10.1111/mmi.12295 (2013).
175 Lembo, A. *et al.* Regulation of CovR expression in Group B Streptococcus impacts blood-brain barrier penetration. *Molecular Microbiology* **77**, 431-443, doi:MMI7215 [pii] 10.1111/j.1365-2958.2010.07215.x (2010).
176 Menegazzi, R., Decleva, E. & Dri, P. Killing by neutrophil extracellular traps: fact or folklore? *Blood* **119**, 1214-1216, doi:10.1182/blood-2011-07-364604 (2012).
177 Sorensen, O. E. & Borregaard, N. Neutrophil extracellular traps - the dark side of neutrophils. *J Clin Invest* **126**, 1612-1620, doi:10.1172/JCI84538 (2016).
178 Lancefield, R. C., McCarty, M. & Everly, W. N. Multiple mouse-protective antibodies directed against group B streptococci. Special reference to antibodies effective against protein antigens. *Journal of Experimental Medicine* **142**, 165-179 (1975).
179 Martin, T. R., Rubens, C. E. & Wilson, C. B. Lung antibacterial defense mechanisms in infant and adult rats: implications for the pathogenesis of group B streptococcal infections in the neonatal lung. *J. Infect. Dis.* **157**, 91-100 (1988).
180 Lembo, A. *et al.* Regulation of CovR expression in Group B Streptococcus impacts blood-brain barrier penetration. *Mol Microbiol* **77**, 431-443, doi:10.1111/j.1365-2958.2010.07215.xMMI7215 [pii] (2010).
181 Rajagopal, L., Vo, A., Silvestroni, A. & Rubens, C. E. Regulation of cytotoxin expression by converging eukaryotic-type and two-component signalling mechanisms in Streptococcus agalactiae. *Mol Microbiol* **62**, 941-957, doi:10.1111/j.1365-2958.2006.05431.x (2006).

182 Whidbey, C. *et al.* A Hyperhemolytic/Hyperpigmented Group B Streptococcus Strain with a CovR Mutation Isolated from an Adolescent Patient with Sore Throat. *Clin Res Infect Dis* **2** (2015).
183 Nizet, V. *et al.* Group B streptococcal beta-hemolysin expression is associated with injury of lung epithelial cells. *Infect Immun* **64**, 3818-3826 (1996).
184 Lilla, J. N. *et al.* Reduced mast cell and basophil numbers and function in Cpa3-Cre; Mcl-1fl/fl mice. *Blood* **118**, 6930-6938, doi:10.1182/blood-2011-03-343962 (2011).
185 Zaitsu, M. *et al.* Estradiol activates mast cells via a non-genomic estrogen receptor-alpha and calcium influx. *Molecular Immunology* **44**, 1977-1985, doi:S0161-5890(06)00626-2 [pii] 10.1016/j.molimm.2006.09.030 (2007).
186 Lin, W. J. *et al.* Threonine phosphorylation prevents promoter DNA binding of the Group B Streptococcus response regulator CovR. *Molecular Microbiology* **71**, 1477-1495, doi:MMI6616 [pii] 10.1111/j.1365-2958.2009.06616.x (2009).
187 Braet, F., De Zanger, R. & Wisse, E. Drying cells for SEM, AFM and TEM by hexamethyldisilazane: a study on hepatic endothelial cells. *Journal of Microscopy* **186**, 84-87 (1997).
188 Brinkmann, V., Laube, B., Abu Abed, U., Goosmann, C. & Zychlinsky, A. Neutrophil extracellular traps: how to generate and visualize them. *J Vis Exp*, doi:10.3791/1724 (2010).
189 Braet, F., De Zanger, R. & Wisse, E. Drying cells for SEM, AFM and TEM by hexamethyldisilazane: a study on hepatic endothelial cells. *J. Microsc.* **186**, 84-87 (1997).
190 Adams Waldorf, K. M. *et al.* Uterine overdistention induces preterm labor mediated by inflammation: observations in pregnant women and nonhuman primates. *Am J Obstet Gynecol* **213**, 830 e831-830 e819, doi:10.1016/j.ajog.2015.08.028 (2015).
191 Vanderhoeven, J. P. *et al.* Group B streptococcal infection of the choriodecidua induces dysfunction of the cytokeratin network in amniotic epithelium: a pathway to membrane weakening. *PLoS Pathog* **10**, e1003920, doi:10.1371/journal.ppat.1003920 [pii] PPATHOGENS-D-13-01329 (2014).
192 Martin, T. R., Rubens, C. E. & Wilson, C. B. Lung antibacterial defense mechanisms in infant and adult rats: implications for the pathogenesis of group B streptococcal infections in neonatal lung. *J. Infect. Dis.* **157**, 91-100 (1988).
193 Musser, J. M., Mattingly, S. J., Quentin, R., Goudeau, A. & Selander, R. K. Identification of a high-virulence clone of type III Streptococcus agalactiae (group B Streptococcus) causing invasive neonatal disease. *Proc Natl Acad Sci U S A* **86**, 4731-4735 (1989).
194 Yost, C. C. *et al.* Impaired neutrophil extracellular trap (NET) formation: a novel innate immune deficiency of human neonates. *Blood* **113**, 6419-6427, doi:10.1182/blood-2008-07-171629 (2009).
195 Goldenberg, R. L., Culhane, J. F., Iams, J. D. & Romero, R. Epidemiology and causes of preterm birth. *Lancet* **371**, 75-84, doi:10.1016/S0140-6736(08)60074-4 (2008).
196 Schleimer, R. P., Kato, A., Kern, R., Kuperman, D. & Avila, P. C. Epithelium: at the interface of innate and adaptive immune responses. *The Journal of allergy and clinical immunology* **120**, 1279-1284, doi:10.1016/j.jaci.2007.08.046 (2007).
197 Muenzner, P. *et al.* Uropathogenic E. coli Exploit CEA to Promote Colonization of the Urogenital Tract Mucosa. *PLoS Pathog* **12**, e1005608, doi:10.1371/journal.ppat.1005608 (2016).

198 Muenzner, P., Rohde, M., Kneitz, S. & Hauck, C. R. CEACAM engagement by human pathogens enhances cell adhesion and counteracts bacteria-induced detachment of epithelial cells. *J Cell Biol* **170**, 825-836, doi:jcb.200412151 [pii] (2005).
199 Muenzner, P., Bachmann, V., Zimmermann, W., Hentschel, J. & Hauck, C. R. Human-restricted bacterial pathogens block shedding of epithelial cells by stimulating integrin activation. *Science* **329**, 1197-1201, doi:10.1126/science.1190892329/5996/1197 [pii] (2010).
200 Byers, S. L., Wiles, M. V., Dunn, S. L. & Taft, R. A. Mouse estrous cycle identification tool and images. *PLoS One* **7**, e35538, doi:10.1371/journal.pone.0035538 (2012).
201 Mu, R. *et al.* Identification of a group B streptococcal fibronectin binding protein, SfbA, that contributes to invasion of brain endothelium and development of meningitis. *Infect Immun* **82**, 2276-2286, doi:10.1128/IAI.01559-13 (2014).
202 Hill, D. R. *et al.* In vivo assessment of human vaginal oxygen and carbon dioxide levels during and post menses. *J Appl Physiol (1985)* **99**, 1582-1591, doi:10.1152/japplphysiol.01422.2004 (2005).
203 Henneke, P. *et al.* Role of lipoteichoic acid in the phagocyte response to group B streptococcus. *J Immunol* **174**, 6449-6455 (2005).
204 Williams, J. M. *et al.* Epithelial cell shedding and barrier function: a matter of life and death at the small intestinal villus tip. *Veterinary pathology* **52**, 445-455, doi:10.1177/0300985814559404 (2015).
205 Giaever, I. & Keese, C. R. A morphological biosensor for mammalian cells. *Nature* **366**, 591-592, doi:10.1038/366591a0 (1993).
206 Lamouille, S., Xu, J. & Derynck, R. Molecular mechanisms of epithelial-mesenchymal transition. *Nature reviews. Molecular cell biology* **15**, 178-196, doi:10.1038/nrm3758 (2014).
207 Hoy, B. *et al.* Distinct roles of secreted HtrA proteases from gram-negative pathogens in cleaving the junctional protein and tumor suppressor E-cadherin. *J Biol Chem* **287**, 10115-10120, doi:10.1074/jbc.C111.333419 (2012).
208 Tian, X. *et al.* E-cadherin/beta-catenin complex and the epithelial barrier. *J Biomed Biotechnol* **2011**, 567305, doi:10.1155/2011/567305 (2011).
209 Handeli, S. & Simon, J. A. A small-molecule inhibitor of Tcf/beta-catenin signaling down-regulates PPARgamma and PPARdelta activities. *Mol Cancer Ther* **7**, 521-529, doi:10.1158/1535-7163.MCT-07-2063 (2008).
210 Streuli, C. H. Integrins as architects of cell behavior. *Mol Biol Cell* **27**, 2885-2888, doi:10.1091/mbc.E15-06-0369 (2016).
211 Sackmann, E. How actin/myosin crosstalks guide the adhesion, locomotion and polarization of cells. *Biochim Biophys Acta* **1853**, 3132-3142, doi:10.1016/j.bbamcr.2015.06.012 (2015).
212 Huang, D., Cheung, A. T., Parsons, J. T. & Bryer-Ash, M. Focal adhesion kinase (FAK) regulates insulin-stimulated glycogen synthesis in hepatocytes. *J Biol Chem* **277**, 18151-18160, doi:10.1074/jbc.M104252200 (2002).
213 Byron, A. *et al.* Anti-integrin monoclonal antibodies. *J Cell Sci* **122**, 4009-4011, doi:10.1242/jcs.056770 (2009).
214 Janes, S. M. & Watt, F. M. New roles for integrins in squamous-cell carcinoma. *Nat Rev Cancer* **6**, 175-183, doi:10.1038/nrc1817 (2006).

215 Hussein, H. A. *et al.* Beyond RGD: virus interactions with integrins. *Arch Virol* **160**, 2669-2681, doi:10.1007/s00705-015-2579-8 (2015).
216 Svoboda, E. *et al.* Secreted aspartic protease 2 of Candida albicans inactivates factor H and the macrophage factor H-receptors CR3 (CD11b/CD18) and CR4 (CD11c/CD18). *Immunol Lett* **168**, 13-21, doi:10.1016/j.imlet.2015.08.009 (2015).
217 Zhao, Y. *et al.* Endothelial Cell Proteomic Response to Rickettsia conorii Infection Reveals Activation of the Janus Kinase (JAK)-Signal Transducer and Activator of Transcription (STAT)-Inferferon Stimulated Gene (ISG)15 Pathway and Reprogramming Plasma Membrane Integrin/Cadherin Signaling. *Mol Cell Proteomics* **15**, 289-304, doi:10.1074/mcp.M115.054361 (2016).
218 Edwards, J. L. & Butler, E. K. The Pathobiology of Neisseria gonorrhoeae Lower Female Genital Tract Infection. *Front Microbiol* **2**, 102, doi:10.3389/fmicb.2011.00102 (2011).
219 Hofman, P. & Vouret-Craviari, V. Microbes-induced EMT at the crossroad of inflammation and cancer. *Gut microbes* **3**, 176-185, doi:10.4161/gmic.20288 (2012).
220 Han, I. H., Kim, J. H., Kim, S. S., Ahn, M. H. & Ryu, J. S. Signaling pathways associated with IL-6 production and EMT induction in prostate epithelial cells stimulated with Trichomonas vaginalis. *Parasite Immunol*, doi:10.1111/pim.12357 (2016).
221 Ha, N. H. *et al.* Prolonged and repetitive exposure to Porphyromonas gingivalis increases aggressiveness of oral cancer cells by promoting acquisition of cancer stem cell properties. *Tumour Biol* **36**, 9947-9960, doi:10.1007/s13277-015-3764-9 (2015).
222 Sougleri, I. S. *et al.* Helicobacter pylori CagA protein induces factors involved in the epithelial to mesenchymal transition (EMT) in infected gastric epithelial cells in an EPIYA- phosphorylation-dependent manner. *FEBS J* **283**, 206-220, doi:10.1111/febs.13592 (2016).
223 MacDonald, B. T., Tamai, K. & He, X. Wnt/beta-catenin signaling: components, mechanisms, and diseases. *Dev Cell* **17**, 9-26, doi:10.1016/j.devcel.2009.06.016 (2009).
224 Pai, P., Rachagani, S., Dhawan, P. & Batra, S. K. Mucins and Wnt/beta-catenin signaling in gastrointestinal cancers: an unholy nexus. *Carcinogenesis* **37**, 223-232, doi:10.1093/carcin/bgw005 (2016).
225 Pez, F. *et al.* Wnt signaling and hepatocarcinogenesis: molecular targets for the development of innovative anticancer drugs. *J Hepatol* **59**, 1107-1117, doi:10.1016/j.jhep.2013.07.001 (2013).
226 Takahashi-Yanaga, F. & Sasaguri, T. Drug development targeting the glycogen synthase kinase-3beta (GSK-3beta)-mediated signal transduction pathway: inhibitors of the Wnt/beta-catenin signaling pathway as novel anticancer drugs. *J Pharmacol Sci* **109**, 179-183 (2009).
227 Blencowe, H. *et al.* Preterm birth-associated neurodevelopmental impairment estimates at regional and global levels for 2010. *Pediatr Res* **74 Suppl 1**, 17-34, doi:10.1038/pr.2013.204 (2013).
228 Tettelin, H. *et al.* Genome analysis of multiple pathogenic isolates of Streptococcus agalactiae: implications for the microbial "pan-genome". *Proc Natl Acad Sci U S A* **102**, 13950-13955, doi:10.1073/pnas.0506758102 (2005).
229 Rajagopal, L., Clancy, A. & Rubens, C. E. A eukaryotic type serine/threonine kinase and phosphatase in Streptococcus agalactiae reversibly phosphorylate an inorganic pyrophosphatase and affect growth, cell segregation, and virulence. *J Biol Chem* **278**, 14429-14441, doi:10.1074/jbc.M212747200 (2003).

230 Cutting, A. S. *et al.* The role of autophagy during group B Streptococcus infection of blood-brain barrier endothelium. *J Biol Chem* **289**, 35711-35723, doi:10.1074/jbc.M114.588657 (2014).
231 Weinberger, D. M., Malley, R. & Lipsitch, M. Serotype replacement in disease after pneumococcal vaccination. *Lancet* **378**, 1962-1973, doi:10.1016/S0140-6736(10)62225-8 (2011).
232 Nance, E. A. *et al.* A dense poly(ethylene glycol) coating improves penetration of large polymeric nanoparticles within brain tissue. *Science translational medicine* **4**, 149ra119, doi:10.1126/scitranslmed.3003594 (2012).
233 Nance, E. *et al.* Non-invasive delivery of stealth, brain-penetrating nanoparticles across the blood-brain barrier using MRI-guided focused ultrasound. *J Control Release* **189**, 123-132, doi:10.1016/j.jconrel.2014.06.031 (2014).
234 Chaffin, D. O., Mentele, L. M. & Rubens, C. E. Sialylation of group B streptococcal capsular polysaccharide is mediated by cpsK and is required for optimal capsule polymerization and expression. *J Bacteriol* **187**, 4615-4626, doi:10.1128/JB.187.13.4615-4626.2005 (2005).
235 Katz, J. *et al.* Mortality risk in preterm and small-for-gestational-age infants in low-income and middle-income countries: a pooled country analysis. *Lancet* **382**, 417-425, doi:10.1016/S0140-6736(13)60993-9 (2013).
236 Blencowe, H. *et al.* National, regional, and worldwide estimates of preterm birth rates in the year 2010 with time trends since 1990 for selected countries: a systematic analysis and implications. *Lancet* **379**, 2162-2172, doi:10.1016/S0140-6736(12)60820-4 (2012).
237 Rubens, C. E., Gravett, M. G., Victora, C. G. & Nunes, T. M. Global report on preterm birth and stillbirth (7 of 7): mobilizing resources to accelerate innovative solutions (Global Action Agenda). *BMC Pregnancy Childbirth* **10 Suppl 1**, S7, doi:10.1186/1471-2393-10-S1-S7 (2010).
238 Slattery, M. M. & Morrison, J. J. Preterm delivery. *Lancet* **360**, 1489-1497, doi:S0140-6736(02)11476-0 [pii] 10.1016/S0140-6736(02)11476-0 (2002).
239 Patel, R. M. *et al.* Causes and timing of death in extremely premature infants from 2000 through 2011. *N Engl J Med* **372**, 331-340, doi:10.1056/NEJMoa1403489 (2015).
240 Nold, C., Anton, L., Brown, A. & Elovitz, M. Inflammation promotes a cytokine response and disrupts the cervical epithelial barrier: a possible mechanism of premature cervical remodeling and preterm birth. *American Journal of Obstetrics and Gynecology* **206**, 208 e201-207, doi:S0002-9378(11)02476-8 [pii] 10.1016/j.ajog.2011.12.036 (2012).
241 Romero, R. *et al.* Infection and labor. VIII. Microbial invasion of the amniotic cavity in patients with suspected cervical incompetence: prevalence and clinical significance. *Am J Obstet Gynecol* **167**, 1086-1091 (1992).
242 Ueno, T. *et al.* Eukaryote-Made Thermostable DNA Polymerase Enables Rapid PCR-Based Detection of Mycoplasma, Ureaplasma and Other Bacteria in the Amniotic Fluid of Preterm Labor Cases. *PLoS One* **10**, e0129032, doi:10.1371/journal.pone.0129032 (2015).
243 Goldenberg, R. L., Hauth, J. C. & Andrews, W. W. Intrauterine infection and preterm delivery. *N Engl J Med* **342**, 1500-1507, doi:10.1056/NEJM200005183422007 (2000).
244 Bastek, J. A., Gomez, L. M. & Elovitz, M. A. The role of inflammation and infection in preterm birth. *Clinics in perinatology* **38**, 385-406, doi:10.1016/j.clp.2011.06.003 (2011).

245 Hillier, S. L. *et al.* A case-control study of chorioamnionic infection and histologic chorioamnionitis in prematurity. *N Engl J Med* **319**, 972-978, doi:10.1056/NEJM198810133191503 (1988).
246 Hitti, J. *et al.* Amniotic fluid tumor necrosis factor-alpha and the risk of respiratory distress syndrome among preterm infants. *Am J Obstet Gynecol* **177**, 50-56, doi:S0002-9378(97)70437-X [pii] (1997).
247 Campbell, J. R. *et al.* Group B streptococcal colonization and serotype-specific immunity in pregnant women at delivery. *Obstet Gynecol* **96**, 498-503 (2000).
248 Akgul, Y., Holt, R., Mummert, M., Word, A. & Mahendroo, M. Dynamic changes in cervical glycosaminoglycan composition during normal pregnancy and preterm birth. *Endocrinology* **153**, 3493-3503, doi:10.1210/en.2011-1950 (2012).
249 Baker, J. R., Yu, H., Morrison, K., Averett, W. F. & Pritchard, D. G. Specificity of the hyaluronate lyase of group-B streptococcus toward unsulphated regions of chondroitin sulphate. *Biochem J* **327 (Pt 1)**, 65-71 (1997).
250 Gochnauer, T. A. & Wilson, J. B. Hyaluronidase production in vitro by streptococci isolated from bovine mastitis cases. *American journal of veterinary research* **12**, 20-22 (1951).
251 Greif, R. L. Colorimetric determination of hyaluronidase activity. *J Biol Chem* **194**, 619-625 (1952).
252 Pioli, P. A. *et al.* Differential expression of Toll-like receptors 2 and 4 in tissues of the human female reproductive tract. *Infect Immun* **72**, 5799-5806, doi:10.1128/IAI.72.10.5799-5806.2004 (2004).
253 Gonzalez, J. M., Xu, H., Ofori, E. & Elovitz, M. A. Toll-like receptors in the uterus, cervix, and placenta: is pregnancy an immunosuppressed state? *Am J Obstet Gynecol* **197**, 296 e291-296, doi:10.1016/j.ajog.2007.06.021 (2007).
254 Wang, Z. *et al.* Two novel functions of hyaluronidase from Streptococcus agalactiae are enhanced intracellular survival and inhibition of proinflammatory cytokine expression. *Infect Immun* **82**, 2615-2625, doi:10.1128/IAI.00022-14 (2014).
255 Hynes, W. L. & Walton, S. L. Hyaluronidases of Gram-positive bacteria. *FEMS Microbiol Lett* **183**, 201-207 (2000).
256 Girish, K. S. & Kemparaju, K. The magic glue hyaluronan and its eraser hyaluronidase: a biological overview. *Life sciences* **80**, 1921-1943, doi:10.1016/j.lfs.2007.02.037 (2007).
257 Ruscheinsky, M., De la Motte, C. & Mahendroo, M. Hyaluronan and its binding proteins during cervical ripening and parturition: dynamic changes in size, distribution and temporal sequence. *Matrix Biol* **27**, 487-497, doi:10.1016/j.matbio.2008.01.010 (2008).
258 Straach, K. J., Shelton, J. M., Richardson, J. A., Hascall, V. C. & Mahendroo, M. S. Regulation of hyaluronan expression during cervical ripening. *Glycobiology* **15**, 55-65, doi:10.1093/glycob/cwh137 (2005).
259 Maul, H., Mackay, L. & Garfield, R. E. Cervical ripening: biochemical, molecular, and clinical considerations. *Clin Obstet Gynecol* **49**, 551-563 (2006).
260 Kavanagh, J., Kelly, A. J. & Thomas, J. Hyaluronidase for cervical ripening and induction of labour. *Cochrane Database Syst Rev*, CD003097, doi:10.1002/14651858.CD003097.pub2 (2006).
261 Spickenreither, M., Braun, S., Bernhardt, G., Dove, S. & Buschauer, A. Novel 6-O-acylated vitamin C derivatives as hyaluronidase inhibitors with selectivity for bacterial

lyases. *Bioorganic & medicinal chemistry letters* **16**, 5313-5316, doi:10.1016/j.bmcl.2006.07.087 (2006).
262 Lancefield, R. C., McCarty, M. & Everly, W. N. Multiple mouse-protective antibodies directed against group B streptococci. Special reference to antibodies effective against protein antigens. *J Exp Med* **142**, 165-179 (1975).
263 Hitti, J. *et al.* Amniotic fluid tumor necrosis factor-alpha and the risk of respiratory distress syndrome among preterm infants. *Am. J. Obstet. Gynecol.* **177**, 50-56, doi:S0002-9378(97)70437-X [pii] (1997).
264 Anthony, B. F., Okada, D. M. & Hobel, C. J. Epidemiology of group B Streptococcus: longitudinal observations during pregnancy. *J Infect Dis* **137**, 524-530 (1978).
265 Rolland, K., Marois, C., Siquier, V., Cattier, B. & Quentin, R. Genetic features of Streptococcus agalactiae strains causing severe neonatal infections, as revealed by pulsed-field gel electrophoresis and hylB gene analysis. *J Clin Microbiol* **37**, 1892-1898 (1999).
266 Jasarevic, E., Howerton, C. L., Howard, C. D. & Bale, T. L. Alterations in the Vaginal Microbiome by Maternal Stress Are Associated With Metabolic Reprogramming of the Offspring Gut and Brain. *Endocrinology* **156**, 3265-3276, doi:10.1210/en.2015-1177 (2015).
267 Jasarevic, E., Rodgers, A. B. & Bale, T. L. A novel role for maternal stress and microbial transmission in early life programming and neurodevelopment. *Neurobiol Stress* **1**, 81-88, doi:10.1016/j.ynstr.2014.10.005 (2015).
268 Balazs, A. B. *et al.* Vectored immunoprophylaxis protects humanized mice from mucosal HIV transmission. *Nat Med* **20**, 296-300, doi:10.1038/nm.3471 (2014).
269 Romero, R. *et al.* Infection and labor. VII. Microbial invasion of the amniotic cavity in spontaneous rupture of membranes at term. *Am J Obstet Gynecol* **166**, 129-133 (1992).
270 Adams Waldorf, K. M., Rubens, C. E. & Gravett, M. G. Use of nonhuman primate models to investigate mechanisms of infection-associated preterm birth. *BJOG* **118**, 136-144, doi:10.1111/j.1471-0528.2010.02728.x (2011).
271 Tazi, A. *et al.* The surface protein HvgA mediates group B streptococcus hypervirulence and meningeal tropism in neonates. *J Exp Med* **207**, 2313-2322, doi:10.1084/jem.20092594 (2010).
272 Castor, M. L. *et al.* Antibiotic resistance patterns in invasive group B streptococcal isolates. *Infect Dis Obstet Gynecol* **2008**, 727505, doi:10.1155/2008/727505 (2008).
273 Langdon, A., Crook, N. & Dantas, G. The effects of antibiotics on the microbiome throughout development and alternative approaches for therapeutic modulation. *Genome Med* **8**, 39, doi:10.1186/s13073-016-0294-z (2016).
274 Bokulich, N. A. *et al.* Antibiotics, birth mode, and diet shape microbiome maturation during early life. *Science translational medicine* **8**, 343ra382, doi:10.1126/scitranslmed.aad7121 (2016).
275 Ortiz, L., Ruiz, F., Pascual, L. & Barberis, L. Effect of two probiotic strains of Lactobacillus on in vitro adherence of Listeria monocytogenes, Streptococcus agalactiae, and Staphylococcus aureus to vaginal epithelial cells. *Curr Microbiol* **68**, 679-684, doi:10.1007/s00284-014-0524-9 (2014).
276 De Gregorio, P. R., Juarez Tomas, M. S., Leccese Terraf, M. C. & Nader-Macias, M. E. Preventive effect of Lactobacillus reuteri CRL1324 on Group B Streptococcus vaginal

colonization in an experimental mouse model. *J Appl Microbiol* **118**, 1034-1047, doi:10.1111/jam.12739 (2015).
277 De Gregorio, P. R., Juarez Tomas, M. S. & Nader-Macias, M. E. Immunomodulation of Lactobacillus reuteri CRL1324 on Group B Streptococcus Vaginal Colonization in a Murine Experimental Model. *Am J Reprod Immunol* **75**, 23-35, doi:10.1111/aji.12445 (2016).
278 Patras, K. A. *et al.* Streptococcus salivarius K12 Limits Group B Streptococcus Vaginal Colonization. *Infect Immun* **83**, 3438-3444, doi:10.1128/IAI.00409-15 (2015).
279 Bernardini, R. *et al.* Neonatal protection and preterm birth reduction following maternal group B streptococcus vaccination in a mouse model. *J Matern Fetal Neonatal Med*, 1-7, doi:10.1080/14767058.2016.1265932 (2016).
280 Baker, J. A. *et al.* Mucosal vaccination promotes clearance of Streptococcus agalactiae vaginal colonization. *Vaccine* **35**, 1273-1280, doi:10.1016/j.vaccine.2017.01.029 (2017).
281 Fabbrini, M. *et al.* The Protective Value of Maternal Group B Streptococcus Antibodies: Quantitative and Functional Analysis of Naturally Acquired Responses to Capsular Polysaccharides and Pilus Proteins in European Maternal Sera. *Clin Infect Dis* **63**, 746-753, doi:10.1093/cid/ciw377 (2016).
282 Dangor, Z. *et al.* Correlates of protection of serotype-specific capsular antibody and invasive Group B Streptococcus disease in South African infants. *Vaccine* **33**, 6793-6799, doi:10.1016/j.vaccine.2015.10.019 (2015).
283 Dangor, Z. *et al.* Association between maternal Group B Streptococcus surface-protein antibody concentrations and invasive disease in their infants. *Expert Rev Vaccines* **14**, 1651-1660, doi:10.1586/14760584.2015.1085307 (2015).
284 Kwatra, G. *et al.* Natural acquired humoral immunity against serotype-specific group B Streptococcus rectovaginal colonization acquisition in pregnant women. *Clin Microbiol Infect* **21**, 568 e513-521, doi:10.1016/j.cmi.2015.01.030 (2015).
285 Heath, P. T. Status of vaccine research and development of vaccines for GBS. *Vaccine* **34**, 2876-2879, doi:10.1016/j.vaccine.2015.12.072 (2016).
286 Kobayashi, M. *et al.* WHO consultation on group B Streptococcus vaccine development: Report from a meeting held on 27-28 April 2016. *Vaccine*, 10.1016/j.vaccine.2016.1012.1029, doi:10.1016/j.vaccine.2016.12.029 (2016).
287 Kobayashi, M. *et al.* Group B Streptococcus vaccine development: present status and future considerations, with emphasis on perspectives for low and middle income countries. *F1000Res* **5**, 2355, doi:10.12688/f1000research.9363.1 (2016).
288 Ramaswamy, S. V., Ferrieri, P., Flores, A. E. & Paoletti, L. C. Molecular characterization of nontypeable group B streptococcus. *J Clin Microbiol* **44**, 2398-2403, doi:10.1128/JCM.02236-05 (2006).
289 Bellais, S. *et al.* Capsular switching in group B Streptococcus CC17 hypervirulent clone: a future challenge for polysaccharide vaccine development. *J Infect Dis* **206**, 1745-1752, doi:10.1093/infdis/jis605 (2012).
290 Hanage, W. P. Serotype replacement in invasive pneumococcal disease: where do we go from here? *J Infect Dis* **196**, 1282-1284, doi:10.1086/521630 (2007).
291 Nishihara, Y., Dangor, Z., French, N., Madhi, S. & Heyderman, R. Challenges in reducing group B Streptococcus disease in African settings. *Arch Dis Child* **102**, 72-77, doi:10.1136/archdischild-2016-311419 (2017).

292 Kim, S. Y. *et al.* Cost-effectiveness of a potential group B streptococcal vaccine program for pregnant women in South Africa. *Vaccine* **32**, 1954-1963, doi:10.1016/j.vaccine.2014.01.062 (2014).